The yeast endosomal/TGN-localized Ysl2p-Arl1p-Neo1p network: search for novel interaction partners

Von der Fakultät für Energie-, Verfahrens- und Biotechnik

der Universität Stuttgart

zur Erlangung der Würde eines Doktors der Naturwissenschaften (Dr. rer. nat)

genehmigte Abhandlung

vorgelegt von Maja Lasić

aus Mostar (Bosnien-Herzegowina)

Institut für Biochemie der Universität Stuttgart

2008

Hiermit versichere ich, dass ich die Arbeit selbst verfasst und dabei keine anderen als die angegebenen Quellen und Hilfsmittel verwendet habe.

Stuttgart, den 16.04.2008

Maja Lasić

Table of contents

Table of figures

Abbreviations

AA	amino acids
ALP	alcaline phosphatase
Amp	ampicilin
AP	clathrin heterotetrameric adaptor protein
APL	amminophospholipid
APS	ammonium persulfate
Arf	ADP-ribosylation factor
Arl	Arf-like
3-AT	3-amonio-1,2,4-triazole
ATP	adenosine 5'-triphosphate
BAR	Bin/Amphiphysin/Rvs
BLAST	Basic Local Alignment Search Tool
BSA	bovine serum albumine
CLAP	chymostatin, leupeptin, antipain, pepstatin
CPY	carboxypeptidase Y
Cy3	indocarbocyanine
DNA	desoxyribonucleic acid
DTT	D,L Dithiohreitol
EE	early endosome
EDTA	ethylenediamine tetraacetic acid
ENTH	epsin N-treminal homology domain
ER	endoplasmatic reticulum
FM4-64	N-(3-triethylammoniumpropyl)-4-(p-diethylaminophenyl-hexatrienyl) pyridinium dubromide
GAP	GTPase activating protein
GEF	guanine nucleotide exchange factor
GFP	green fluorescent protein
GGA	Golgi-associated, γ-adaptin homologous, Arf-interacting protein
GST	glutathione S-transferase
HA	hemagglutin
HSP	high speed pellet
IEF	isoelectrical focusing
IF	indirect immunofluorescence
IgG	immunoglobulin G

IPTG	isopropyl-beta-D-thiogalactopyranoside
IP	immunoprecipitation
kDa	kiloDalton
LE	late endosome
M	molar
ß-ME	ß-mercaptoethanol
mM	millimolar
MVB	multivesicular body
NEB	New England Biolabs
NP-40	nonident P-40
OD_{600}	opical density at 600 nm
PCR	polymerase chain reaction
PGK	phosphoglycerokinase
pH	$-\log_{10} c(H^+)$
pI	isoelectrical point
SD	synthetic growth medium
SDS-PAGE	sodium dodecyl sulfate-polyacrylamide gel electrophoresis
SNARE	soluble *N*-ethylmaleimide-sensitive factor attachment protein receptor
TAP	tandem affinity purification
TCA	trichloracetic acid
TEMED	tetramethylethylemdiamine
TEV	tobacco etch virus
TGN	*trans*-Golgi network
ts	temperature sensitive
Triton X-100	alkylpehnylpolyethylenglycol
Tween-20	polyoxyethylensorbitolmonolaureate
v/v	volume/volume
wt	wild type
w/v	weight/volume
YPD	yeast complete medium

Abstract

Vesicle transport is crucial for the communication between the compartments of a eukaryotic cell during the internalisation of endocytosed material, secretion of proteins into the extracellular space and biosynthetic transport to the vacuole. During each transport step the budding, tethering and fusion of the vesicle has to be regulated by numerous proteins to ensure the specificity of transport. Arfs and Rabs, small GTPases of the Ras superfamily, are crucial switches in these processes due to their GDP/GTP cycle. Arf GTPases regulate mainly the budding of vesicles by recruiting adaptor proteins to membranes, which in turn ensure the packaging of appropriate cargo into the vesicle and enable the coat assembly.

Ysl2p is a large protein, which has in the group of Dr. Birgit Singer-Krüger been shown to play a role in both the endocytic and biosynthetic route. Sequence analysis has further revealed homologies of Ysl2p to Sec7 family Arf GEFs. Due to this homology and the interaction of the N-terminus of Ysl2p, which contains the Sec7 domain, with the Arf-like GTPase Arl1p, Ysl2p was proposed to be a guanine nucleotide exchange factor for Arl1p. *ARL1* was as well identified as a suppressor of the growth defect of Δ*ysl2* cells. Arl1p localises to TGN and endosomes, where it recruits GRIP domain proteins to the membrane. Since GRIP-domain proteins are regarded as regulators of vesicle tethering, Arl1p was also proposed to be mainly involved in the tethering of vesicles. The *NEO1* gene, which encodes an aminophospholipid translocase, has been identified as a second suppressor of the Δ*ysl2* mutant. Same study of the Dr. B. Singer-Krüger group has demonstrated an *in vivo* interaction between Neo1p and Ysl2p. Thus, Neo1p is together with Ysl2p and Arl1p a further component of a common network. The work presented in this PhD thesis focussed on the role of Ysl2p within this network.

Former analysis from the Dr. B. Singer-Krüger group have demonstrated strong diferencies between some protein levels of Δ*ysl2*- and wild type cells when compared by one-dimensional electrophoresis. In the present study, the protein composition of vacuoles isolated from Δ*ysl2*- and wild type cells were compared using two dimensional electrophoresis. Subsequently, the differing proteins were analysed by mass spectroscopy (collaboration with Dr. A. Sickmann group, Würzburg) to identify which protein levels are affected by the deletion. From all observable changes upon *YSL2* deletion, the most prominent was the increase of the vacuolar levels of Erg6p. Additionally, a reduction of the vacuolar levels of some of the V-ATPase subunits and actin could be observed in Δ*ysl2* cells.

Subcellular fractionation experiments were performed to analyse if the changes of vacuolar levels of the V-ATPase were accompanied by changes in its distribution between TGN and endosomes. Additionally, other marker proteins of the TGN and endosomes were analysed for their distribution. However, no significant changes in the distribution of the

analysed proteins could be observed. Interestingly, the cellular levels of Kex2p were significantly reduced in Δ*ysl2* cells, which indicates on a possible role for Ysl2p in sorting of Kex2p on TGN/endosomes. For Ysl2p the subcellular distribution indicates a primarily early endosomal localisation.

To identify novel interaction partners of Ysl2p, a two hybrid screen was performed in collaboration with the group of Dr. P. Uetz (Karlsruhe) with different subdomains of this large protein. Surprisingly, although several putative interaction partners of Ysl2p were identified in the screens, only the putative interactors of the central region of the protein (Ysl2PILT) could be confirmed in my subsequent studies. Ent4p appears to be the most interesting candidate since its homologues Ent3p and Ent5p have recently been found to interact with Gga2p, a putative binding partner of Ysl2p. A weak interaction of Ent4p and Ysl2p could be detected by a GST-pull down but not by a co-immunoprecipitation experiment.

An alternative approach to identify novel interaction partners of Ysl2p was a large scale immunoprecipitation of Ysl2p-TAP. Although Ysl2p could be enriched with high purity no additional band could be specifically co-purifed by Ysl2p-TAP. This is surprising, since in a similar study Gillingham *et al*. (2006) isolated the protein Dop1p equimolar to Ysl2p, suggesting that the two proteins exist in a complex. Possible explanation for the failure in the present study could be a false purification method, since cells were lysed by grinding under liquid nitrogen while Gillingham *et al*. used spheroblasts for the detection.

To analyse the importance of different domains of the Ysl2p protein, a deletion series was generated, in which 100 to 900 amino acids from the C-terminus of Ysl2p were exchanged by the TAP-epitope and the corresponding effect on the cell growth was analysed. Interestingly, already the deletion of C-terminal 100 amino acids caused the same growth defect as the deletion of the complete *YSL2* gene. Further, it was demonstrated by a co-immunoprecipitation experiment that Ysl2p interacts with itself and that the C-terminal 100 amino acids are crucial for this interaction. Thus, the dimerisation of Ysl2p by the C-terminus could be highly important for cellular function.

Former study from the group of Dr. B. Singer-Krüger analysed the role of the APL translocase Neo1p within the Ysl2p-Arl1p network. There it was demonstrated, that at restrictive temperatures the temperature-sensitive *neo1-69* mutant accumulates aberrant membrane protrusions within the cell. Interestingly, the same study showed that the deletion of the *ARL1* gene restores the growth of the *neo1-69* mutant at the restrictive temperature, possibly by preventing the accumulation of Arl1p and effectors at the aberrant membrane protrusions. To identify possible Arl1-effectors, the experiment was repeated in the present study with deletions of several known TGN/endosomal adaptors. While the deletion of *GGA1* had no effect on the growth of the *neo1-69* mutant and the deletion of AP-1 and AP-3

subunits caused only partial suppression, the deletion of the adaptor *GGA2* could suppress the *neo1-69* growth defect to the same extent as the deletion of *ARL1*. Analogous analysis with several small GTPases demonstrated that, while the deletion of Ypt GTPases *YPT7* and *YPT51* had no effect on the growth of the *neo1-69* mutant, the deletion of *ARF1* caused partial and deletion of *ARL3* caused suppression comparable to the deletion of *ARL1*. The connection between Gga2p and the Ysl2-Arl1-Neo1 network indicated by genetical analysis was supported by indirect immunofluorescence analysis, which demonstrated that the deletions of either *ARL1* or *YSL2* caused a loss of punctuate structures in the Gga2p-HA staining while in some *neo1-69* mutant cells an accumulation of Gga2p in the aberrant structures could be observed. Further, a genetic interaction of *ARL1* with the *GGA*s as well as an interaction of the VHS-GAT domain of Gga2p with Arl1p and Ysl2p by a GST-pull down experiment could be demonstrated. Thus, Arl1p and its network seem to play a role not only in tethering as indicated by former analysis but as well in vesicle budding together with the adaptor protein Gga2p.

Finally, the protein Tvp38p has earlier been demonstrated to interact with Ysl2p in a two hybrid assay and a co-immunoprecipitation. Interestingly, Miller *et al*., (2005) have recently demonstrated an interaction between Sys1p and Tvp38p in a split ubiquitin screen. Both interactions could be confirmed in the present study, the Ysl2p-Tvp38p interaction by a GST-pull down assay and the Sys1p-Tvp38p interaction by a co-immunoprecipitation experiment. Thus, Tvp38p appears to be a link between the networks Ysl2-Arl1-Neo1 and Sys1-Arl3-Arl1. That could be a hint for a common role of these proteins.

In summary, the present study provides evidence that the Ysl2-Arl1-Neo1 network plays an important role in membrane recruitment of the adaptor Gga2p to membranes and thus may participate in vesicle budding processes. Further, Ysl2p may play a role in the localisation of Erg6p, which regulates one of the final maturation steps in ergosterol synthesis.

Zusammenfassung

Die interne Kompartimentalisierung ermöglicht es der eukaryotische Zelle den Transport sowohl von extrazellulärem Material zur Vakuole/Lysosom als auch von sekretorischen Proteinen nach außen von zytosolischem Milieu zu trennen. Die meisten Transportschritte zwischen den Kompartimenten werden durch Vesikel ermöglicht. Arfs und Rabs, kleine GTPasen der Ras Super-Familie, sind dabei entscheidend für die Spezifität der Auswahl sowohl des Transportguts als auch der Zielmembran. Proteine beider Familien werden durch Guaninnukleotid-Austauschfaktoren (GEF) aus der GDP- in die GTP-gebundene, aktive Form überführt, die Interaktion mit entsprechendem GEF entscheidet darüber hinaus an welche Membran die GTPase rekrutiert wird. Hauptaufgabe der Arf GTPasen liegt darin Adaptoren an die Membran zu mobilisieren, diese wiederum interagieren gleichzeitig mit Clathrin und den Proteinen, die als Ladung in den Vesikel eingeschlossen werden. Clathrinmoleküle bilden Netzwerke, die wiederum die Deformation der Membran bis zur endgültigen Abschnürung des fertigen Transportvesikels unterstützen.

Ysl2p ist ein großes Hefe-Protein von 186 kDa, dessen Verlust zur Folge Defekte sowohl in der Endozytose als auch im Sortieren vakuolärer Enzyme hat. Sequenzanalysen zeigten Homologien zwischen Ysl2p und den Mitgliedern der Sec7 Familie der Arf GEFs auf, die zwar in der Sec7 Domäne selbst nur niedrig ist, sich dafür aber über die gesamte Länge des Proteins erstrecken. Gleichzeitig wurde das Arf-ähnliche Protein, Arl1p, bei der Suche nach Suppressoren der Δysl2 Mutante identifiziert. Die Interaktion zwischen dem N-Terminus von Ysl2p und Arl1p, die *in vitro* nachgewiesen werden konnte, unterstützt die These, dass Ysl2p ein GEF für Arl1p sein könnte. Weiterhin wurde das *NEO1* Gen, das eine Amminophospholipid (APL) Translokase kodiert, als Suppressor der Wachstums- und Endozytosedefekte der Δysl2 Zellen identifiziert, sowie eine Interaktion zwischen Neo1p und Ysl2p mittels Koimmunopräzipitationsexperimenten nachgewiesen. Aufgrund dieser Ergebnisse wurde in Analogie zu dem Netzwerk aus Arf1p, dem GEF Gea2p und der APL Translokase Drs2p vorgeschlagen, dass das Ysl2-Arl1-Neo1 Netzwerk an der Biogenese von Endosomen beteilig ist. Dabei soll Neo1p die APL auf die cytosolische Seite der Lipiddoppelschicht überführen und somit möglicherweise zu der Membrankrümmung beitragen. Gleichzeitig interagiert Neo1p mit Ysl2p, welches Arl1p aktiviert. Im Rahmen dieser Doktorarbeit habe ich mich mit der Frage befasst, mit welchen weiteren Proteinen Ysl2p in diesem Prozess interagiert.

In der Gruppe von Dr. B. Singer-Krüger konnte gezeigt werden, dass die Deletion des *YSL2* Gens eine starke Fragmentierung der Vakuole verursacht und dass diese Fragmentierung mit starken Veränderungen der Proteinlevels in der Vakuole einhergeht, wie durch eindimensionale Elektrophorese gezeigt. Aus diesem Grund wurden in der vorliegenden Arbeit als erstes isolierte Vakuolen von Δysl2- und Wildtypzellen mittels zweidimensionaler

Gelelektrophorese aufgetrennt und die Proteine, deren vakuolären Levels durch die *YSL2* Deletion stark beeinflusst wurden, mittels Massspektoskopie bestimmt (Kollaboration mit der Gruppe von Dr. A. Sickmann, Würzburg). Von den Proteinen, von denen Informationen gewonnen werden konnten, am stärksten auffallende Protein wurde als Erg6p identifiziert, ein Protein das an der Synthese von Ergosterol beteiligt ist und als Folge der *YSL2* Deletion stark an Vakuolen angereichert wird. Außerdem konnten Reduktionen der vakuolären Levels von Aktin und einiger V-ATPase Untereinheiten verzeichnet werden.

Da die *YSL2* Deletion zu einer Reduktion des vakuolären Levels der V-ATPase führt, wurde mittels Zellfraktionierung untersucht, ob sich in der Δ*ysl2* Mutante die Verteilung der V-ATPase zwischen den TGN und endosomalen Kompartimenten verändert hat. Bei der Fraktionierung konnten jedoch weder für die V-ATPase noch für die meisten anderen untersuchten Markerproteine Veränderungen in der Verteilung nachgewiesen werden. Interessanterweise konnte in Δ*ysl2* Zellen eine starke Reduktion des Kex2p-Levels nachgewiesen werden. Dies deutet darauf hin, dass Ysl2p möglicherweise eine Rolle im Kex2p-Transport zwischen TGN und Endosomen haben könnte. Die subzelluläre Fraktionierung deutet außerdem auf eine primär frühendosomale Lokalisierung von Ysl2p.

Um weitere Interaktionspartner von Ysl2p zu finden, wurde mittels eines robotisierten Verfahrens (Kollaboration mit der Gruppe von Dr. P. Uetz, Karlsruhe) eine Zweihybridanalyse mit verschiedenen Domänen von Ysl2p durchgeführt. Interaktionspartner wurden in der kompletten Genbank von *S. cerevisiae* gesucht und für mehrere Domänen gefunden. Erstaunlicherweise konnten nur die Interaktionspartner der mittleren Unterdomäne von Ysl2p (Ysl2PILT) bei meinen anschließenden Analysen bestätigt werden. Von den putativen Interaktionspartnern von Ysl2PILT war Ent4p von größtem Interesse, da kürzlich eine Wechselwirkung zwischen dessen Homologen Ent3p und Ent5p und Gga2p, einem potentiellen Bindungspartner von Ysl2p, aufgezeigt wurde. Eine schwache Interaktion zwischen Ent4p und Ysl2p konnte *in vitro*, jedoch nicht mittels Koimmunopräzipitation gezeigt werden.

Ergänzend zu der Zweihybridanalyse wurde eine Immunopräzipitation von Ysl2p-TAP im Großansatz durchgeführt, in der Hoffnung weitere Interaktionspartner mittels Koimmunoprezipitation identifizieren zu können. Jedoch konnten keine spezifischen Banden in den Ysl2-Eluaten entdeckt werden. Dies ist umso erstaunlicher, da in einer ähnlichen Studie von Gillingham *et al*. (2006) das Protein Dop1p in äquimolaren Mengen isoliert wurde wie Ysl2p selbst, woraus geschlossen werden kann, dass Dop1p und Ysl2p als Komplex vorliegen. Der Grund für den Misserfolg in der hier präsentierten Arbeit könnte in der falsch gewählten Präparationsmethode liegen. Der Aufschluss wurde z.B. in dieser Studie durch Mörsern in flüssigem Stickstoff durchgeführt während Gillingham *et al.* sphäroblastierte

Zellen durch Homogenisation aufgeschlossen haben, was möglicherweise die Wechselwirkung erhält.

Bisher war nicht viel bekannt über die Relevanz der jeweiligen Unterdomänen von Ysl2p für die Proteinfunktion. Eine Deletionsreihe wurde in der vorliegenden Arbeit konstruiert, bei der 100 bis 900 Aminosäuren von C-Terminus von Ysl2p durch ein TAP-Epitop ersetzt wurden. Daraufhin wurde das Wachstum der jeweiligen Deletionsmutanten mit Wildtyp- und Δ*ysl2*-Zellen verglichen. Bemerkenswerterweise führte schon der Verlust von 100 Aminosäuren zu dem gleichen Wachstumsdefekt wie die Deletion des gesamten Gens. Folglich ist der C-Terminus von großer Bedeutung für die Ysl2p Funktion. Mittels Koimmunopräzipitation konnte in der vorliegenden Studie nachgewiesen werden, dass Ysl2p mit sich selbst interagiert. Weiterhin wurde gezeigt, dass die C-terminalen 100 Aminosäuren für diese Interaktion entscheidend sind. Somit liegt die Vermutung nahe, dass die Dimerisierung von Ysl2p mittels C-Terminus entscheidend für dessen Funktion innerhalb der Zelle ist, möglicherweise als gerüstbildendes Protein an endosomalen/TGN Membranen.

Bei der Analyse der Funktion der APL Translokase Neo1p wurde in einer vorherigen Studie der Gruppe von Dr. B. Singer-Krüger (Wicky *et al*., 2004) die *neo1-69* Mutante untersucht, die unnatürliche Verlängerung der endosomalen Strukturen akkumuliert. Diese Akkumulation der endosomalen Strukturen könnte wiederum den schweren Wachstumsdefekt dieser Mutante verursachen. Interessanterweise supprimiert die Deletion von *ARL1* diesen Wachstumsdefekt der *neo1-69* Mutante, möglicherweise durch Verhinderung der Akkumulation der Arl1p-Effektoren in den unnatürlichen Verlängerungen der *neo1-69* Mutante. Im Einklang mit diesem Modell, sollte die Deletion der Arl1p Effektoren einen ähnlichen Effekt auf das Wachstum der *neo1-69* Mutanten haben. Folglich, um zu überprüfen ob weitere potentielle Arl1p-Effektoren in der *neo1-69* Mutante akkumulieren, wurde der Einfluss der Deletionen einer Reihe von Adaptorproteinen, die am TGN/endosomalen Transport beteiligten sind, auf das Wachstum der *neo1-69* Mutante untersucht. Im Einklang mit dem Modell, haben die Deletionen der Adaptoren signifikante Unterschiede im Suppressionsverhalten bezüglich der *neo1-69* Mutante gezeigt. Während Deletion von *GGA1* keinen Einfluss auf das Wachstum hatte und Deletionen von AP-1 und AP-3 Untereinheiten den Wachstumsdefekt leicht supprimieren, bewirkte die Deletion von *GGA2* in der *neo1-69* Mutante ein wildtypartiges Wachstum und somit dasselbe Suppressionsverhalten wie die Deletion von *ARL1*. Deletionen von einigen Arf und Ypt-GTPasen zeigte auch, dass nur die Deletion von Arf-GTPasen den Wachstumsdefekt der *neo1-69* Mutante supprimieren. Während Deletionen von *YPT7* und *YPT51* keinen Einfluss auf das Wachstum von *neo1-69* Zellen hatten, konnte die Deletion von *ARF1* das Wachstum der Zellen zum Teil und Deletion von *ARL3* genau wie *ARL1* vollständig wiederherstellen. Diese Ergebnisse sind im Einklang

mit dem Modell in dem die Akkumulation der Vesikelknospungsmaschinerie für den Wachstumsdefekt der *neo-69* Mutante verantwortlich ist.

Da die Deletion von *GGA2* die beste Suppression des Wachstumsdefekts der *neo1-69* Mutante erreicht hatte, war es am wahrscheinlichsten, dass dieser Adaptor ein Arl1p-Effektor ist. Um eine mögliche Verbindung zu überprüfen wurde die Lokalisation von Gga2p in den Δ*ysl2* und Δ*arl1* sowie der *neo1-69* Mutante mittels indirekter Immunofluoreszenz untersucht. In der *neo1-69* Mutante konnte für Gga2p gezeigt werden, dass in den meisten Zellen das punktierte Färbungsmuster verloren geht. In den restlichen Zellen konnte eine stärkere Assoziation von Gga2p mit Membranen beobachtet werden. Die Deletion von *ARL1* und *YSL2* hat einen vollständigen Verlust der punktierten Lokalisierung von Gga2p zur Folge. Folglich scheinen sowohl Neo1p als auch Ysl2p und Arl1p an der Rekrutierung von Gga2p zu Membranen beteiligt zu sein. GST-*pull down* Experimente konnten eine Interaktion zwischen der VHS-GAT Domäne von Gga2p sowohl mit Arl1p als auch Ysl2p nachweisen. Weiterhin konnte auch eine genetische Interaktion zwischen *ARL1* und den *GGA*s gezeigt werden, die Trippelmutante Δ*arl1*Δ*gga1*Δ*gga2* zeigt ein deutlich schlechteres Wachstum als die Einzel- oder Doppelmutanten. Zusammengefasst deuten die Immunofluoreszenzen, sowie die genetischen und biochemischen Daten auf eine Einbindung des Adaptors Gga2p in das Ysl2-Arl1-Neo1 Netzwerk. Somit ist auch ein Hinweis auf eine Rolle des Ysl2-Arl1-Neo1-Netzwerks in der Vesikelknospung geliefert worden.

Als letztes wurden die Interaktionen des Transmembranproteins Tvp38p mit Ysl2p und Sys1p untersucht. Die Interaktion zwischen Tvp38p und Ysl2p wurde bisher mit der Zweihybridanalyse sowie durch Koimmunopräzipitationen gezeigt, während die Interaktion von Tvp38p mit Sys1p aus einem *Split-ubiquitin screen* bekannt ist. Beide Interaktionen konnten bestätigt werden. Die Interaktion von Tvp38p mit dem N-Terminus von Ysl2p wurde *in vitro* mit einem GST-*pulldown* nachgewiesen. Die Interaktion zwischen Tvp38p und Sys1p konnte *in vivo* mittels Koimmunopräzipitation gezeigt werden. Diese beiden Nachweise liefern einen gemeinsamen Interaktionspartner für Komponenten der Ysl2-Arl1-Neo1 und Sys1-Arl3-Arl1 Netzwerke und somit einen Hinweis auf die Möglichkeit einer gemeinsamen Funktion.

Zusammenfassend kann gefolgert werden, dass das Ysl2-Arl1-Neo1 Netzwerk eine Rolle im Prozess der Vesikelknospung hat, indem es den Adaptor Gga2p zu Membranen rekrutiert. Ysl2p könnte auch eine Funktion in der Lokalisation von Erg6p haben, einer Komponente der Ergosterolsynthese-Maschinerie.

1 Introduction

1.1 Vesicular transport in yeast

1.1.1 Endocytic and biosynthetic route are interconnected at the TGN/endosome network

A hallmark of eukaryotic cell is the compartmentalization of metabolic processes by the development of endomembrane systems. One of the most complex functions of the organelles of the exocytic and endocytic pathways is the maintenance of the organelle structure, composition and function with regard to the continuous flow of protein and membrane along these pathways.

The secretory system of eukaryotic cells is organised as a series of membrane-enclosed compartments that include the endoplasmatic reticulum (ER), Golgi cisternae, the trans-Golgi network (TGN), secretory vesicles and the plasma membrane. Among these organelles, the TGN has a central role as a site of protein sorting. The transport of newly synthetised proteins through the ER and Golgi cisternae occurs with almost no diversion to alternative routes (Fig.1, arrow 1). However, once proteins reach the TGN they face several possible destinations: the extracellular space and plasma membrane on the one side (Fig. 1, arrow 2) or early endosomes (EE; Fig. 1, arrow 3), late endosomes (LE; Fig. 1, arrow 4) and vacuole on the other side (Fig. 1, arrow 6) (reviewed by Gu *et al*., 2001). The TGN is thereby the interconnecting point of the secretory system with the endosomal-lysosomal system, another array of membrane-enclosed compartments that comprises different types of endosomes and lysosome/vacuole. This interconnection is necessary for the biosynthetic delivery of proteins and membranes from the TGN to the vacuole (Fig. 1, arrow 3-5; reviewed by Pelham, 2002). Proteins of the TGN, like the CPY-receptor Vps10p and the endopeptidase Kex2p, that reach endosomes, are recycled back to the TGN (Fig. 1, arrow 7 and 8; reviewed by Conibear and Stevens, 1998; Cooper and Stevens, 1996). An alternative direct pathway from the TGN to the vacuole bypassing endosomal compartments has been described for the vacuolar membrane protein alkaline phosphatase (ALP) (Fig. 1, arrow 6; Odorizzi *et al*., 1998b).

The endosomal-lysosomal system is used for the transport of endocytosed material. Through endocytosis, cells internalize plasma membrane components (e.g. downregulate signalling receptors) and nutrients in response to environmental cues or intracellular signals (Szymkiewicz *et al*., 2004).

The first step in the process of endocytosis is the internalization at the plasma membrane, where extracellular material and plasma membrane proteins become enclosed into transport vesicles by invagination of the plasma membrane (Fig. 1, arrow 9; Kaksonen *et al*., passes through at least two kinds of endosomes to the vacuole (Fig. 1, follow arrows 9–10–5; Singer-Krüger and Riezman, 1990; Vida *et al*., 1993). Internalized material moves first through a compartment of a higher density, the early endosomes, which are located at the cell periphery. At the ultrastructural level, the early endosomes display a highly complex and pleiomorphic organisation (Prescianotto-Baschong and Riezman, 1998; Mulholland *et al*., 1999). Tubular domains of the early endosomes extend from the large spherical vesicle and these tubular extensions are critical for all recycling processes. The recycling back to the plasma membrane (Fig. 1, arrow 11 and 2) has been well studied in mammalian cells, where many proteins follow this pathway (reviewed by Gruenberg, 2003). In yeast cells, only few proteins are known to return to the plasma membrane, among which are the a-factor receptor Ste3p, the v-SNARE protein Snc1p, and the chitin synthase Chs3p (Chen and Davis, 2000; Lewis *et al*., 2000; Ziman *et al*., 1996; Holthuis *et al*., 1998).
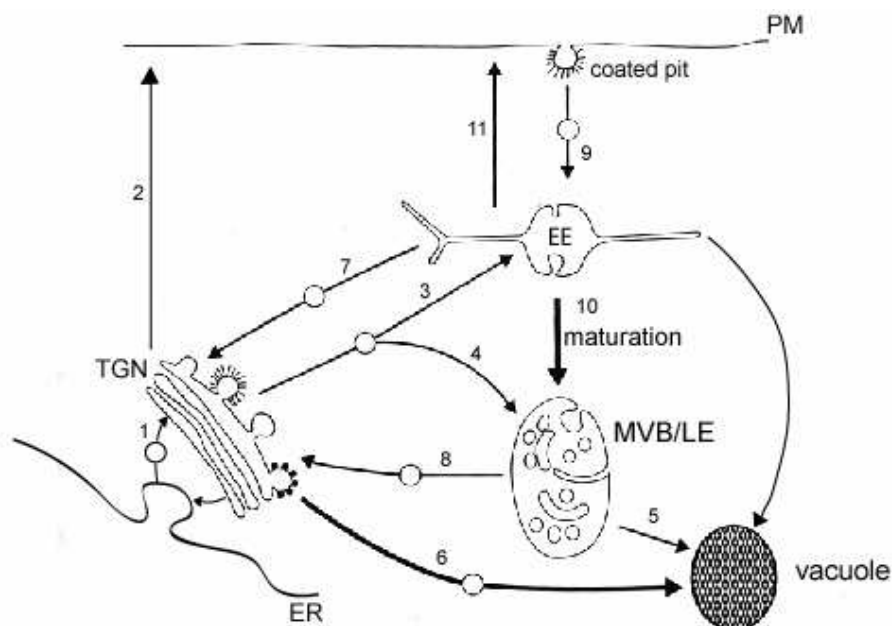
Fig. 1: Overview of the transport pathways in the endomembrane system in yeast. In the biosynthetic pathway, newly synthetised proteins are sorted from the ER through the Golgi apparatus to their final destination (1-6). Resident proteins are recycled back to the TGN (7 and 8). Conversely, newly internalized material is transported to the early endosomes (9). At this compartment, proteins destined for recycling are sorted back to the plasma membrane (11 and 2), whereas proteins destined for degradation are transported to the late endosomal compartment/MVB (10) and subsequently to the lysosome/vacuole (5). Alternative route transports metarial directly from TGN to the vacuole (6). The cellular compartments are indicated: plasma membrane (PM), early endosome (EE), late endosome (MVB/LE), vacuole, and *trans*-Golgi network (TGN) (adapted from Lemmon and Traub, 2000).

After delivery to early endosomes, these proteins transit to the TGN and return to the cell surface via the secretory pathway (Fig. 1, following arrows 9–7–2). The retrograde transport from endosomes to the TGN (Fig. 1, arrow 7) is mainly used by a specific set of transmembrane proteins that cycle between these two organelles. Most notable among these are acid-hydrolase receptors (Vps10p), transmembrane enzymes (Kex2p, Ste13p) and SNAREs (soluble N-ethylmaleimide-sensitive fusion protein (NSF) attachment protein receptors) (reviewed by Bonifacino and Rojas, 2006).

Proteins destined for degradation are transported from the early endosome to the late endosomal compartment (LE), which is of lower density than the early endosome and fuses with the vacuole (Fig. 1, arrow 10 – 5; Prescianotto/Baschong and Riezman, 2002; Singer-Krüger *et al*., 1993). This pathway is the principal route for material internalized by bulk phase endoctosis and for proteins destined for downregulation such as the pheromone α-factor receptor Ste2p (Chvatchko *et al*., 1986; Jenness and Spatrick, 1986). The biogenesis of late endosomes occurs by a process of maturation from vacuolar elements of early endosomes (Fig. 1, arrow 10) by budding of the endosomal membrane toward the compartment lumen and pinching off to form vesicles (Prescianotto-Baschong and Riezman, 2002). Due to this invagination late endosomes are commonly referred to as multivesicular bodies (MVBs). Membrane proteins destined for degradation within the vacuolar lumen are sorted into luminal MVB vesicles through the concerted action of the conserved ESCRT machinery (Babst *et al*., 2002; Katzmann *et al*., 2003). On the other hand, membrane proteins destined for the plasma membrane or TGN are excluded from these membrane subregions to be recycled back (Fig. 1, arrow 8; Nikko *et al*., 2003).

The vacuole is the terminal compartment for most of the endocytosed material. Apparently, the delivery of endocytosed macromolecules for the final degradation occurs by direct fusion of late endosomes with the lysosomes/vacuole (Fig. 1, arrow 5; Russell *et al*., 2006; Luzio *et al*., 2001). The vacuole contains a wide variety of acidic hydrolases, which degrade the endocytosed proteins (Teter and Klionsky, 2000). In addition to this role in the protein degradation, the vacuole participates in buffering the pH of the cytoplasm and in the regulation of water and ion homeostasis (Davis and Goodman, 1986; Nelson *et al*., 1989).

1.1.2 Vesicular traffic between TGN/endosomal compartments

Every step of the secretory, biosynthetic or endocytic pathway (see section 1.1.1) is mediated by vesicles. The vesicle-mediated transport is roughly divided into three steps: vesicle formation or budding mediated by a coat protein complex, which is intimately involved in cargo packaging (see section 1.1.2.1), vesicle positioning on the right acceptor membrane (tethering) mediated by specific tethering factors (see section 1.1.2.2) and vesicle fusion mediated by the interaction of a vesicle-SNARE (v-SNARE) with SNAREs on the target membrane (t-SNAREs) (see section 1.1.2.3) (Grosshans *et al*., 2006).

1.1.2.1 Vesicle budding

One of the crucial steps during the formation of transport vesicles is the recruitment of cytosolic coat proteins to the donor membrane. Four different types of vesicle coats, COP-I, COP-II, retromer and clathrin, have been identified to be implicated in distinct transport steps between organelles (Bonifacino and Rojas, 2006).

COPI and COPII coats regulate transport between the ER and cis-Golgi (Fig. 2). COPII coated vesicles mediate the anterograde ER-to-Golgi transport (Barlowe *et al*., 1994), whereas retrograde Golgi-to-ER vesicles use the COPI coat (Orci *et al*., 1986). The COPII coat consists of the small GTPase Sar1p and two protein complexes, Sec23/24p and Sec13/31p (Barlowe *et al*., 1994; Bednarek *et al*., 1996), whereas the COPI coat contains the small GTPase Arf1p and a heptameric protein complex called coatomer (Orci *et al*., 1986; Serafini *et al*., 1991; Bednarek *et al*., 1996).

After reaching the Golgi apparatus, the cargo proteins are transported to the TGN from where they are selected for the specific destination, e.g. hydrolases, which are destined for the vacuole, are brought to the endosomes by the appropriate receptor. After these acid-hydrolase receptors (Vps10p in yeast and cation-independent mannose 6-phosphate receptor (CI-MPR) in mammals) have released the cargo in the acidic environment of the endosome, they are recycled back to the TGN by a heteropentameric complex named "retromer" (Seaman *et al*., 1997; Arighi *et al*., 2004; Fig.2). The yeast retromer consists of two subcomplexes. The membrane-bound subocomplex comprises Vps5p and Vps17p, members of the sorting nexins family which heterodimerize on phosphatidylinositol-3-phosphate (PtdIns3)-enriched endosomes (Bravo *et al*., 2001; Peter *et al*., 2004; Horazdovsky *et al*., 1997). Additionally to Vps5p and Vps17p there is the cargo-selective subcomplex, composed of Vps26p, Vps29p and Vps35p (Seaman *et al*., 1997). Vps35p interacts with the cytosolic domains of retrograde cargo proteins such as Vps10p (Nothwehr *et al*., 2000).

The best-characterized transport vesicles are clathrin-coated vesicles (CCVs). The clathrin coat is a lattice of pentagons and hexagons that curves around to enclose a vesicle. The main proteins of these coated vesicles are clathrin-heavy chain (Chc1p) and clathrin-light chain (Clc1p). Three clathrin heavy chains form a trimer that appears as a triskelion, each leg extending radially. The legs are joined at a central trimerization domain and each leg is associated with a light chain (Kirchhausen, 2000). The globular N-terminal domain of the heavy chain protrudes to fom a inner layer, thereby binding to various mono- and heterotetrameric adaptor proteins and other clathrin-binding-box containing proteins (Maldonado-Baez and Wendland, 2006).

Recruitment and assembly of clathrin on membranes is facilitated by a direct interaction with clathrin adaptors (Gallusser and Kirchhausen, 1993; Dell'Angelica *et al*., 1998). Adaptors bind simultaneously to clathrin, membrane lipids, and in many cases to transmembrane cargo proteins (Kirchhausen, 1999; Robinson, 2004). In addition, the adaptors interact with numerous accessory factors, which regulate or participate directly in clathrin-coated vesicle formation (reviewed by Slepnev and DeCamilli, 2000). There are currently two major classes of adaptors that cooperate with clathrin: the tetrameric APs (adaptor protein) and monomeric GGAs (Golgi-localized, γ-ear containing, ADP-ribosylation-factor binding), (Bonifacino, 2004).

The adaptin complexes are each composed of four subunits with conserved structure: two large subunits (100 kDa; γ and β1 in AP-1, α and β2 in AP-2, δ and β3 in AP-3), one medium (50 kDa; μ1-μ3), and one small (20 kDa; σ1-σ3). AP-2 recruits clathrin to the plasma membrane (Munn, 2001; Fig. 2) while AP-3 transports proteins from endosomes and the TGN to lysosomes/vacuole (Cowles *et al*., 1997; Stepp *et al*., 1997; Theos *et al*., 2005; Fig. 2). AP-1 is implicated in transport of proteins like Kex2p from the TGN to endocytic intermediates (Stepp *et al*., 1995; Deloche *et al*., 2001) and also in retrograde transport from early endosomes to the TGN (Valdivia *et al*., 2002; Foote and Nothwehr, 2006; Fig. 2).
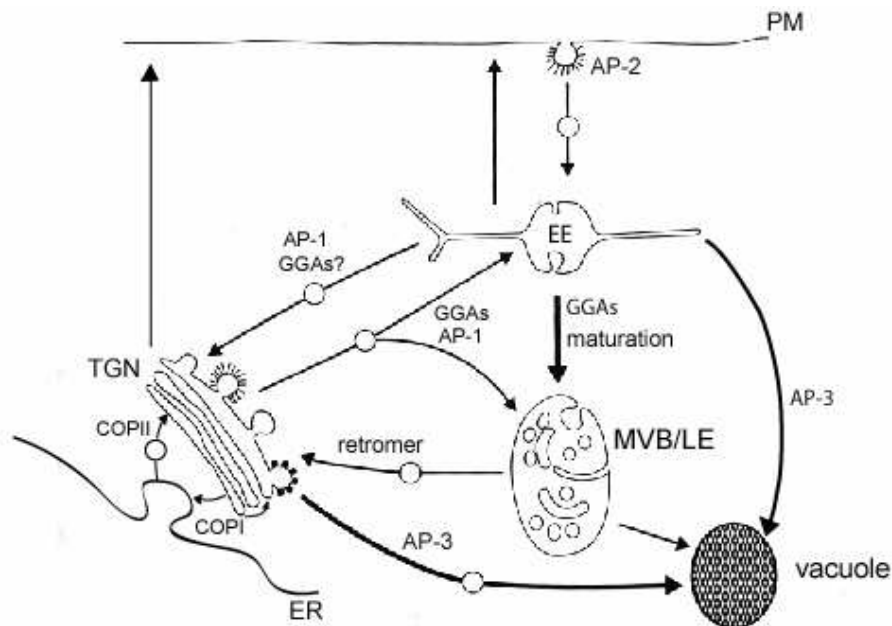
Fig. 2: Proposed roles for different adaptors in cellular transport. While COPI and COPII regulate retrograde and anterograde transport from ER to Golgi, respectively, and AP-2 is localised on the plasma membrane, AP-1, AP-3 and the GGAs regulate with a common effort the complex vesicular transport between the TGN, endosomes and the vacuole. AP-1 regulates both the anterograde and retrograde transport between TGN and endosomes, GGAs as well but additionally seem to play a role in the protein sorting into the MVB vesicles during endosome maturation. AP-3 regulates the transport from TGN or EE to the vacuole which bypasses the LE (adapted from Lemmon and Traub, 2000)

The GGAs (Golgi-localized, γ-ear-containing, Arf (ADP-ribosylation factor)-binding) are a family of monomeric, clathrin-binding adaptors (Hirst *et al*., 2000; Dell'Angelica *et al*., 2000; Boman *et al*., 2000). Three Ggas are present in human cells (GGA1, GGA2 and GGA3) and two are present in *S. cerevisiae* (Gga1p and Gga2p). GGAs have a modular organization, consisting of first a VHS (Vps27, HRS, and STAM) domain that recognizes acidic-cluster-dileucine signals present in the cytosolic tails of cargo like mannose 6-phosphate receptors (MPRs) (Puertollano *et al*., 2001; Zhu *et al*., 2001), second, a GAT (GGA and TOM) domain that interacts with the GTP-bound form of Arfs (Boman *et al.*, 2000; Dell'Angelica *et al*., 2000; Puertollano *et al*., 2001b) as well as ubiquitin (Scott *et al*., 2004; Puertollano and Bonifacino, 2004), third, a hinge domain that binds clathrin (Zhu *et al*., 2001; Puertollano *et al*., 2001b) and fourth, a GAE (γ-adaptin ear) domain that interacts with accessory proteins (Wasiak *et al*., 2002; Mattera *et al*., 2003; Lui *et al*., 2003).

GGAs have up to date been implicated in multiple trafficking pathways between TGN and the endosomes (Fig.2). First, several lines support a model of GGAs in the anterograde TGN-endosome transport. The GGAs sort the mammalian cation–independent mannose-6-phosphate receptor (CI-MPR) into clathrin-coated vesicles at the TGN (Doray *et al*., 2002b;

Mattera *et al*, 2003). Further, in yeast Kex2p and Vps10p, the yeast homologue of MPR, are missorted and falsely degraded in the vacuole of Δ*gga1*Δ*gga2* cells, instead of cycling between TGN and late endosome (Costaguta *et al*., 2001; Mullins and Bonifacino, 2001). Similar, the late endosomal SNARE Pep12p is missorted from the TGN to early instead of late endosomes in Δ*gga1*Δ*gga2* cells (Black and Pelham, 2000). Finally, Scott *et al*. (2004) demonstrated that the binding to GGAs is necessary to sort ubiquitylated cargo (i.e. Gap1p) from the TGN to the endosome. Thus, all these aspects support a model in which the GGAs function as adaptors for the sorting of both ubiquitylated and non-ubiquitylated cargo from TGN to endosomes (Scott *et al*., 2004). Second, the study from Puertollano and Bonifacino (2004) demonstrates that in addition to the known block in TGN-to endosome transport mammalian cells depleted of GGAs also exhibit a strong defect in the endocytosis and degradation of epidermal growth factor receptors (EGFRs), transmembrane proteins that undergo internalization into membrane invaginations during endosomal maturation by a process that is dependent on their post-endocytic ubiquitylation (Longva *et al*., 2002; Reggiori *et al*., 2001; Reggiori *et al*., 2002). This study argues for an additional role of GGAs in MVB sorting: GGAs may retain ubiquitylated cargo proteins in the early endosome and may concentrate these cargo molecules for sorting into the MVB vesicles by the ESCRT machinery (Puertollano and Bonifacino, 2004). Third, recent studies have implicated GGAs in retrograde transport from endosomal compartments to the TGN, like retrograde transport of internalised BACE1 (Alzheimer-associated beta-secretase; Wahle *et al*., 2005) and retrieval of MPRs from early endosomes to the TGN (Ghosh *et al*., 2003; Puertolano and Bonifacino, 2004).

The functional relationship between the GGA proteins and the heterotetrameric adaptor AP-1 has to date not been clearly defined. Both yeast and mammalian GGA proteins physically interact with AP-1 (Costaguta *et al*., 2001; Doray *et al*., 2002; Bai *et al*., 2004), and studies of MPR sorting in mammalian fibroblasts suggest a sequential role for the two adaptors (Doray *et al*., 2002). In contrast, the triple Δ*gga1*Δ*gga2*Δ*apl2* mutant is defective in growth, alpha-factor maturation, and transport of carboxypeptidase S to the vacuole although the double Δ*gga1*Δ*gga2* mutant or Δ*apl2* mutant show no phenotypes, indicating that GGAs and AP-1 function in distinct pathways between the TGN and endosomes (Costaguta *et al*., 2001). Thus, it remains to be defined which transport pathways are regulated by GGAs and AP-1 together and which independently.

A long-recognised commonality between COPI, COPII and the clathrin budding pathways is that small G-proteins of the Arf family regulate membrane recruitment of the

adaptors and coat (Dascher and Balch, 1994; Barlowe *et al.*, 1994; Dell'Angelica *et al.*, 2000; Dittie *et al.*, 1996; Ooi *et al.*, 1998). COPI components and clathrin adaptors are recruited by Arf1p, whereas the COPII coat depends on the Arf-related protein Sar1p.

Arfs represent a family of small GTPases, which have been implicated in a large number of cellular processes, including vesicular membrane traffic, Golgi morphology, lipid metabolism, cell motility and cytokinesis (Kahn, 2003). The cycle of coat recruitment and vesicle formation is intimately tied to the GTP cycle of the Arf GTPase. Its activation results not only in a conformational change that allows an interaction with numerous effectors, but also in a change in localisation from the cytoplasm to a membrane by insertion of the N-terminal amphiphatic helix that carries a myristoyl group into the lipidbilayer (Antonny *et al.*, 1997). The membrane localisation and conformational change upon nucleotide exchange of Arf-GTP are crucial for the recruitment of coat proteins to a membrane surface.

The interconversion between the two conformation states of small GTPases is promoted by two types of activities: guanine nucleotide exchange factors (GEFs) increase the level of activated (GTP-bound-from) and GTPase activating proteins (GAPs) accelerate the intrinsic hydrolysis of the bound GTP (Kahn, 2003). All Arf GEFs identified to date possess a Sec7 domain, a module of approximately 200 amino acids that is necessary and sufficient for catalyzing nucleotide exchange on Arf1p *in vitro*. While the smaller (<100 kDa) Arf GEFs (ARNO, cytohesin-1, EFA6) have so far only been identified in higher eukaryotes, the larger Gea/GBF/GNOM and Sec7/BIG subfamilies (>100 kDa) have orthologues in all eukaryotes examined and are therefore suggested to play highly conserved roles in membrane dynamics (Jackson and Casanova, 2000). Four Sec7 domain proteins of this class have been described to date in *S. cerevisiae*: Sec7p (Franzusoff and Scheckman, 1989), Gea1p, Gea2p (Peyroche *et al.*, 1996), and Syt1p, the last one being the most distant relative (Jones *et al.*, 1999). The localisation of Arf GEFs determines where in the cell the Arf GTPase will be activated. Hence, the GEFs control not only the timing but also the spatial organisation of Arf-activation (Jackson, 2003) and are therefore crucial components of the vesicle budding machinery.

1.1.2.2 Role of golgins in vesicle attachment

When a transport vesicle is destined to fuse with an acceptor compartment, it first needs to recognize its partner membrane by physical contact in a specific location. This process of membrane attachment or tethering requires the precise positioning of participating membranes (Jahn *et al.*, 2003). Central to this process are the Rab/Ypt GTPases. In most tethering reactions, GTP bound Rabs on the donor membrane mediate membrane attachment

by interacting with specific effectors on target membranes (Jahn *et al*., 2003). Like Arf GTPases, Rab GTPases function as molecular switches, cycling between GTP- and GDP-bound states. The active, GTP-bound form is attached to membranes by a C-terminal modification with hydrophobic geranylgeranyl groups (Araki *et al*., 1990)

The different tasks of Rab GTPases are carried out by a diverse collection of effector molecules that bind to specific Rabs in their GTP-bound state (Grosshans *et al*., 2006). A group of Rab effectors belong to the so called golgins. Golgins are long coiled-coil proteins that are implicated in several processes: tethering of transport vesicles, connecting adjacent Golgi cisternae, and/or assembling or scaffolding other proteins (Barr and Short, 2003; Gillingham and Munro, 2003). They associate with Golgi membranes in a variety of ways. Some have a transmembrane domain near their C-terminus (Giantin, Golgin-84, CASP) while others are peripheral membrane proteins. Peripheral golgins may associate with the membrane either by an interaction with an adaptor protein of the GRASP family (GRASP65-GM130, GRASP55-Golgin45) or are recruited to Golgi membranes in a nucleotide-dependent manner by small GTPases of the Rab (p115 by Rab1, BicaudalD1/D2 and TMF by Rab6), Arf-like (Golgin-245, Golgin-97 and Imh1p) and Arf (GMAP-210, Rud3p) families (Short *et al*., 2005).

All golgins recruited by Arl1p comprise the GRIP-domain, a ~45 amino acid motif found in at least four mammalian golgins (p230/golgin245, golgin-97, GCC88, and GCC185) and one yeast golgin (Imh1p) (Van Valkenburgh *et al*., 2001; Panic *et al*., 2003a; Setty *et al*., 2003; Lu *et al*., 2003). The GRIP-domain forms a homodimer, with each monomer separately binding an Arl1p-GTP molecule. The simultaneous binding of two Arl1p molecules likely stabilizes the association of the golgin with the membrane (Panic *et al*., 2003b; Wu *et al*., 2004). GRIP domain proteins seem to primarily regulate endosome-to-Golgi transport via tethering of endosome-derived vesicles to the TGN (Lu *et al*., 2004; Tsukada *et al*., 1999).

By analogy to the GRIP domain, Rud3p binds to the GTPase Arf1p via its C-terminal "GRIP-related Arf-binding" (GRAB) domain and seems to function as a dimer, proposing a similar mechanism (Gillingham *et al*., 2004).

1.1.2.3 Membrane fusion

After the tethering of the vesicle to the target membrane, the fusion of the vesicle and acceptor lipid bilayers is enabled by action of a variety of protein families. First, the membranes are brought into close proximity, where counteracting electrostatic forces need to be overcome before the lipids of the proximal leaflets can interact. Second, the boundary

between the hydrophilic and hydrophobic portion of the bilayer is destabilized and non-bilayer transition states are generated that culminate in the formation of an aqueous fusion pore (Jahn *et al*., 2003).

Crucial for the first step is the SNARE (soluble N-ethylmaleimide-sensitive factor attachment protein receptor) family of small, C-terminally-anchored coiled-coil membrane proteins (Söllner *et al*., 2003). When two membranes fuse, SNAREs on the vesicle membrane (v-SNAREs) interact with the t-SNAREs on the target membrane. The SNAREs then intertwine in a tight *trans* complex, which brings the two membrane into close proximity (Hong, 2005). After fusion, v-SNAREs and t-SNAREs unite their anchors in the fused membrane, so forming a *cis* complex (Fig. 3A).
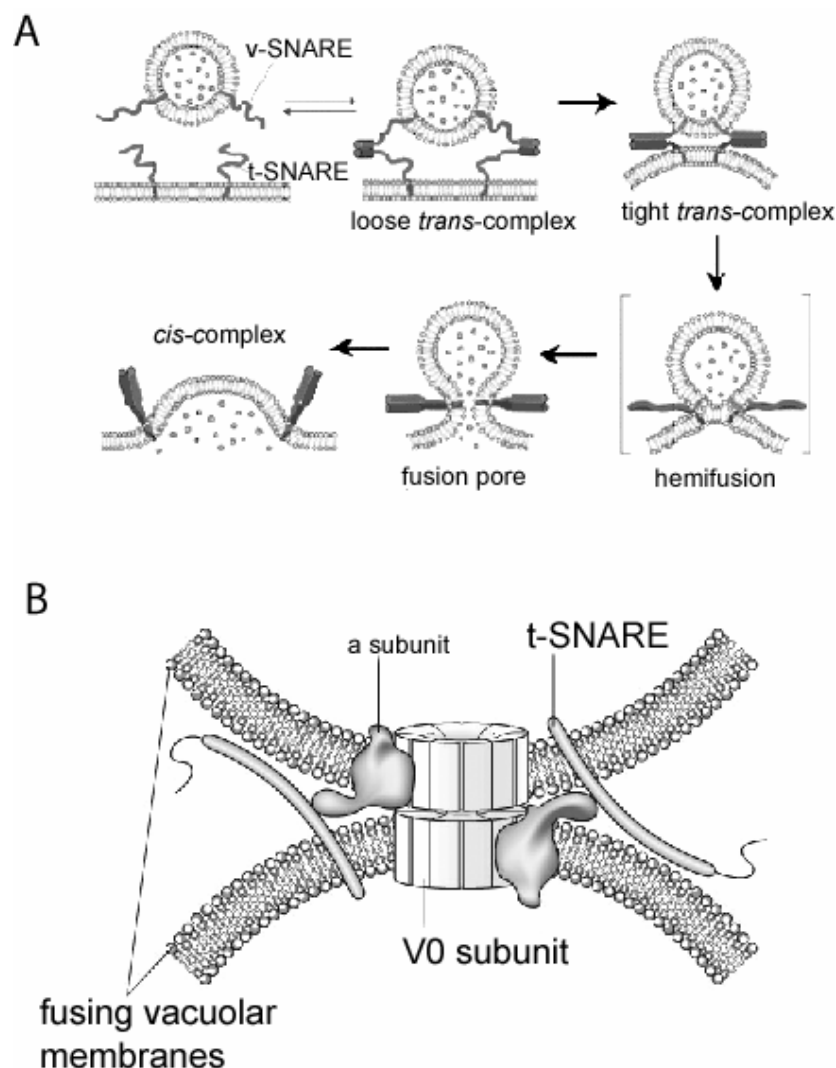
Fig. 3: Modell of vesicle fusion: (A) Model of the SNARE role in the membrane fusion (adapted from www.ibpc.fr/UPR1929/jph/41.htm) (B) Model of the V-ATPase role in the membrane fusion (adapted from Almers, 2001).

For the second step of the fusion process, additionally to the SNAREs is the V_0 domain of the vacuolar ATPase necessary. Trans-pairs of V-ATPase V_0 subunits are formed between the two fusing membranes. These trans-pairs promote the mixing of the lipid bilayers by virtue of the highly hydrophobic proteolipid subunits (Peters *et al*., 2001; Bayer *et al*., 2003) and enable by that the final fusion (Fig. 3B).

Since SNAREs exhibit a specific subcellular localisation, they are often used as markers to identify distinct organelles, e.g. yeast Tlg1p and Pep12p are used as markers for early and late endosomes, respectively (Holthuis *et al*., 1998; Becherer *et al*., 1996), while the t-SNARE Vam3p is used as a vacuolar marker (Darsow *et al*., 1998).

1.1.3 Role, transport and assembly of the V-ATPase

Vacuolar (H^+)-ATPases (V-ATPases) are multisubunit enzymes composed of a peripheral complex V_1 attached to a membrane-bound V_0 complex (Nelson and Harvey, 1999; Nishi and Forgac, 2002). They reside mainly within the vacuole but also within endosomes and secretory vesicles. The major function of the V-ATPase consists in the maintenance of the pH gradient within these intracellular compartments by the ATP-driven transport of protons from the cytosol into acidic organelles. It functions in processes such as receptor-mediated endocytosis, intracellular targeting of vacuolar enzymes, protein processing and degradation (Nishi and Forgac, 2002). During the receptor-mediated endocytosis, a reduced pH within early endosomes, produced by action of the V-ATPase, can trigger the dissociation of internalized ligand-receptor complexes. This may allow the recycling of receptors to the plasma membrane, which provides a mechanism for controlling both the rate of ligand uptake and the density of cell-surface receptors (Forgac, 1999; Stevens and Forgac, 1997). A similar mechanism governs the uncoupling of the newly synthetised lysosomal enzymes from the Golgi to lysosomes. Acidification of late endosomes causes the release of lysosomal enzymes from the receptors, and permits the recycling of the respective receptor to the TGN (Nishi and Forgac, 2002) (see section 1.1.1).

The assembly and disassembly of the V-ATPase is regulated accurately to ensure the temporal and spatial control of the acidification and as well to avoid useless ATP consumption. A complex containing Skp1p, Rav1p, and Rav2p (termed RAVE for 'regulator of the (H+)-ATPase of vacuolar and endosomal membranes') regulates the assembly of the V-ATPase (Seol *et al*., 2001, Smardon *et al*., 2002) while restricting the process spatially to the early endosomes (Sipos *et al*., 2004). Disassembly of the V-ATPase under less favourable conditions might conserve ATP when energy sources are limited, while rapid reassembly

could help to prevent cytosolic acidification when metabolism resumes. The glycolytic enzyme aldolase was found to bind directly to several subunits of the V_1 and V_0 sectors and mutants lacking aldolase ($\Delta fba1$) grew better at pH 5 than at pH 7.5, suggesting a connection between the aldolase and the V-ATPase activity. Further, the level of free V_1 complex was found to be increased in the $\Delta fba1$ mutants (Lu *et al*., 2001; Lu *et al*., 2004). Thus, the extracellular glucose availability might be signalled to V-ATPases at the vacuolar membrane via aldolase levels to induce the reversible disassembly of V-ATPase complexes.

1.1.4 Role of ergosterol in yeast

Lipids provide the physical support of organelle membranes, acting as a barrier for water-soluble molecules and as a solvent for the hydrophobic domains of membrane proteins. By contributing to the intrinsic properties of membranes, such as thickness, asymmetry, and curvature, lipids regulate protein movement and distribution (Huttner and Zimmerberg, 2001; van Meer and Sprong, 2004). Some short- and long-lived lipids have a restricted distribution in the plane of the bilayer, thereby forming transient or more stable microdomains (Mukherjee and Maxfield, 2004). In particular, cholesterol and sphingolipids were proposed to form a separate liquid-ordered phase (lipid rafts), thereby functioning as platforms that can incorporate distinct classes of proteins, and thus regulate numerous cellular processes, including signalling, sorting and infection (Parton and Richards, 2003; Simons and Vaz, 2004; Lafont *et al*., 2004). Detergent-resistant membranes (DRMs) are the yeast equivalent to lipid rafts (Kübler *et al*., 1996; Bagnat *et al*., 2000; Wachtler and Balasubramian, 2006). They are enriched in sphingolipids and in ergosterol (Bagnat *et al*., 2000), the structural sterol of fungi.

There are multiple roles for sterols in yeast endocytosis. First, specific sterols are required in receptor-mediated endocytosis at or before receptor hyperphosphorylation arguing for a specific role at an early step in the process (Munn *et al*., 1999). Second, based on experiments analysing FM4-64 and LY accumulation, sterol structures also have a general role at a postinternalization step. Third, ergosterol is as well required for the Sec18/ATP-dependent priming step of homotypic vacuole fusion (Heese-Peck *et al*., 2002; Kato and Wickner, 2001, see section 1.1.3). An obstruction of ergosterol synthesis inhibits also all these processes.

In both yeast and mammalian cells, sphingolipids and sterols are predominantly found in the plasma membrane (Lange *et al*., 1989; Patton *et al*., 1991; Hechtberger *et al*., 1994; Zinser and Daum, 1995), but they are synthesized in compartments of the early secretory

pathway (Daum *et al*., 1998; Futerman and Riezman, 2005). Ergosterol biosynthesis requires a large number of genes encoded by *ERG* genes in yeast (see Fig. 4). The *ERG* genes encoding enzymes involved in later steps of ergosterol biosynthesis (*ERG6*, *ERG2*, *ERG3*, *ERG5*, and *ERG4*) are not essential for cell viability, whereas those involved in earlier steps (*ERG9*, *ERG1*, *ERG7*, and *ERG11*) are required for viability. Interestingly, three enzymes of the sterol biosynthetic pathway, Erg1p, Erg6p and Erg7p, are located in the lipid droplets (Leber *et al*., 1994; Müllner *et al*., 2004; Zinser *et al*., 1993) and not in the ER as the other components of the ergosterol synthesis machinery. These droplets serve mainly for storage of neutral lipids and consist of a highly hydrophobic core of triacylglycerols and/or steryl esters, surrounded by a phospholipid monolayer with only a few protein embedded, like e.g. Erg6p (Zweytick *et al*., 2000).
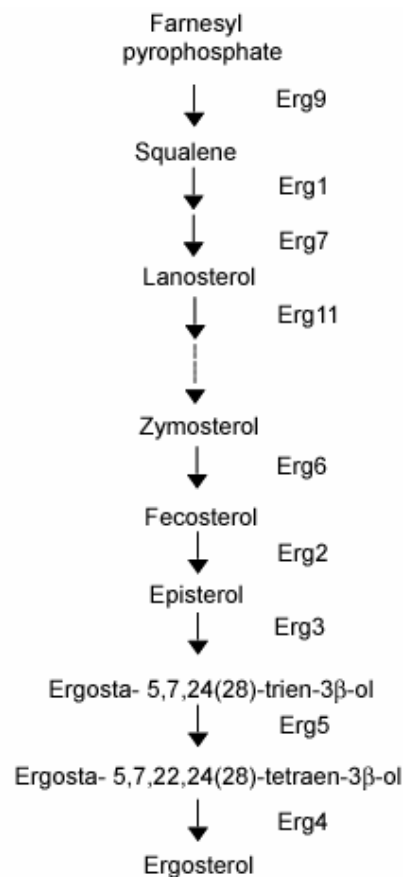
Fig. 4: Sterol synthesis pathway in yeast

The *ERG6* gene, encoding the S-adenosylmethionineΔ24-methyltransferase, which catalyzes C-24 methylation of zymosterol, is the first non-essential enzyme during the ergosterol synthesis process (see Fig. 4). For that reason, mutants of the *ERG6* gene are often used in the analysis of the ergosterol role. Erg6p localised in lipid particles acquires its substrate, free zymosterol, from the endoplasmic reticulum, where it is synthesized.

Conversion of zymosterol to fecosterol occurs at contact zones between the endoplasmic reticulum and lipid particles (Zinser *et al*., 1993). The product of the methyltransferase reaction, fecosterol, must then be translocated from lipid particles to the endoplasmic reticulum for further conversion to ergosterol. *ERG6* mutant cells exhibit pleiotropic phenotypes that include defective conjugation, hypersensitivity to cycloheximide, resistance to nystatin, a severely diminished capacity for genetic transformation, defective tryptophan uptake (Gaber *et al*., 1989) and are sensitive to brefeldin A (Vogel *et al*., 1993; Graham *et al*., 1993). These phenotypes reflect the role of ergosterol as a regulator of membrane permeability and fluidity.

Upon synthesis in the ER, sphingomyelin and cholesterol (ergosterol) are transported to the later secretory organelles mainly by nonvesicular pathways. As support, they are excluded from the retrograde COPI-coated vesicles, a process which may contribute to the enrichment of these lipids in the late Golgi network and the plasma membrane (Brugger *et al*., 2000). Plasma membrane cholesterol constitutively recycles via recycling endosomes, which appear to be cholesterol rich (Hornick *et al*., 1997; Hao *et al*., 2002; Gagescu *et al*., 2000), while lysosomes are cholesterol poor (Sokol *et al*., 1988; Lange *et al*., 1998; Schoer *et al*., 2000). The association of the yeast ergosterol with detergent-resistant membranes (DRMs) (Simons and Ikonen, 1997; Brown and London, 2000) is believed to play an important role in these distribution processes (Ridgway, 2000).

1.2 Ysl2p network and its role in vesicular transport

1.2.1 Role of Ysl2p in TGN/endosomal traffic

Ysl2p/Mon2p was originally identified by B. Singer-Krüger in a screen for mutants, which are synthetically lethal with the deletion of *YPT51*, a gene encoding a Rab GTPase that regulates transport from early to late endosomes (Singer-Krüger and Ferro-Novick, 1997). Additionally, it was found in screens for mutants that are sensitive to the drugs monensin and brefeldin A (Muren *et al*., 2001), defective in endocytosis (Wiederkehr *et al*., 2001) and defective in protein transport to the vacuole (Avaro *et al*., 2002; Bonangelino *et al*., 2002).

Ysl2p is a large protein of 186 kDa with a weak homology to the large Arf GEFs of the Sec7 family (see section 1.1.2.1). It is well conserved in evolution with homologues from humans to *Dictyostelium*. Efe *et al*. (2005) defined the Mon2p family due to the sequence homology over six conserved regions (A to F). Domains A, E and F are found solely in the members of the Mon2p family. The alignments of the A and F domains between the members

of the Mon2 family show a sequence similarity of 42% and 40%, respectively, with a predominance of charged and hydrophobic residues. The type of conserved amino acids, the small size, and the predicted secondary structure for these two domains suggest that they could be involved in protein binding activity (Efe *et al*., 2005). Originally, the homology to the Sec7 family members was recognized in B-domain (corresponds to the DCB (Dimerisation and Cyclophilin-Binding) domain), which precedes the Sec7 domain (Bonangelino *et al*., 2002; Jochum *et al*., 2002). A multiple sequence alignment and secondary structure prediction performed in the group of B. Singer-Krüger showed a clear relationship between Ysl2p and the Sec7 family members (Jochum *et al*., 2002). Domains B, C and D of Ysl2p are also present in large Sec7 GEFs and closely correspond to the conserved upstream and downstream regions of the Sec7 catalytic domain, as recently defined (Mouratou *et al*., 2005; Efe *et al*., 2005; Gillingham *et al*., 2006). The homology of the Mon2 and Sec7 families raises the question of the role of the domains shared between Ysl2p and the large Arf GEFs. Recently, it has been shown for the GBF and BIG ArfGEF groups that the DCB (B domain) can homodimerize and can also interact with the HUS domain (C domain) (Ramaen *et al*., 2007). Since for Ysl2p the dimerisation could as well be demonstrated (Efe *et al*., 2005), and Ysl2p has both of these domains (B and C) it is possible that its dimerisation is mediated through the interaction of B-B or B-C domains.

Multiple genetic and biochemical evidence indicated an interaction between Ysl2p and the Arf-like protein Arl1p. The deletion of *ARL1* in Δ*ysl2* cells resulted in synthetic lethality of the cells while the overexpression of *ARL1* suppressed specifically the defects of Δ*ysl2* cells in growth, endocytosis and vacuole formation (Jochum *et al*., 2002). A physical interaction between the N-terminal region of Ysl2p including the Sec7 domain and Arl1p was shown by the yeast two hybrid system and by *in vitro* binding studies. These data together with the structural homology (see section 1.2.1) indicate that Ysl2p represents a Sec7 family GEF for Arl1p (Jochum *et al*., 2002; see section 1.1.2.1). On the opposite, Gillingham *et al*. (2006) demonstrated that the punctuate distribution of Arl1p and Imh1p is unaffected in Δ*ysl2* cells. Whether or nor Ysl2p is implicated in the activation of Arl1p as a GEF remains to be shown.

From differential centrifugation experiments one could presume that a major fraction of Ysl2p is a homodimer, which is peripherally associated with TGN and/or endosomes (Jochum *et al*., 2002, Efe *et al*., 2005). In agreement, the microscopic analysis revealed that Ysl2p co-localised with the endocytic marker FM4-64 and collapsed into the *vps27* class E compartment (Jochum *et al*., 2002), both characteristics of endosomal proteins. In another

study, Ysl2p co-localised partially with Sec7p-DsRed chimera and the PH$_{(FAPP1)}$-DsRed fusion, both markers of the TGN (Efe *et al.*, 2005), however it did not collapse in the *sec7* mutant (Jochum *et al.*, 2002), known to perturb the localisation of Golgi resident proteins. Thus, the microscopic studies support the TGN/endocytic localisation for Ysl2p, the membrane association seems to be achieved by the N-terminal domains A-C. Interestingly, Arl1p may not be required for the association of Ysl2p with membranes (Efe *et al.*, 2005).

YSL2-deleted cells are viable but exhibit strong growth delays at all temperatures. Although Δ*ysl2* cells were not impaired in the kinetics of α-factor internalisation at the plasma membrane, they exhibited a strong delay in Ste2p turnover (Jochum *et al.*, 2002), indicating a role for Ysl2p in post-internalisation steps of endocytosis. Internalisation experiments with Lucifer Yellow (LY) and electronmicroscopic analysis of temperature sensitive mutants demonstrated the highly fragmentated vacuole as an immediate, and therefore most likely a direct consequence of the heat inactivation of Ysl2p (Jochum *et al.*, 2002). Thus, Ysl2p also participates in the maintenance of the vacuolar structure probably by regulating the biosynthetic transport. Together these results suggest a role for Ysl2p on the crossing between the endocytic and biosynthetic route. The result that *YSL2* displays synthetic lethality with *vps1*, *vps26*, *vps52*, *vps54*, *rcy1*, *vps45* and *arf1* (Efe *et al.*, 2005), all known to block vesicular transport to and from the TGN, supports this idea. Recently, Ysl2p was also found to be implicated in the transport of Ape1p, a hydrolase transported from cytoplasm to the vacuole via the Cvt pathway. The processing of prApe1p was found to be almost completely defective in the Δ*ysl2* mutant (Efe *et al.*, 2005). Interestingly, the late-Golgi GARP complex, known to be an effector of Arl1p (Panic *et al.*, 2003), is required for the formation of Cvt vesicles (Reggiori *et al.*, 2003). This may indicate a common role for Ysl2p and Arl1p in this process.

Recent studies have identified Dop1p as an interaction partner of Ysl2p, the two proteins seem to function in a stochiometric complex (Gillingham *et al.*, 2006; Efe *et al.*, 2005). Dop1p is a large, essential protein represented in all eukaryotes from yeast to human. The founding member of the family is the DopA gene from *Aspergillus nidulans*. DopA contains several putative domains, including three leucine zipper-like domains. It is required for correct cell morphology and spatiotemporal organization of multicellular structures (Pascon *et al.*, 2000). Further analysis of the *S. cerevisae* homologue revealed that Ysl2p seems to be crucial for the membrane localisation of Dop1p (Gillingham *et al.*, 2006). Together, Ysl2p and Dop1p seem to be required for transport between endosome and Golgi,

since their loss causes an accumulation of v-SNARE Snc1p and syntaxin Sso1p on internal membranes (Gillingham *et al*., 2006).

Recent studies have reported a number of novel interaction partners for the large Arf GEFs and have by that shown that being an Arf GEF is not their only function. Yeast Gea1p and Gea2p are reported to bind to Gmh1p, a conserved Golgi membrane protein of unknown function, through the region C-terminal to their Sec7 domain, and Gea2 also binds to a Golgi P-type ATPase through its Sec7 domain (Chantalat *et al*., 2003; Chantalat *et al*., 2004). In addition, mammalian GBF1 was found to bind to the Golgi coiled-coil protein p115 via a "poorly conserved" region at the C terminus, but removal of this region from GBF1 did not affect its Golgi localization (Garcia-Mata *et al*., 2003). The mammalian large Arf GEFs BIG1 and BIG2 have been reported to interact with a number of proteins (Xu *et al*., 2005; Padilla *et al*., 2003; Li *et al*., 2003). Present model explains the multiple interactions of large ARF GEFs with their role as scaffolds, which recruit or retain a number of proteins in a particular part of the Golgi. Gillingham *et al*. (2006) proposed that Ysl2p may serve as well as a scaffold to recruit a subset of Dop1p, and potentially other proteins, to the membranes. The interaction of Ysl2p with Dop1 (Efe *et al*., 2005; Gillingham *et al*., 2006), Arl1p (Jochum *et al*., 2002), Neo1p (Wicky *et al*., 2004; see section 1.2.3) itself (Efe *et al*., 2005) and probably additional interaction partners supports this role for Ysl2p.

1.2.2. Arl1p recruits GRIP-domain Golgins to TGN/endosomal membranes

Arl1p, the GTPase interacting with Ysl2p (Jochum *et al*., 2002; see section 1.2.1), was originally identified in a search for Arf1p-homologues. Arl1p has all of the typical features of an Arf-family GTPase, including an amphipathic N-terminal helix and the myristylation site (Lee *et al*., 1997). It bound and hydrolysed GTP, but lacked 'Arf' activity in the G_s ADP-ribosylation assay (Tamkun *et al*., 1991; see section 1.1.2.1) and was therefore named Arf-like. A single homologue of Arl1p is present in the genome of most eukaryotes so far examined.

Localisation studies in mammalian cells identified TGN as the major organelle of Arl1p (Lowe *et al*., 1996; Lu *et al*., 2001). In yeast, the punctuate pattern together with co-localisation studies identified as well Golgi, but also endosomes as major compartments of Arl1p (Setty *et al*., 2003; Jochum *et al*., 2002). *ARL1* depletion in mammalian cells causes an accumulation of TGN proteins such as TGN46 on endosomal compartments (Lu and Hong,

2003; Yoshino *et al.*, 2003). In agreement with this observation, the overexpression of a constitutively active *ARL1* mutant (Arl1Q71L) resulted in large, unstacked Golgi cisternae while a dominant negative mutant (Arl1T32N) caused the disappearance of the Golgi (Lu *et al.*, 2001). Thus, Arl1p seems to play an important role in the maintenance of the Golgi structure.

These phenotypes could recently be explained by the identification of the GRIP-domain Golgin Imh1p as a direct effector of Arl1p (Van Valkenburgh *et al.*, 2001; Panic *et al.*, 2003a; Setty *et al.*, 2003; Lu and Hong, 2003). Golgins are known to function as vesicle tethers and as well in the maintenance of the TGN structure (see section 1.1.2.2). Nevertheless, GRIP-domain proteins are not the only effectors of Arl1p. The GARP-VFT complex, which is also a putative vesicle tether that has been implicated in endosome-to-Golgi trafficking, has recently been identified as an additional Arl1p effector (Panic *et al.*, 2003b). Due to the role of Arl1p effectors as vesicle tethers (see also section 1.1.2.2), it has been proposed that Arl1p regulates retrograde trafficking (Munro, 2005). Several proteins known to be effectors of Arf1p, like Arfaptin2 (also termed POR1) and MKLP1, have as well the ability to bind to Arl1 *in vitro*. Further, the expression of the GTP-restricted form of Arl1p in mammalian cells leads to an increased membrane association of vesicle coat proteins, COPI and AP-1 (Lu *et al.*, 2001; Van Valkenburgh *et al.*, 2001). These results imply that Arl1p shares overlapping roles with Arf1p, in addition to its functions that are carried out by unique effectors such as GRIP domain proteins (Lu *et al.*, 2001).

Genetic studies in yeast have shown that Golgi recruitment of Arl1p requires a second Arlf-like GTPase, Arl3p (ARFRP1 in humans), and a small transmembrane protein Sys1p (Setty *et al.*, 2003; Setty *et al.*, 2004; Behnia *et al.*, 2004; Panic *et al.*, 2003). Arl3p is an atypical Arf family member, in that it lacks a myristoylation site and instead is N-terminally acetylated, with this modification being required for recruitment of the protein to the Golgi by Sys1 (Behnia *et al.*, 2004; Setty *et al.*, 2004; Lu *et al.*, 2003; Lu *et al.*, 2001; Yoshino *et al.*, 2003; Lu *et al.*, 2004). This Arl3p/Arl1p GTPase cascade demonstrates the exquisite regulation mechanism involved in localising effectors such as the GRIP domain protein.

1.2.3 Neo1p is functionally connected to Ysl2p and Arl1p

Recently, in the group of B. Singer-Krüger Neo1p was identified as a new binding partner of Ysl2p (Wicky *et al.*, 2004). This 130 kDa large protein belongs to the Drs2-family of P-type ATPases, proposed to function as aminophospholipid translocases (APTs) (Gomes *et al.*, 2000; Pomorski *et al.*, 2003; Tang *et al.*, 1996; Zachowski *et al.*, 1989). APTs couple

ATP hydrolysis to the translocation of primarly phosphatidylserine (PS) and phosphatidylethanolamine (PE) but also other phospholipids to the cytosolic leaflet of biological membranes (Balasubramanian and Schroit, 2003; Natarajan *et al*., 2004). Among the five Drs2-family members present in *S. cerevisiae*, deletion of *DNF1*, *DNF2*, and *DNF3*, either individually or in combination, does not affect growth, and Δ*drs2* cells fail to grow only at 23°C or below (Chen *et al*., 1999; Hua *et al*., 2002). However, the lethality of the quadruple Δ*drs2*Δ*dnf1*Δ*dnf2*Δ*dnf3* mutant indicated that *DRS2* and the *DNF* genes constitute an essential subfamily with functional overlap (Hua *et al*., 2002). On the contrary, the role of Neo1p seems to be unique due to the lethality of the single deletion mutant.

NEO1 has first been identified in a screen for genes that upon overexpression confer the resistance to the aminoglycoside antibiotic neomycin (Prezant *et al*., 1996). The group of B. Singer-Krüger has identified the *NEO1* gene as a high-copy and low-copy suppressor of the growth defect of the Δ*ysl2* mutant (Wicky *et al*., 2004). The major fraction of Neo1p localises to the endosomal compartments, while a smaller part associates with late Golgi membranes. Consistent with a role of Neo1p within the endomembrane system, temperature-sensitive *neo1* mutants exhibited defects in endocytosis, vacuolar protein sorting, and vacuole biogenesis (Wicky *et al*., 2004). Neo1p interacts *in vivo* with Ysl2p and the subcellular localisation and the stability of Ysl2p are affected in the *neo1-69* mutant. Furthermore, the subcellular distribution of Arl1p was also found to be impaired in *neo1-69* cells.

Interestingly, the deletion of *ARL1* suppresses the *neo1-69* growth defect (Wicky *et al*., 2004). The present model explains the strong growth phenotype by a detrimental interaction of Neo1p with Arl1p and interacting partners that are functionally connected. Such assemblies may impair the process of membrane trafficking within the TGN/endosomes (for example by accumulating at endosomal membrane protrusions), thereby causing the growth inhibition in the *neo1-69* mutant at nonpermissive temperatures. Deletion of specific components of the Neo1p-dependent machinery, e.g. Arl1p, would then prevent the accumulation of further downstream effectors and restore the growth in the *neo1-69* mutant.

A higher concentration of aminophospholipids in the cytosolic leaflet is believed to induce the recruitment of specific proteins or help to deform membranes during vesicle budding. Recent publications, which demonstrate that a complex composed of Drs2p, Arf1p and the Sec7 family Arf GEF, Gea2p, is functionally implicated in membrane transformation events (Chen *et al*., 1999; Chantalat *et al*., 2004) and that Neo1p is involved in the Ysl2p-Arl1p network (Wicky *et al*., 2004), provided further evidence for this idea.

1.3 Goal of this project

The goal of this PhD work was to gain new insights into the role of the yeast protein Ysl2p on TGN/endosomes. Due to its sequence homology to Sec7 family members and biochemical and genetic interactions with the Arf-like GTPase Arl1p, Ysl2p was proposed to be a GEF (guanine nucleotide exchange factor) for Arl1p. The putative aminophospholipid translocase Neo1p was identified as a part of the Ysl2-Arl1 network as well. Together these proteins are supposed to regulate vesicular transport on TGN/endosomes. Nevertheless, the precise role of this common network was unclear.

Loss of *YSL2* perturbs severely the morphology of intracellular membranes within the cell. The fragmentation of the vacuole is one of the strongest phenotypes. One of the goals of the work presented here was to analyse the importance of the Ysl2p presence for the vacuole composition and distribution of TGN/endosomal proteins. Since Ysl2p is a very large protein of 186 kDa, its functions may probably be attributed to different subdomains. Due to that, a further aspect of this work was the specification of the importance of the Ysl2p C-terminal subdomains. A search for novel interaction partners of Ysl2p as well as a confirmation of the interaction with Tvp38p was performed to help to define the role of Ysl2p in the vesicular transport. Finally, it was of interest to examine if the Ysl2-Neo1-Arl1 network has a role in vesicle budding. Therefore, the possible implication of clathrin adaptors in this network was analysed.

2 Material and Methods

2.1 Materials

2.1.1 Saccharomyces cerevisiae strains

The *Saccharomyces cerevisiae* strains used in this study are listed below.

Yeast Strain	Genotype	Source
BS64	*MATa his4 ura3 leu2 lys2 bar1-1*	Singer-Krüger *et al.*, 1994
BS695	*MATα his4 ura3 leu2 lys2 ysl2::kan^r bar1-1*	Jochum *et al.*, 2002
BS714	strain Y190 transformed with plasmids pAS1-YPT51 and p67	B. Singer-Krüger
BS727	*MATa/α his4/his4 ura3/ura3 leu2/leu2 lys2/lys2 YSL2/ YSL2::3-HA-kan^r bar1-1/bar1-1*	B. Singer-Krüger
BS747	*MATa/α his4/his4 ura3/ura3 leu2/leu2 lys2/lys2 ysl2::kan^r/ysl2::kan^r bar1-1/bar1-1*	B. Singer-Krüger
BS811	*MATa/α his4/his4 ura3/ura3 leu2/leu2 lys2/lys2 NEO1/neo1::kan^r bar1-1/bar1-1*	Wicky *et al.* 2004
BS862	*MATa his4 ura3 leu2 lys2 neo1::kan^r bar1-1* + pRS315-HA-NEO1	Wicky *et al.* 2004
BS906	*MATα his4 ura3 leu2 lys2 SJL2::TAP-URA3 (K. lactis) bar1-1*	B. Singer-Krüger
BS912	*MATa his4 ura3 leu2 lys2 YSL2::TAP-URA3 (K. lactis) neo1::kan^r bar1-1* + pRS315-HA-NEO1	Wicky *et al.* 2004
BS917	*MATa his4 ura3 leu2 lys2 neo1::kan^r bar1-1* + pRS315-neo1-69	Wicky *et al.*, 2004
BS934	strain Y190 transformed with plasmids pAS1-Sjl2-588 and pYPR171-C1#9	B. Singer-Krüger
BS986	*MATα his4 ura3 leu2 lys2 YSL2::TAP-URA3 (K. lactis) bar1-1*	B. Singer-Krüger
BS1105	*MATa his4 ura3 leu2 lys2 arl1::URA3 bar1-1*	Wicky *et al.*, 2004
BS1121	*MATα his4 ura3 leu2 lys2 YSL2::3-HA-His5 (S.pombe) bar1-1*	Wicky *et al.*, 2004
BS1299	*MATα his4 ura3 leu2 lys2 YKR088c::3-HA-HIS3(S. Pombe) bar1-1*	B. Singer-Krüger
BS1323	*MATa ura3 leu2 lys2 neo1::kan^r arl1::kan^r bar1-1* + pRS315-neo1-69	Wicky *et al.*, 2004
BS1488	*MATa his4 ura3 leu2 lys2 NEO1::3-HA-kan^r bar1-1*	B. Singer-Krüger
BS1519	*MATα ade2 his4 ura3 leu2 lys2 CLC1::3-HA-kan^r bar1-1*	Böttcher *et al.*, 2006
BS1557	*MAT? his4 ura3 leu2 lys2 CLC1::3-HA-kan^r neo1::kan^r bar1-1* + pRS315- neo1-69	B. Singer-Krüger
CB8	*MATa ade2 ura3 leu2 lys2VPS13-HA bar1-1*	Claudia Böttcher
CB223	*MATα his4 ura3 leu2 lys2 vps27 SYS1::13-Myc-kan^r YKR088c::3-HA-kan^r bar1-1*	Claudia Böttcher
CB255	*MATa his4 ura3 leu2 lys2 gga1::kan^r gga2::kan^r bar1-1*	Claudia Böttcher
RH1201	*MATa/α his4/his4 ura3/ura3 leu2/leu2 lys2/lys2 bar1-1/bar1-1*	H. Riezman
Y190	*MATa ura3-52 his3-200 ade2-101 lys2-801 trp1-901 leu2-3,112 gal4Δ gal80Δ cyh^r2*	Steve Elledge, Houston, Tex.
YML35	*MATα his4 ura3 leu2 lys2 ysl2Δ500::TAP-URA3 (K. lactis) neo1::kan^r bar1-1* + pRS315-HA-NEO1	this study
YML97	*MATα his4 ura3 leu2 lys2 ysl2Δ400:TAP-URA3 (K. lactis) bar1-1*	this study

YML101	*MATα his4 ura3 leu2 lys2 ysl2Δ200::TAP-URA3 (K. lactis) bar1-1*	this study
YML102	*MATα his4 ura3 leu2 lys2 ysl2Δ200::TAP-URA3 (K. lactis) bar1-1*	this study
YML103	*MATa his4 ura3 leu2 lys2 ysl2Δ300::TAP-URA3 (K. lactis) bar1-1*	this study
YML107	*MATα his4 ura3 leu2 lys2 ysl2Δ500::TAP-URA3 (K. lactis) bar1-1*	this study
YML109	*MATa his4 ura3 leu2 lys2 ysl2Δ750::TAP-URA3 (K. lactis) bar1-1*	this study
YML110	*MATa his4 ura3 leu2 lys2 ysl2Δ750::TAP-URA3 (K. lactis) bar1-1*	this study
YML113	*MATa his4 ura3 leu2 lys2 ysl2Δ900::TAP-URA3 (K. lactis) bar1-1*	this study
YML121	*MATα his4 ura3 leu2 lys2 ysl2Δ400::TAP-URA3 (K. lactis) bar1-1*	this study
YML138	*MATα his4 ura3 leu2 lys2 ysl2Δ100::TAP-URA3 (K. lactis) bar1-1*	this study
YML164	*MATα ura3 leu2 lys2 ERG6::GFP ysl2::kan^r bar1-1*	this study
YML165	*MATα ura3 leu2 lys2 ERG6::GFP bar1-1*	this study
YML172	*MATα ura3 leu2 lys2 TSA1::GFP ysl2::kan^r bar1-1*	this study
YML173	*MATa ura3 leu2 lys2 TSA1::GFP bar1-1*	this study
YML174	*MATa/α his4/his4 ura3/ura3 leu2/leu2 lys2/lys2 YSL2::TAP-URA3 (K. lactis) / YSL2::3-HA-kan^r bar1-1/bar1-1*	this study
YML221	*MATa his4 ura3 leu2 lys2 Ent4::3-HA-kan^r bar1-1*	this study
YML231	*MATα his4 ura3 leu2 lys2 Ysl1::3-HA-kan^r bar1-1*	this study
YML233	*MATα his4 ura3 leu2 lys2 Ysl1::3-HA-kan^r ysl2::kan^r bar1-1*	this study
YML268	*MATα his4 ura3 leu2 lys2 gga1::kan^r bar1-1*	this study
YML269	*MATα his4 ura3 leu2 lys2 gga2::kan^r bar1-1*	this study
YML271	*MATa/α his4/his4 ura3/ura3 leu2/leu2 lys2/lys2 YSL2::3-HA-His5 (S.pombe) /ysl2Δ100::TAP-URA3 (K. lactis) bar1-1/bar1-1*	this study
YML278	*MATα his4 ura3 leu2 lys2 apl6::kan^r neo1::kan^r bar1-1 + pRS315- neo1-69*	this study
YML281	*MATa his4 ura3 leu2 lys2 gga2::kan^r neo1::kan^r bar1-1 + pRS315- neo1-69*	this study
YML290	*MATα his4 ura3 leu2 lys2 gga1::kan^r neo1::kan^r bar1-1 + pRS315- neo1-69*	this study
YML296	*MATα his4 ura3 leu2 lys2 apl2::kan^r neo1::kan^r bar1-1 + pRS315- neo1-69*	this study
YML303	*MATα his4 ura3 leu2 lys2 GGA2::3-HA-kan^r bar1-1*	this study
YML307	*MATa his4 ura3 leu2 lys2 GGA2::3-HA-kan^r neo1::kan^r bar1-1 + pRS315- neo1-69*	this study
YML318	*MATα his4 ura3 leu2 lys2 gga2::kan^r arl1::URA3 bar1-1*	this study
YML333	*MATa his4 ura3 leu2 lys2 vps27 Gga2::3-HA-kan^r bar1-1*	this study
YML341	*MATα his4 ura3 leu2 lys2 arl3::kan^r neo1::kan^r bar1-1 + pRS315- neo1-69*	this study
YML346	*MATa his4 ura3 leu2 lys2 ARL1::3-HA-HIS3 bar1-1*	this study
YML355	*MATα his4 ura3 leu2 lys2 gga1::kan^r arl1::URA3 bar1-1*	this study
YML360	*MATa his4 ura3 leu2 lys2 GGA2::3-HA-kan^r arl1::URA3 bar1-1*	this study
YML363	*MATα his4 ura3 leu2 lys2 GGA2::3-HA-kan^r ysl2::kan^r bar1-1*	this study
YML371	*MATα his4 ura3 leu2 lys2 ypt51::LYS2 neo1::kan^r bar1-1 + pRS315- neo1-69*	this study
YML376	*MATα his4 ura3 leu2 lys2 ypt7::URA3 neo1::kan^r bar1-1 + pRS315- neo1-69*	this study
YML397	*MATα his4 ura3 leu2 lys2 vps27 Gga2::3-HA-kan^r arl1::URA3 bar1-1*	this study
YML413	*MATα his4 ura3 leu2 lys2 arf1::kan^r neo1::kan^r bar1-1 + pRS315- neo1-69*	this study
YML440	*MATa his4 ura3 leu2 lys2 ysl2Δ100::3-HA-kan^r bar1-1*	this study
YML460	*MATa his4 ura3 leu2 lys2 gga1::kan^r gga2::kan^r arl1::URA3 bar1-1*	this study

2.1.2 *Escherichia coli* strains

The *E. coli* DH5α strain was used for all plasmid amplifications and DNA ligations, the strain *E.coli* BL21 for purification of GST-fusion proteins.

DH5α	F'/endA1 hsdR17(r_k-m_{k+}) supE44 thi- 1 recA1 gyrA (Nal$_r$) relA1 Δ(lacZYA-argF)$_{U169}$ (Φ80lacZΔM15)	Hanahan, 1983
BL21	B, F-, *dcm*, *omp*T, *hsd*S(rB-mB-), *gal*/(DE3) [pLysS Camr]	Novagene, Madinson, WI

2.1.3 Plasmids

The plasmids used in this study are listed below.

Plasmid name	Characteristics	Source
pFA6-kanMX6	contains *kan*^{r}	Wach *et al.*, 1994
pFA6a-3xHA-KanMX6	contains 3xHA *Kan*^{r}	Longtine *et al.*, 1998
pBS1539	Contains *TAP-URA3* (*K.lactis*)	Rigaut *et al.*, 1999
pRS315-HA-NEO1	contains *SpeI/EcoRI* fragment of *3-HA-NEO1*, cloned by *SpeI/SalI*	B. Singer-Krüger
pRS315-neo1-69	carries *neo1-69*, derived from pRS315-NEO1 by PCR mutagenesis	Wicky *et al.*, 2004
pRS426-ARL1	Contains *BamHI/XhoI* fragment of ARL1 including 446 bp 5' of ATG and 136 bp of stop codon	Jochum *et al.*, 2002
pFL-ARF1	ARF1, 2 µm, URA3	Cathy Jackson, Bethesda, Md.
pmycTLG1	*myc-TLG1* in pRS316; *URA3* CEN	J. Holthuis, Utrecht, NL
pHAKex2	*HA-KEX2* in pRS426	B. Singer-Krüger
pGEX-4T-1	Encodes *GST*	
pGEX-Gga2(1-326)	*Sma*I/*Sal*I fragment of Gga2 (encodes amino acids 1-326) in pGEX4-1	This study
pGEX-YPT7		B. Singer-Krüger
yEp24/YSL2	*Nhe*I/*Sal*I fragment of *YSL2* inserted into yEp24	B. Singer-Krüger
pGEX5-Ysl2Nterm	*Bam*HI/*Sal*I fragment of *YSL2* (encodes amino acids 2 to 514) in pGEX5-3	Jochum *et al.*, 2002
pGEX-EPLL	*Sma*I/*Sal*I fragment of *YSL2* (encodes amino acids 1100 to 1636) in pGEX4-1	This study
pGEX-PILT	*Bam*HI/*Sal*I fragment of *YSL2* (encodes amino acids 662 to 1077) in pGEX5-1	This study
pAS1-Ysl2Nterm	*Bam*HI/*Sal*I fragment of *YSL2* (encodes amino acids 2 to 514) in pAS1	This study
pAS1-Ysl2MKLF	*Bam*HI/*Sal*I fragment of *YSL2* (encodes amino acids 529 to 723) in pAS1	This study
pAS1-Ysl2Cterm	*Bam*HI/*Sal*I fragment of *YSL2* (encodes amino acids 505 to 1071) in pAS1	B. Singer-Krüger
pAS1-Ysl2PELD	*Sma*I/*Sal*I fragment of *YSL2* (encodes amino acids 1417 to 1636) in pAS1	This study
pAS1-Sjl2-588	*Bam*HI/*Sal*I fragment of Sjl2 (encodes amino acids 1-588) in pAS1	Wicky *et al.*, 2003
pAS1-Ypt51	*Bam*HI/*Sal*I fragment of *YPT51* in pAS1	B. Singer-Krüger
pACTII-Vps10	Contains parts of *VPS10*	B. Singer-Krüger

pYPR171-C1#9	Contains *BSP1* in modified pGAd424	Wicky *et al.*, 2003
pGBD-C2-Ysl2	Contains *YSL2*	B. Singer-Krüger
pAS1-Ysl2PILT	*BamHI/SalI* fragment of *YSL2* (encodes amino acids 662 to 1077) in pAS1	This study
yPR171 #18	*BSP1* in pSEY8 (*URA3*, 2 µm), isolated from genomic pSEY8 library, includes *EcoRI/Nru* fragment of *YPR171w*	Wicky *et al.*, 2003
pACTII-Ent4	*SmaI/XhoI* fragment of *ENT4* (encodes amino acids 2 to 248, including 212 bp after stop codon	This study
pOAD-YLR154c	contains *RNH203* in pOAD	P. Uetz, Karlsruhe
pOAD-YML011c	contains *RAD33* in pOAD	P. Uetz, Karlsruhe
pOAD-ATR1	contains *ATR1* in pOAD	P. Uetz, Karlsruhe
pOAD-YOL101c	contains *IZH4* in pOAD	P. Uetz, Karlsruhe
pOAD-Bud27	contains *BUD27* in pOAD	P. Uetz, Karlsruhe
pOAD-YMR279c	contains *YMR279c* in pOAD	P. Uetz, Karlsruhe
pOAD-MRS6	contains *MRS6* in pOAD	P. Uetz, Karlsruhe

2.1.4 Antibodies

Antibodies used in this study are listed below with specification of dilutions used for immunoblotting and immunofluorescence.

2.1.4.1 Antibodies used for immunoblotting

Antibodies	dilution	source
Mouse monoclonal purified anti-HA, clone 16B12	1:2000	Covance
Mouse monoclonal anti-c-Myc	1:1000	Oncogene
Rabbit serum or purified anti-Ysl2p	1:500	Jochum *et al.*, 2002
Mouse monoclonal anti-V-ATPase 60 kDa	1:1000	Molecular Probes
Mouse monoclonal anti-V-ATPase 69 kDa	1:1000	Molecular Probes
Mouse monoclonal anti-V-ATPase 100 kDa	1:1000	Molecular Probes
Mouse monoclonal anti-CPY	1:2000	Molecular Probes
Mouse monoclonal anti-ALP	1:1000	Molecular Probes
Mouse monoclonal anti-PGK	1:2000	Molecular Probes
Mouse monoclonal anti-Pep12p	1:500	Molecular Probes
Rabbit polyclonal anti-Tlg2p	1:500	B. Singer-Krüger
Rabbit polyclonal anti-Vps10p	1:1000	B. Singer-Krüger
Rabbit polyclonal anti-Kex2p	1:250	B. Singer-Krüger
Rabbit polyclonal anti-actin (C4)	1:500	Boehringer
Rabbit polyclonal anti-GFP	1:200	Clontech
Rabbit polyclonal anti-Fba1p	1:1000	Ming Lu, UCSF, USA
Goat anti-mouse IgG, alkaline phosphatase conjugated	1:1000	Kirkegaard & Perry laboratories
Goat anti-rabbit IgG, alkaline phosphatase conjugated	1:1000	Kirkegaard & Perry laboratories

2.1.4.2 Antibodies used for indirect immunofluorescence and/or immunoprecipitations

Antibodies	Dilution	Source	Used for
Mouse monoclonal anti-HA, clone 16B12	1:2000	Covance	IF
Rabbit polyclonal anti-c-Myc A-14 (789)	1:300	Santa-Cruz Biotechnologies, Inc.	IF + IP
Cy3-conjugated affinity purified goat anti-mouse Fab fragment	1:1000	Jackson ImmunoResearch	IF
Alexa594-conjugated goat anti-rabbit IgG (H+L) highly cross-adsorbed	1:1000	Molecular Probes	IF

2.1.5 Enzymes and kits used for molecular biology

The QIAprep Spin Miniprep Kit (Qiagen) was used for DNA isolation from *E. coli* cells, the QIAEX II Gel extraction Kit (Qiagen) for DNA extraction from agarose gels, and the QIAquick PCR purification Kit (Qiagen) for PCR fragment purification. Restriction endonucleases used in this study were provided either by Roche or by New England Biolabs (NEB). The *Vent* DNA polymerase (NEB) and the *Taq* DNA polymerase (Roche) were used for DNA amplifications by the polymerase chain reaction (PCR).

2.1.6 Chemicals

Unless otherwise indicated, the chemicals used in this study were provided by the companies Genaxxon, Merck, Roth and Sigma.

2.1.7 Media

Yeast cells were grown either in complete medium (YPD) (1% (w/v) Bacto® yeast extract, 2% (w/v) Bacto® peptone, 2% (w/v) glucose, pH 5.5) or in synthetic growth medium (SD medium) (0.67% (w/v) yeast nitrogen base, 2% (w/v) glucose, pH 5.6) containing 0.3 mM adenine, 0.4 mM tryptophan, 1 mM lysine, 0.3 mM histidine, 1.7 mM leucine and 0.2 mM uracil (final concentration) (complete SD medium). Cells were grown to early logarithmic phase (0.1-0.8 OD_{600} units/ml) at 25°C or 30°C on a rotary shaker, unless otherwise indicated. Yeast transformants carrying a plasmid were grown in SD medium lacking an amino acid depending on the selection marker (e.g. *LEU2* or *URA3*) present on the plasmid. Solid medium contained 2% (w/v) Bacto® Agar in addition to the YPD or SD

medium components. Selective growth of yeast cells carrying a gene deletion marked by the kan^r gene for geneticine resistence was performed by incubation on YPD plates containing 0.2 mg/ml geneticine (G-418 sulfate).

The sporulation of diploid cells was induced by incubation at 25°C on presporulation plates (0.8% (w/v) Bacto® yeast extract, 0.3 % (w/v) Bacto® peptone, 10% (w/v) glucose, 2% (w/v) Bacto® Agar) for 1 day and sporulation plates (1% (w/v) potassium acetate, 0.1% (w/v) Bacto® yeast extract, 0.05% (w/v) glucose, 2% (w/v) Bacto® agar, 0.075 mM adenine, 0.1 mM tryptophan, 0.25 mM lysine, 0.075 mM hisidine, 0.42 mM leucine, 0.05 mM uracil) for 5 to 10 days at 25°C until tetrads were formed.

E. coli cells transformed with plasmids carrying the gene Amp^r for ampicillin resistance as selection marker were grown in LB medium (0.5% (w/v) yeast extract, 1% (w/v) Bacto® trypton, 0.5 % (w/v) NaCl, pH 7.5) containing 100 µg/ml ampicillin.

2.2 Methods

2.2.1 Generation of DNA constructs

All DNA manipulations were performed by standard techniques (Sambrook *et al.*, 1989). Enzymes were used as suggested by the provider. *E. coli* cells were transformed by heat shock or electroporation. All PCR-amplified DNA fragments subcloned in a vector were sequenced (MWG, Martinsried) to exclude the presence of PCR errors.

2.2.1.1 Generation of plasmids

To generate the constructs for the yeast two hybrid screen, DNA fragments containing subdomains of *YSL2* were amplified by PCR using the *Vent* DNA polymerase and as a template *YSL2* in yEp24. The flanking primers (provided by MWG) contained restriction sites for the enzymes as listed below. After isolation and purification, the PCR products were digested and subcloned into the pAS1 vector (bait vector) opened with corresponding enzymes. *ENT4* was amplified from genomic DNA and inserted into the pACTII vector (prey vector) opened with corresponding enzymes (*Sma*I/*Xho*I).

For GST pull down experiments a new pGEX-Gga2$_{(1-326)}$ plasmid was constructed by inserting a PCR fragment encoding amino acids 1-326 of *GGA2* into the bacterial expression vector pGEX-4T-1 (GE Healthcare). To generate the pGEX constructs containing subdomains of *YSL2*, the corresponding pAS1 plasmids were digested by appropriate enzymes and the inserts subcloned into the pGEX-4-1 vector, except for Ysl2N-term where the equivalent

method was used to create pAS1-Ysl2N-term by subcloning from the pGEX-5-3 construct. The PCR amplified regions were analysed by sequencing for the presence of PCR errors (MWG).

Nr.	Primer name	sequence
M10	5'PELD, *Sma*I	5'- ACA ATC CCG GGT CCA GAG CTC GAT AAT TTA -3'
M11	3'realstopYsl2,*Sal*I	5'- GCA AGT CGA CTA GTC TAG TTT CGT AAA TCC -3'
M12	5'PILT, *Bam*HI	5'- CGT AGG ATC CCA CCA ATA CTG ACT AAA TCA -3'
M13	3'PILT, *Sal*I	5'- GCA AGT CGA CTA TGG TTC AAT AAC CTC TAA -3'
M14	5'MKLF, *Bam*HI	5'- CGT AGG ATC CCA ATG AAA TTG TTT TCG ATT -3'
M15	3'MKLF, *Sal*I	5'- GCA AGT CGA CTA AGG ATG ATA GCC AAT GTC -3'
M20	5'Ent4, *Sma*I	5'-ACG ATA CCC GGG GCC TTT GTT AGA TAC CTT CAA G-3'
M21	3'Ent4, *Xho*I	5'- GAT ACT CGA GAT CCA GGA TTA TTC TAG AAC G -3'
M53	5'Gga2(1-326), *Sma*I	5'- ACA ATC CCG GGT ATG TCC CAT CCG CAC TCA -3'
M54	3'Gga2(1-326), *Sal*I	5'- GCA AGT CGA CTA AGC GTT GGA GTC ACC GTT -3'

2.2.1.2 Gene disruptions and epitope tagging of open reading frames

The disruptions of genes were performed by replacement of the complete ORF with the *kan*[r] ORF of *E. coli*. For this, a simple PCR-based strategy was used to amplify the KanMX module from plasmid pFA6-kanMX6 plus flanking regions of the genes to be disrupted (Wach *et al*., 1994). The PCRs were performed with following primers: M36 and M37 for deletion of *APL2*, M38 and M39 for *APL6*, M40 and M41 for *GGA1*, M42 and M43 for *GGA2*. The generated PCR products were approximately 1,500 bp long and were transformed into homozygous diploid strain RH1201, which was subsequently subjected to sporulation and dissection to obtain haploid deletion strains.

For the generation of C-terminal HA-epitope tags the same strategy was used. Specific fragments containing the HA-epitope were generated by PCR using pFA6a-3xHA-KanMX6 as template (Longtine *et al*., 1998) with oligonucleotids described below, and were inserted downstream of and in frame with the chromosomal loci by homologous recombination, which was enabled through overlapping 45 bp regions in primers and the target sequence. The primer M9 and M75 were used for the generation of Ysl2Δ100p-HA, primer M24 and M25 for Ent4p-HA and primer M49 and M50 for Gga2p-HA.

Similarly, the Ysl2ΔX-TAP-specific PCR fragments were generated by amplification from the plasmid pBS1539 with the oligonucleotides described below and were inserted downstream of and in frame with the *YSL2* ORF. For the PCR reaction primer M1-7 were combined with the primer BS570 to generate the appropriate cassette.

All transformants were purified and correct integration was verified by immunoblotting and sometimes by PCR.

The primers were provided by MWG.

Nr.	Primer name	sequence
BS570	3'TAP, Ysl2	5'- CAC ACA ACT ATT TCT ATA AGC ATA TCA TAC ATA CTA CAA TCT TAT GTA TTA CGA CTC ACT ATA GGG -3'
M1	5'TAPYsl2 1537AA	5'- TTG GTT AAT TTT ATG TTG AAC ACA AAC GAG AAA TTA AGA AAG TTA ACT GCT CCT TCC ATG GAA AAG AGA AG -3'
M2	5'TAPYsl2 1417AA	5'- TTT TGT GAT TTA TTT ATA AAT GTT ATT GTT GTC ACA TTA CAA AGA ATC AAC CCA TCC ATG GAA AAG AGA AG -3'
M3	5'TAPYsl2 1309AA	5'- ATA ACA AAA AAA CTT GGA CCA AAG CTT CCA AAA GCA TCA CTT AAC AGG TTA CCA TCC ATG GAA AAG AGA AG -3'
M4	5'TAPYsl2 1206AA	5'- TCG AGC AAA ACT GAA TAC GAT TGT ATA TAC GAA CTA ATA ACC GGA TTT CCT CCT TCC ATG GAA AAG AGA AG -3'
M5	5'TAPYsl2 1107AA	5'- AAT GAA ACT GAT TTT ATA AAT GTA ACA TTG CAA GGA TTA ATT AAG CTT TAT CCG TCC ATG GAA AAG AGA AG -3'
M6	5'TAPYsl2 890AA	5'- GGT GAA CTG TTA ATG AAC TCT TGG ACC AAT ATT TTC AAC ATC ATT AAT TCA CCA TCC ATG GAA AAG AGA AG -3'
M7	5'TAPYsl2 723AA	5'- CTC ACT TTA GAA CAA ACG AAC CTC AAC CTG AAT AAT GAC ATT GGC TAT CAT CCT TCC ATG GAA AAG AGA AG -3'
M9	5' 3XHAKan Ysl2Δ100	5'- TTG GTT AAT TTT ATG TTG AAC ACA AAC GAG AAA TTA AGA AAG TTA ACT GCT CCC GGG TTA ATT AAC ATC -3'
M24	5' 3xHA Kan Ent4	5'- GGA ATA AGC AAG CTC TCA TTT AGA CCC AAG TCT TCA AAT AAC CCG TTC AGA CCC GGG TTA ATT AAC ATC-3'
M25	3' 3xHAKan Ent4	5'- ATC AGG ATA TAT TCT AGA ACG TTC TAG AAA CAA TAC TGA CCA CAA AGA CTT TTC GGT CGA TGA ATT CGA GCT CG-3'
M36	S1 Apl2	5'- GCT TTA TTG TCA TAA TAC ACC AAT TAT CTG GGT ACG AAC TCA CTT CCT GCA GCT TAC GTA CGC TGC AGG TCG AC-3'
M37	S2 Apl2	5'- CGG ACG TTT ATA GTC AGA ATA AAT CGA GGA GAT CCT GTG ACA CTA TAT TGC CGC CCG TCG ATG AAT TCG AGC TCG -3'
M38	S1 Apl6	5'- GAC AGC AAA CAA TCG AAA AGT GGA CAA CCA GCA ATG GTA GAT TCA ATT CAC CGC GTA CGC TGC AGG TCG AC -3'
M39	S2 Apl6	5'- CTC CGA GTT CTA AAG CTC CAG ATG CGA AGA AGA CGT TCC CGA AGA AGA CGT TCC CTC GAT GAA TTC GAG CTC G -3'
M40	S1 Gga1	5'- CTT AAT AAA GAA GCA ATT TGG GAC AAG TCA CTA CTT CAA GTA TAA CCC AGA CAA GAC GTA CGC TGC AGG TCG AC -3'
M41	S2 Gga1	5'- CTG GTT TAG TAT GTT GGC GTA ACA CTC TGT TCT CTG TAA TAT AAT ATG GCA TCT ACT CGA TGA ATT CGA GCT CG -3'
M42	S1 Gga2	5'- GCT GAA TTG CTA ATC GTG ATA CTG CAT CAT GTC CCA TCC GCA CTC ACA TAG CCG TAC GCT GCA GGT CGA C -3'
M43	S2 Gga2	5'- CAT AGA GAA GAG AAA GGA TTG ATA AGA AAC GCC AGA GGA TTA TAC ATT AGG TAA CGT CGA TGA ATT CGA GCT CG -3'
M49	5'3xHAKan Gga2	5'- TTC TGT CAA CTC CAC CCA AGC TGA AGA AAC TGC TGT TTT TAC GTT ACC TAA TGT ACC CGG GTT AAT TAA CAT C -3'
M50	3'3xHAKan Gga2	5'- CCT TTA CAC GAT CTA GCA TTG CTA ACT ACT TTT GAT GCA TGA AAA CGC AAC TCG ATG AAT TCG AGC TCG -3'
M75	3'3xHAKan, Ysl2	5'- CAC ACA ACT ATT TCT ATA AGC ATA TCA TAC ATA CTA CAA TCT TAT GTA TTC GAT GAA TTC GAG CTC G- 3'

2.2.2 Mating, sporulation, transformation of yeast cells and two-hybrid assays

Heterozygous strains were generated by mating of a particular strain of mating type **a** with a particular strain of mating type α on YPD plates. After an overnight incubation at 25°C, the mixture was streaked out at 25°C on YPD or on selective SD plates to obtain single colonies. The biggest colonies were analysed under the light microscope for diploid cells. Colonies of such diploids were streaked out overnight on presporulation plates at 25°C and the material was transferred to sporulation plates (for recipes for all plates see section 2.1.7). After incubation at 25°C for at least 5 days, cells were prepared for tetrad dissection in dissection buffer (1.2 M sorbitol, 50 mM Tris/HCl pH 7.5) containing oxalyticase (4 µl of the 5 mg/ml stock). Tetrads were separated under the light microscope using a needle fo. tetrad dissection (Singer Instruments) coupled to a micromanipulator.

Transformation of cells was performed according to the lithium acetate method (Ito *et al.*, 1983).

The two hybrid method is commonly used to identify novel protein-protein interactions. The system is based on the modular organisation of the transcription factor Gal4. The two genes of interest are inserted into vectors (pAS1 and pACTII) containing the DNA binding or activator domain of Gal4, respectively. The Gal4 DNA binding domains were fused to different subdomains of Ysl2p: pAS1-Ysl2N-term (amino acid 1-505), pAS1-Ysl2C-term (amino acid 505-1071), pAS1-Ysl2PILT (amino acid 662-1077), pAS1-Ysl2MKLF (amino acid 529-723), pAS1-Ysl2EPLL (amino acid 1100-1636) and pAS1-Ysl2PELD (amino acid 1417-1636) (see section 2.2.1.1). The two hybrid screen was performed by P. Uetz group (Karlsruhe), who have the complete *S. cerevisiae* library inserted into the pOAD vector (Uetz *et al.*, 2000), which contains the Gal4 transcriptional activation domain. In the screen performed by the P. Uetz group several positive interaction partners of the Ysl2p-subdomains were identified. The two hybrid analysis was repeated in the present work with the vectors pOAD-YLR154C, pOAD-YML011C, pOAD-ATR1, pOAD-YOL101C, pOAD-Bud27, pOAD-YMR279C, pOAD-MRS6 (provided by P. Uetz group), pACTII-Ent4 was made in the present work (see section 2.2.1.1), vector yPR171 #18 was provided by B. Singer-Krüger (*BSP1* in pSEY8; Wicky *et al.*, 2003) and served as a negative control. The pOAD plasmids (and pACTII-Ent4) were co-expressed with the respective pAS1 plasmid containing the Ysl2p subdomain in the yeast strain Y190 according to the results from the two hybrid screen in the P. Uetz group. The reporter genes (*lacZ* or *HIS3*) which are dependent on the functional Gal4 transcription factor could only be expressed if the two proteins of interest

can interact with each other. The activation of the reporter *lacZ* gene was analysed using the ß-galactosidase colony filter assays (Fields and Song, 1989). The activation of the reporter *HIS3* gene was tested by incubation of the Y190 transformants on selective SD plates lacking leucine, tryptophan and histidine and containing 25 mM 3-amino-1,2,4-triazole (3-AT).

2.2.3 Biochemical methods

2.2.3.1 Generation of cell extracts and quantitative analysis of protein solubility

Total cell extracts were prepared by a lysis method using glass beads as follows. 1 x 10^8 cells were collected, washed in 0.5 ml TE-buffer (50 mM Tris/HCl pH 7.5/ 5 mM EDTA) and resuspended in 100 µl TE-buffer with protease inhibitors (1x CLAP; pepstatin, antipain, leupeptin, chymostatin each 5 µg/ml final concentration). After addition of ~100 µg of glass beads the cells were lysed by vortexing and cooling on ice for 1 min for five rounds and of after addition of 100 µl 2x SDS-PAGE sample buffer (see below) finally boiled for 5 min at 95°C and centrifuged at 13,000 rpm for five minutes.

Alternatively, total cell extracts were prepared by alkaline lysis as follows. One OD_{600} unit of cells grown in YPD at 25°C to early logarithmic phase (0.1-0.3 OD_{600} units/ml) was washed once with ddH_2O and resuspended in 1 ml ddH_2O. 100 µl of 2 N NaOH/ 5% (v/v) ß-mercaptoethanol were added and cells were lysed for 10 min on ice. Proteins were precipitated by the addition of 6% (w/v) trichloracetic acid (TCA) (final concentration) for 30 min on ice. After a 20 min centrifugation at 13,000 rpm, pellets were washed with 1 ml ice-cold acetone. After air-drying at 37°C, pellets were resuspended in 100 µl SDS-PAGE sample buffer (see below). Samples were vortexed for 20 min at 37°C and incubated at 95°C for 5 min and centrifuged at 13,000 rpm for five minutes.

To determine the percentage of membrane-associated Gga2p-HA in wild-type (YML303), Δ*ysl2* (YML364) and Δ*arl1* (YML360) cells the amounts of Gga2p-HA in the pellet and supernatant fractions upon centrifugation at 100,000 x g were compared by immunoblotting. For that the following procedure was applied. 50 OD_{600} cell aliquots of each strain (see section 2.2.3.7) were lysed with glass beads in the presence of protease inhibitors [1x PIC (0.1 µg/ml leupeptin, 0.5 mM phenantroline, 0.5 µg/ml pepstatin, 0.1 mM Pefabloc, each final concentration), 1 mM phenylmethylsulfonylfluoride (PMSF)]. Lysates were immediately precleared at 13,000 rpm for 20 min. The supernatants (880 µl) were re-centrifuged at 100,000 x g for 1 h in a TLA 120.2 rotor (Beckman Instruments). Pellets were

resuspended in 250 µl IP buffer (see section 2.2.3.6) and the protein concentrations of the pellet and supernatant fractions were determined by the Microassay Bradford procedure (Bradford, 1976) using an IgG standard. Each fraction was adjusted with SDS-PAGE sample buffer to 1µg proteins/µl. Determination of the percentage of membrane associated Gga2p was performed by loading several amounts (µg) of the pellet and supernatant fractions on a SDS-polyacrylamid gel. After immunoblotting, the intensity of the Gga2p bands derived from the pellet fractions was compared to that derived from the supernatant fractions. The pellet and supernatant fractions showing the same intensity of the Gga2p-HA bands for a given strain were determined. The values (µg) of the respective fraction were divided by the total protein amounts of the pellet and supernatant fractions, respectively. The two ratios were expressed using a common denominator, allowing the determination of the percentage of total Gga2p present in each fraction (see section 3.5.4; Fig.14).

2.2.3.2. SDS-PAGE, Western- and Immunoblotting

SDS-PAGE (sodium dodecyl sulphate – polyacrylamide gel electrophoresis) is a method used for separation of proteins according to their molecular mass (Laemmli, 1970). In the present work gels were mainly poured using a Mini Protean III equipment and wre 1.5 mm thick. By variation of acrylamide concentration the pore size of the polymerized gele were varied (usually 7-15%) according to the size of the protein to be analysed. Additionally to the acrylamide/bisacrylamide solution (37.5:1) in the desired percentage, the gel solution contains 0.375 M Tris (pH 8.8 for the resolving gel and pH 6.8 for the stacking gel), 0.1% SDS, 0.04% APS and 0.04% TEMED. The addition of APS and TEMED catalyses the polymerisation of acrylamide, therefore these two components are added just prior to pouring of the gel. By pouring a low percentage (~ 4%) stacking gel above the resolving gel, it is ensured that each sample is adjusted to one lane before entering the resolving gel so that the protein separation according to the molecular mass is ensured. For electrophoresis, the polymerised gel was transferred into the Biorad Miniprotean III electrophoresis chamber and overlayed with approximately 300 ml SDS running buffer (25 mM Tris; 190 mM glycine; 0.1 % SDS).

Unless otherwise indicated, proteins were denatured in SDS-PAGE sample buffer (50 mM Tris/HCl pH 6.8, 2.5 mM EDTA/NaOH pH 8, 2 % (w/v) SDS, 5 % (w/v) glycerol, 0.01 % (w/v) bromphenol blue, 2.5 % (v/v) ß-mercaptoethanol) or in SDS-PAGE sample buffer containing 9 M urea for transmembrane proteins. 5-30 µl of samples and 2.5 µl of

protein molecular mass standard (high range or low range molecular weight marker, Biorad) were loaded into the slots and proteins were separated at 23 mA per gel during running in the stacking gel and 37 mM per gel in the resolving gel for 1-2 h. After electrophoresis, proteins were either stained directly in the gel with silver, Coomassie Brilliant Blue or Colloidal coomassie (see section 2.2.3.4) or transferred onto a nitrocellulose membrane by Western blotting (Towbin *et al.*, 1979) and the Mini-Trans-Blot cell system (Bio-Rad Laboratories). A `sandwich` for Western blotting consisting of one layer of Whatman paper (GB002), a sponge, three layers of Whatman paper, a nitrocellulose membrane, the SDS gel and again three layers of Whatman paper, a sponge, and one Whatman paper was positioned into the blotting apparatus (Mini Trans-Blot Cell, BioRad) filled with tank blotting buffer (150 mM glycine, 20 mM Tris, 20 % [v/v] methanol). Proteins were then transferred to the membrane for 4 h at 200 mA on ice. After transferring, the nitrocellulose membrane was stained for 5 min in Ponceau S solution (5 % [v/v] acidic acid; 0.2 % [w/v] Ponceau S) and washed with ddH$_2$O to detect the transfer of the proteins, dried, and stored at room temperature.

Immunoblotting was performed in low fat milk buffer [2.5% (w/v) low fat milk powder, 1x phosphate saline buffer (PBS) (2.7 mM KCl, 137 mM NaCl, 5.6 mM Na$_2$PO$_4$, 1.4 mM NaH$_2$PO$_4$, 1.5 mM KH$_2$PO$_4$), 0.2% (v/v) Tween 20]. Secondary antibodies conjugated to alkaline phosphatase (see section 2.1.4.1) were used. The alkaline phosphatase-catalysed colour reaction was performed in development reaction buffer (0.1 M Tris/HCl pH 9.5, 0.1 M NaCl, 50 mM MgCl$_2$) containing 0.015% (w/v) of BCIP (5-bromo-4- chloro- 3- indolyl- phosphate) and 0.03% (w/v) of NBT (nitroblue tetrazolium) (Bio-Rad Laboratories).

2.2.3.3 Two dimensional gel electrophoresis

Two-dimensional gel electrophoresis is the combination of two high-resolution electrophoretic procedures (isoelectric focusing and SDS-PAGE) to optimize the resolution compared to either procedure alone. In the first-dimension gel, solubilised proteins are separated according to their isoelectric point (pI) by isoelectric focusing. This gel is then applied to the top of an SDS-slab gel and submitted to PAGE. The proteins in the first dimension migrate into the second-dimension gel where they are separated on the basis of their molecular weight.

The two-dimensional gel electrophoresis was performed according to manufacturers instructions (GE Healthcare; http://www5.gelifesciences.com/aptrix/upp01077.nsf/Content/ 2d_electrophoresis). Before starting the isoelectrical focusing the commercially available Immobiline DryStrip gel strips (GE Healthcare; 7cm, pH 3-10) were rehydrated over night in

reswelling trays in 125 µl of rehydratation solution (8 M urea, 2 % (w/v) CHAPS, 0.0025 % (w/v) Bromphenol blue, 1x IPG buffer pH 3-10 (GE Healthcare), and 20 mM DTT) covered with IEF Cover Fluid (GE Healthcare). 50 µg (for qualitative analysis) or 125 µg (for mass spectrometry) of isolated vacuoles (see 2.2.3.9) were precipitated in the presence of 6 % (w/v) TCA and 0.015 % (w/v) desoxycholic acid and the dried pellet was resuspended in 100 µl rehydration buffer. After positioning the rehydrated strips in the Multiphor II apparatus (GE Healthcare) according to manufacturer instructions and covering them with the IEF Cover Fluid, the samples were loaded onto the strips with the help of sample holders positioned next to the anode and the focusing was performed at 0.2 kV for 1 min, 0.5 kV for 5 min, 1 kV for 30 min and 2 kV for 4.5 h. After isoelectrical focusing the strips were shortly washed with water and then incubated two times for 15 min in equilibration buffer (2 % (w/v) SDS, 50 mM Tris pH 8.8, 6 mM urea, 30 % (w/w) glycerol, 0.002 % (w/v) bromphenol blue). The first equlibration was performed in presence of 1% DTT (w/v) and the second in the presence of 2.5 % (w/v) iodoacetamid. After the final washing, the strips were positioned onto the second dimension, which corresponds to the classical SDS-PAGE (preferentially 12 % SDS-gel), sealed with melted agarose sealing solution (0.5 % (w/v) agarose, 0.004 % (w/v) bromphenol blue in the SDS running buffer) and separated according to the molecular weight. Depending on the direct purpose of the analysis the gels were stained either with silver (qualitative analysis) or with colloidal Coomassie (mass spectrometry) (see section 2.2.3.4).

2.2.3.4 Staining methods

Silver staining. After SDS-PAGE the gels were fixed for 30 min in 40 % (v/v) ethanol / 10 % (v/v) acetic acid, then incubated in sensitizing solution for further 30 min (30 % (w/v) ethanol / 0.125 % (w/v) glutardialdehyde / 0.2 % (w/v) sodium thiosulfate / 6.8 % (w/v) sodium acetate) and washed three times for five minutes in ddH$_2$O. The silver reaction lasted 20 min in 0.25 % (w/v) silver nitrate / 0.015 % (w/v) formaldehyde. After two short washes in distilled water the separated proteins were detected with the developing solution (2.5 % (w/v) sodium carbonate / 0.008 % (w/v) formaldehyde). The detection lasted between 5 and 15 minutes depending on the quantity of the proteins and had to be stopped after reaching the desired intensity of staining by incubation in a solution containing 1.5 % (w/v) Na-EDTA for 10 min. After washing in water for 3 x 5 min, the gels were prepared for drying by incubation in 30 % (v/v) ethanol / 4 % (w/v) glycerol for 2 x 30 min and dried at room temperature for 3-4 h.

Colloidal Coomassie staining. The Colloidal Coomassie staining is very time-consuming (5 days) but is almost as sensitive as silver staining and in contrast to silver it does not disturb the following mass spectroscopical analysis. After the SDS-PAGE the gel was fixed for 16 h in 50 % (v/v) methanol / 2 % (v/v) phosphoric acid, washed afterwards 3x 30 min in water and preincubated for 1 h in 34 % (v/v) methanol / 2 % (v/v) phosphoric acid / 17 % (w/v) ammoniumsulfate prior to the final staining in 34 % (v/v) methanol / 2 % (v/v) phosphoric acid / 17 % (w/v)ammoniumsulfate / 0.066 % (w/v) Coomassie G-250 for five days at 4°C.

Coomassie staining. Coomassie staining was used for qualitative analysis after purification of GST-fusion proteins and after GST-pull down assays. After SDS-PAGE the gel was stained for at least 1 h in 0.25 % (w/v) Coomassie Brilliant Blue R250/ 7.5 % (v/v) acetic acid/ 50 % (v/v) methanol and destained in 45 % (v/v) methanol/ 1 % (v/v) acetic acid until the background staining was washed out. The gels were then prepared for drying by incubation in 30 % (v/v) ethanol / 4 % (w/w) glycerol for 2x 30 min and dried at 60°C for 2 h.

2.2.3.5 Expression and purification of GST fusion proteins in *E. coli*

For the expression of GST fusion proteins the protease deficient *E. coli* strain BL21 (Novagene, Madinson, WI) was used. The desired plasmids were transformed using heat shock method. One positive clone was transferred in 100 ml LB$_{amp}$ media and grown over night at 37°C. In the morning, the 1 l culture was diluted 1:50 (20 ml for 1 l) and grown at 30°C. When the culture reached the density of 0.5 OD$_{600}$/ml, expression of the GST fusion proteins was induced by the addition of 0.5 mM IPTG. After further 3.5 h of incubation at 30°C cells were harvested at 4,000 x g for 10 min at room temperature and frozen at -20°C. The frozen pellet was thawed and resuspended in 30 ml ice-cold 1 x phosphate saline (PBS)/EDTA buffer containing 1 mM PMSF. The resuspended cells were transferred to a 30 ml Corex tube and lysed by sonification (Supersonic Sonificator *Sonic Power*) for three times 8-9 sec each (level 4) on ice. The cell lysate was cleared at 12,000 rpm at 4°C for 30 min (Sorval, SS-34 rotor). The supernatant was transferred to ultracentrifuge tubes and further cleared at 100,000 x g for 1 h at 4°C. To isolate the GST-fusion proteins the resulting supernatant was added to 600 µl glutathione Sepharose beads and incubated for 1 h at 4°C while overhead shaking. Glutathione Sepharose beads were spun down at 500 x g for 5 min and washed twice with 40 ml ice-cold 1 x PBS/ 5 mM EDTA, transferred to a 15 ml Falcon tube and washed twice with 14 ml ice-cold 1 x PBS/ 5 mM EDTA. Bound proteins were eluted by three consecutive treatments with 250 µl of glutathione buffer (20 mM reduced

glutathione, 100 mM Tris/HCl pH 8.0). The three eluates were dialysed in separate hoses at 4°C in 2 l of dialysis buffer (10 mM HEPES/NaOH pH 7.8, 1 mM MgCl$_2$, 1 mM DTT, 0.2 mM PMSF) with slow stirring. After 2 h the samples were transferred to fresh dialysis buffer and dialysed over night. Next day, the samples were centrifuged for 1 min at 13,000 rpm at 4°C to remove precipitates. The supernatants were frozen in liquid nitrogen in aliquots of 80 µg protein and stored at -80°C.

2.2.3.6 Affinity chromatography with glutathione S-transferase fusion proteins

Glutathione S-transferase (GST) or GST-fusion proteins were expressed in the *E. coli* strain BL21 (Novagene, Madinson, WI) and were affinity purified using glutathione Sepharose beads as described in section 2.2.3.5. To prepare the yeast protein extract, a total of 1.75-2 x 10^{10} cells were harvested at 4,000 x g for 10 min at room temperature, resuspended in 50 ml of 10 mM Tris/HCl (pH 7.5), 0.8 M sorbitol, 1 mM DTT, 0.5 mM PMSF, and converted into spheroblasts by incubation for 1h at 30°C upon addition of 0.5 mg zymolyase 100T. Spheroblasts were collected at 4°C and 1,500 rpm for 15 min and lysed by Dounce homogenisation in 7 ml ice-cold lysis buffer by 15 strokes (20 mM HEPES/KOH [pH 7.2], 0.1 M KCl, 2 mM MgCl$_2$, 0.2 M sorbitol, 0.6% (w/v) Triton X-100 [0.01% NP-40 for BS1488 (HA-Neo1p)], 1 mM DTT) containing protease inhibitors (0.5 mM PMSF, CLAP [each 5 µg/ml]). The lysate was centrifuged at 22,000 x g for 30 min and one millilitre of the supernatant was incubated with 40 µl bed volume of glutathione-Sepharose 4B preloaded with 80 µg of GST or GST-fusion proteins at 4°C for 1 h. After washing the beads four times (200 x g, 2 min) with lysis buffer, bound proteins were eluted by three consecutive incubations with 250 µl of 20 mM reduced glutathione (100 mM Tris/HCl [pH 9.0], 0.2 M NaCl, 5 mM DTT, 0.1 % TritonX-100 [0.005% NP-40 for BS1488]). Proteins were TCA precipitated from the pooled eluates and the resulting precipitates resuspended in 80 µl 1x SDS sample buffer, vortexed for 20 min at 37°C, and boiled at 95°C for 5 min or 10 min at 50°C for detection of HA-Neo1p. Samples were analysed by SDS-PAGE with subsequent Coomassie Brilliant Blue staining (15 µl sample) or immunoblotting with anti-HA antibody (30 µl sample) for detection of GST-fusions or HA-tagged proteins, respectively.

2.2.3.7 Co-immunoprecipitation experiments

50 OD_{600} aliquots of cells used for co-immunoprecipitation experiments were prepared in advance and stored at -80°C. For that, cells grown at 30°C in 1.6 l of YPD to density of 0.8 OD_{600} units/ml were harvested by centrifugation for 5 min at 4,000 rpm. Cell pellets were washed twice with 200 ml ddH$_2$O and once with 50 ml cold IP buffer (115 mM KCl, 5 mM NaCl, 2 mM MgCl$_2$, 1 mM EDTA/NaOH pH 8, 20 mM HEPES/KOH pH 7.8). Cells were resuspended in IP buffer to a concentration of 166 OD_{600} units/ ml of cell suspension. Aliquots containing 300 µl (50 OD_{600}) of cell suspension were frozen in liquid nitrogen and stored at -80°C for subsequent immunoprecipitations.

The procedure used to purify Ysl2p-TAP assemblies was based on the tandem affinity purification (TAP) method described by Rigaut *et al*. (1999). The aliquoted cells were lysed with glass beads (~200 mg) in the presence of protease inhibitors (1x CLAP) by vortexing for 45 sec and cooling on ice for one min for ten rounds. Cell lysates were transferred to fresh precooled Eppendorf tubes and glass beads were washed with 800 µl IP buffer. DTT was added to 1 mM (final concentration) and proteins were extracted in the presence of 0.01 % (for detection of Ysl2p-Neo1p interaction; strains YML35, BS912, BS862) or 0.8 % (w/v) (for Ysl2p-Ysl2p interaction; strains YML174, YML178, YML271) NP-40 (final concentration) for 20 min on ice. After 20 min centrifugation at 13,000 rpm, 60 µl of a 1:3 slurry of IgG-sepharose beads (GE Healthcare) were added to the supernatants and the affinity purification of Ysl2p-TAP assemblies was performed for 2 h at 4°C on an overhead shaker. The IgG-sepharose beads were washed twice with 500 µl IP buffer (containing desired NP-40 concentration) and twice with 500 µl TEV cleavage buffer (10 mM Tris/HCl pH 8, 150 mM NaCl, 0.5 mM EDTA/NaOH pH 8, 1 mM DTT, 0.01 or 0.8 % (w/v) NP-40). Bound proteins were eluted in 100 µl TEV cleavage buffer containing 5 µl of TEV protease for 2 h at 15ºC. The eluates were transferred to a fresh tube and the IgG-sepharose beads were washed twice with 400 µl TEV cleavage buffer. The proteins present in the complete eluates were precipitated in the presence of 6 % (w/v) TCA, 0.015 % (w/v) desoxycholic acid and 5 µg of IgG and were resuspended in 65 µl SDS-PAGE sample buffer either containing 9 M urea (for detection of Neo1p-HA) or without (for detection of Ysl2p-HA). Subsequently, samples were vortexed for 20 min at 37°C and incubated at 50°C for 10 min (for samples in urea buffer) or 95°C for 5 min (for samples in SDS-sample buffer). 20-30 µl (for detection of Ysl2p-TAP) and 5-10 µl (for detection of Ysl2p- or Neo1p-HA) of samples were separated by SDS-PAGE. Proteins were detected by immunoblotting using rabbit anti-Ysl2p (Jochum *et al*., 2002) and mouse anti-HA (16B12, Covance) as primary antibodies.

For the detection of the Sys1-Tvp38 interaction (strains BS1299, CB223) the aliquoted cells were lysed with glass beads (~200 mg) in the presence of protease inhibitors (1x CLAP) and the Sys1-Myc assemblies extracted in the presence of 0.01% NP-40. To exclude the possibility that after treatment with only 0.01% NP-40 the interaction between Sys1p-Myc and Tvp38p-HA is enabled solely by membranes, the supernatants obtained after centrifugation of cell extracts for 20 min at 13,000 rpm were recentrifuged at 100,000 x g for 1 h at 4°C (TLA 120.2 rotor; Beckman Instruments). The 100,000 x g supernatants of three aliquots were unified and incubated for 1 h with 15 µl rabbit anti-Myc antibody and for one additional hour with 100 µl rehydrated protein A-Sepharose. Proteins were eluted by heating for 10 min at 50°C in 60 µl SDS-PAGE sample buffer containing 9 M urea. Finally, 20 µl (for detection of Tvp38p-HA) and 10 µl (for detection of Sys1p-Myc) of the eluates were analysed by SDS-PAGE and immunoblotting with anti-HA and anti–Myc antibodies.

2.2.3.8 Large scale co-immunoprecipitation by Ysl2p-TAP

Cells (strains BS986 and BS906) grown to 0.8-1 OD_{600} units/ml in 2 l of YPD at 30°C were harvested by centrifugation for 5 min at 4,000 rpm. Alternatively to the 2 l flask culture, cells were also grown in 20 l batch fermenter. For that, 20 l of YPD were inoculated with 2 l of preculture and cells were grown for 7 h at 30°C until the early stationary phase (25 OD_{600}/ml). The pH was held constant at 5.5, initial concentration of glucose was 2 %. For both methods, pelleted cells were washed twice with ice cold ddH_2O and once with IP buffer (115 mM KCl, 5 mM NaCl, 2 mM $MgCl_2$, 1 mM EDTA, 20 mM HEPES pH 7.8). Finally, cells were resuspended in IP buffer (2 ml buffer/ 1 g cells) and squeezed into liquid nitrogen forming small uniform drops. The cell clumps were stored at –80°C.

The lysis method used in this approach is considered to preserve the protein-protein interactions more efficiently than e.g. glass beads lysis (Kellogg and Moazed, 2002). The cells (~ 5 g aliquoted cell pellets, corresponds to ~ 1.66 g wet weight of cells) were lysed by grinding at high speed for 20 min with a mortar and pestle under liquid nitrogen to obtain a fine powder with the consistency of flour. Before adding additional IP buffer the powder thawed for 5-10 min to avoid formation of ice crystals. The powder was resuspended in 4/3 volume of cold IP buffer (with 0.2 % NP-40, 1 mM DTT and 1 mM PMSF) and the proteins extracted for 20 min while stirring at 4°C. After centrifugation at 4,500 x g for 15 min the exact protein concentration in the extract was estimated by a Bradford test (Bradford, 1976) to compare the lysis efficiency of experimental repetitions. 25 µl bed volume of IgG Sepharose

beads (GE Healthcare) were added to the supernatant and the affinity purification of Ysl2p-TAP assemblies was performed for 2 h at 4°C on an overhead shaker. The IgG Sepharose beads were washed twice with 15 ml IP-buffer (containing 0.2 % NP-40, 1 mM DTT) and twice with 15 ml TEV cleavage buffer (10 mM Tris/HCl pH 8.0, 150 mM NaCl, 0.5 mM EDTA, 1 mM DTT, 0.2 % NP-40). Then the beads were transferred into a 1.5 ml tube and the bound proteins were eluted in 1 ml TEV cleavage buffer (+ 1 mM PMSF) containing 1.5 µl TEV protease for 2 h at 15°C. After the eluates were transferred to a fresh tube 6 ml (3 volumes) of calmodulin binding buffer (10 mM ß-mercaptoethanol, 10 mM Tris/HCl pH 8.0, 150 mM KCl, 1 mM Mg-acetate, 1 mM imidazole, 2 mM $CaCl_2$, 0.2 % NP-40) (+ 8 mM $CaCl_2$ for titration of the EDTA from the TEV cleavage buffer) and 25 µl calmodulin affinity resin were added to it. After incubation for 2 h at 4°C the calmodulin affinity resin was washed three times with 10 ml calmodulin binding buffer and the proteins were eluted from the resin with 3x 1 ml calmodulin elution buffer (10 mM ß-mercaptoethanol, 10 mM Tris/HCl pH 8.0, 1 M KCl, 1 mM Mg-acetate, 1 mM imidazole, 20 mM EGTA, 0.2 % NP-40) for 15 min each. The proteins of united eluates were precipitated in the presence of 6% (w/v) TCA, 0.015 % (w/v) desoxycholic acid and 5 µg of IgG. The pellet was resuspended in 50 µl SDS-PAGE sample buffer, vortexed for 20 min at 37°C and incubated at 95°C for 5 min. 20 µl of samples were separated by SDS-PAGE and the isolated proteins detected by silver staining.

2.2.3.9 Subcellular fractionation of cells on a sucrose gradient for separation of early endosomes from late endosomes and TGN

Fractionation procedure followed published methods (Sipos and Fuller, 2002). Cells (strains YML231 and YML233) grown at 25°C to a density of 1.5-2 OD_{600}/ml were harvested by centrifugation for 8 min at 5,000 x g in the presence of 20 mM NaF and 20 mM NaN_3. After washing with 300 ml ddH_2O the cells were resuspended in pre-treatment buffer (150 mM Tris/HCl pH 9.4, 40 mM ß-mercaptoethanol, 10 mM NaN_3, 10 mM NaF) to the density of 50 OD_{600} equivalents/ml and incubated for 10 min at room temperature. After centrifugation for 5 min at 4,000 rpm the pelleted cells were resuspended to 50 OD_{600} equivalents/ml in spheroblasting buffer (50 mM HEPES/KOH pH 6.8, 10 mM NaN_3, 10 mM NaF, 1.2 M sorbitol) and spheroplasted with 0.8 mg oxalyticase/ml culture (Enzogenetics, Corvallis, OR) for ~35 min at 30°C (the efficiency of spheroblast formation was tested by the decrease of turbidity, due to the lysis of spheroplasts, after aliquots of the cell/spheroblast suspension were diluted 50-fold with ddH_2O). Spheroplasts were collected at ≥ 90%

spheroblasting efficiency by centrifugation at room temperature at 2,500 g for 5 min. The pellet was resuspended at 250 OD_{600} equivalents/ml in ice-cold storage buffer (25 mM HEPES/KOH pH 6.8, 50 mM KOAc, 0.5 M sorbitol) and frozen as 200 µl aliquots over N_2 vapour (10 cm distance) for 35-40 min. Samples can be stored safely at –80°C for at least 2 months. Tubes were thawed by immersion in a 25°C water bath with shaking and then placed on ice.

After thawing the aliquoted spheroblasts were mixed with 400 µl of lysis buffer [25 mM HEPES/KOH pH 6.8, 50 mM KOAc, 0.2 M sorbitol, 1 mM PMSF, 1x CLAP (pepstatin, antipain, leupeptin, chymostatin, each 5 µg/ml final concentration)] resulting in a sorbitol concentration of 0.3 M. After homogenisation of four unified aliquots with 20 strokes in a ground-glass homogenizer (5 ml, Wheaton, Millville, NJ) the sorbitol concentration was adjusted to 0.7 M by adding 560 µl of 2.4 M sorbitol and the lysate was precleared by two centrifugations at 500 x g for 5 min. The precleared lysate was centrifuged for 15 min at 15,000 x g at 4°C, and the resulting supernatant for 30 min at 200,000 x g and 4°C to generate the high speed pellet (HSP). The HSP membranes were resuspended in 500 µl membrane buffer (25 mM HEPES/KOH pH 6.8, 50 mM KOAc, 0.7 M sorbitol, 1 mM PMSF, 1x CLAP) prior to fractionation on a sucrose gradient.

0.5 ml of resuspended HSP membranes, equivalent to 200 ml of cells (OD_{600}=1), were loaded on the top of the following sucrose gradient (from the bottom): 0.5 ml of 60 % / 2 ml of 48 % / 2.5 ml of 40 % / 2.5 ml of 36 % / 2.5 ml of 32 % / 2 ml of 29 % [all the dilutions for the sucrose gradient were made from a 60 % (w/w) stock and diluted with 20 mM HEPES/NaOH, pH 6.8]. The gradient was centrifuged at 41,000 rpm for 18 h at 4°C (Beckman Coulter SW41 rotor). 890 µl fractions were collected and precipitated in the presence of 6 % (w/v) TCA, 0.015 % (w/v) desoxycholic acid and 5 g of IgG. After resuspending in 150 µl SDS-PAGE sample buffer, the fractions were vortexed for 20 min at 37°C and incubated at 95°C for 5 min. 30 µl of samples were separated by SDS-PAGE and the separated proteins were detected by immunobloting with antibody dilutions as described in 2.1.4.1.

2.2.3.10 Subcellular fractionation of cells on a Ficoll gradient for isolation of vacuoles

The procedure to isolate vacuoles from yeast cells was based on the method described by Haas (1995). Cells used for vacuolar isolation were grown in 1.2 l of YPD to 0.6-0.8 OD/ml at 25°C (Δ*ysl2* strains: BS747, YML164, YML172) or 30°C (wild type strains:

RH1201, YML165, YML173). The strains BS747 and RH1201 were used for 2-dimensional electrophoresis (see section 2.2.3.3), the strains YML164, YML165 and YML172 and YML173 for analysis of the cellular levels of Erg6p-GFP and Tsa1p-GFP in wild type and $\Delta ysl2$ cells. After centrifugation for 5 min at 4,000 rpm the pellet was resuspended in 50 ml 100 mM PIPES/10 mM DTT pH 9.4 followed by incubation in a water bath for 10 min at 30°C with constant shaking (80 rpm). Cells were harvested for 5 min at 5,000 rpm and 4°C and subsequently resuspended in 15 ml spheroblasting buffer (600 mM sorbitol, 500 mM KPO_4, 0.16 X YPD) and spheroblasted for 25 min at 30°C and 80 rpm in a water bath by addition of 0.8 mg oxalyticase / 1,000 OD_{600} cells. After gradual centrifugation at 2,500 rpm for one minute and 3,500 rpm for one further minute and removal of the complete supernatant, the pellet was resuspended carefully in 15 % (w/v) Ficoll solution (15 % (w/v) Ficoll, 10 mM PIPES, 200 mM sorbitol, pH 6.8). After addition of 100 µl of 0.04 % (w/v) dextran in 15 % (w/v) Ficoll solution, the spheroblasts were shaken gently immediately and incubated first for one minute on ice then for 1'30" in 30°C water bath, then again on ice. The lysate was transferred into centrifuge tubes and a density gradient was created by carefully layering 3 ml 8% (w/v), 3,5 ml 4% (w/v) and 700 µl 0% (w/v) Ficoll solution (each in 10 mM PIPES, 200 mM sorbitol, pH 6.8) over it. After ultracentrifugation at 30,000 rpm for 90 min at 4°C (rotor SW41Ti, Contron) the vacuoles accumulate in the 4% / 0% (w/v) Ficoll interphase. The vacuoles should be collected without removing the 0% Ficoll phase. Each gradient tube yielded approximately 600 µl vacuole solution with a protein concentration of 0.25 to 0.9 mg/ml protein. The aliquoted vacuoles were shock frozen in liquid N_2 and stored at -80°C. For qualitative analysis of the vacuolar composition, the two-dimensional gel electrophoresis approach was used (section 2.2.3.3).

2.2.3.11 Fluorescence microscopy

Prior to indirect immunofluorescence, cells were grown overnight at 25°C in YPD medium or in selective SD medium to early logarithmic phase (0.1-0.3 OD_{600} units/ml). Four OD_{600} units of cells were fixed for 4 h at room temperature with gentle shaking (100 rpm) in growth medium containing additionally 100 mM potassium phosphate buffer (KPi, pH 6.5) and 4 % formaldehyde (final concentration, respectively). Upon harvest (5 min, 2,000 rpm), cells were washed three times with 1 ml sorbitol buffer (1.2 M sorbitol, 100 mM KPi pH 6.5). Spheroblasting of the cells was performed for 30 min at 30°C in 1 ml sorbitol buffer containing 20 mM ß-mercaptoethanol and 20 µg/ml Zymolyase 100T (final concentration; Seigagaku Kyogo, Japan). Collected spheroblasts were washed twice with 1 ml sorbitol buffer

(5 min, 1,000 rpm), resuspended in 400 µl sorbitol buffer and stored at 4°C for up to two days. The fixed cells were labelled on 10-well immunofluorescence microscope slides (Polysciences, Inc.). Slides were prepared by placing 15 µl of poly-L-lysine solution (1 mg/ml in 10 mM NaN_3, stored at 4°C) in each well. After 1 min of incubation, the solution was aspirated and slides were allowed to dry. Each well was washed five times with 20 µl ddH_2O. Fixed cells (15 µl/well) were applied to the dried wells and allowed to settle for 15 min. The unbound cells were removed by washing three times with 20 µl PBS (53 mM Na_2HPO_4, 13 mM NaH_2PO_4, 75 mM NaCl). Subsequently, cells were preincubated for 30 min in PBT (PBS, 1% (w/v) BSA, 0.1% (w/v) Tween 20) to reduce the unspecific binding of antibodies. PBT was aspirated and 15µl of primary antibody (diluted in PBT and centrifuged for 2 min at 13,000 rpm before use to pellet possible antibodies aggregates) were applied. After 1 h incubation in a humid chamber, each well was washed ten times with PBT. The secondary antibody diluted in PBT and centrifuged as described before was applied (15 µl/well) and incubated in the dark as described for first antibody. After washing each well with PBT and PBS (six times each), cells were covered with one drop of 99% glycerine for immunofluorescence (Fluka). Coverslips were sealed to the slides using nail polish and stored at 4°C in the dark for several days.

The mouse monoclonal anti-HA (16B12, Covance; used for detection of Gga2p-HA and Clc1p-HA) and rabbit polyclonal anti–Myc (Santa-Cruz Biotechnologies, Inc; used for detection of Tlg1p-Myc) were used as primary antibodies (diluted to 1:1,000 and 1:100, respectively), and the indocarbocyanine (Cy3)-conjugated goat anti-mouse Fab fragment (Jackson ImmunoResearch) and Alexa594-conjugated goat anti-rabbit IgG (Molecular Probes) as secondary antibodies (diluted to 1:1,000) (see section 2.1.4.2).

To observe localisation of GFP-tagged Erg6p by direct fluorescence, cells were grown at 25°C to early logarithmic phase (0.1-0.2 OD_{600} units/ml) in complete SD medium. The GFP-tagged proteins were viewed in the fluorescence microscope on cover slips using the appropriate filter for GFP.

3 Results

3.1 Effect of YSL2 deletion on the vacuolar composition

Ysl2p/Mon2p was previously identified and characterised in the group of B. Singer-Krüger as an important regulator of the vesicle transport on yeast TGN/endosomes (Singer-Krüger *et al.*, 1993; Jochum *et al.,* 2002; see section 1.2.1). Deletion of *YSL2* has severe effects on the cell phenotype, e.g. strong growth inhibition and fragmentation of the vacuole. The analysis of the vacuolar protein composition for wild type and Δ*ysl2* cells with one-dimensional SDS-PAGE in the group of B. Singer-Krüger revealed differences in the protein pattern of the silver-stained gel (unpublished data). On the one hand, quantities of several proteins were reduced in Δ*ysl2* vacuoles compared with wild type, what indicated that some vacuolar proteins (e.g. components of the homotypic vacuole fusion) may be missorted away from the vacuole or falsely degraded. On the other hand, novel bands in Δ*ysl2* vacuoles indicated that some proteins, which may play an important role elsewhere in the cell (e.g. on TGN/endosomes), are missorted to the vacuole. Identification of these proteins, whose vacuolar levels are either falsely increased or reduced in Δ*ysl2* vacuoles, could help to further specify the role of Ysl2p in the sorting on TGN/endosomes. Therefore, in the present study, a two-dimensional (2-D) gel electrophoresis was used to separate the vacuolar proteins first according to their isoelectric point (pI) and subsequently according to their molecular weight. Vacuoles of wild type (RH1201) and Δ*ysl2* (BS747) cells were isolated by differential centrifugation in a 0-15% Ficoll gradient and subsequently subjected to 2-D gel electrophoresis (see section 2.2.3.9. and 2.2.3.3, respectively). Experiments with IEF stripes of different pH range confirmed that the isoelectric focussing (IEF) was optimal when performed with IEF-stripes with pH 3-10, since the composition of proteins with marginal isoelectric points did not differ between wild type and Δ*ysl2* vacuoles (data not shown). The second dimension was performed on 12% SDS-gels due to their improved resolution compared to low percentage SDS-gels (7 -10%).

For the qualitative analysis, gels were stained according to the silver staining protocol, while for the final analysis the gels were stained according to a colloidal Coomassie procedure (see section 2.2.3.4) and protein spots, which were identified as specific for either the wild type or Δ*ysl2* vacuoles were cut out and sent for mass spectroscopic analysis (by the group of Dr. A. Sickmann, Würzburg). The mass spectroscopic results revealed that the heat shock proteins of the Hsp70 family, Ssb1p and Ssb2p (Fig. 5; arrow 4+5 respectively) and the fructose-bisphosphate aldolase II, Fba1p (Fig. 5; arrow 6), were less abundant in Δ*ysl2*

vacuoles. On the other hand, Erg6p (Fig. 5; arrow 1+2), which plays a role in the ergosterol biosynthesis pathway by catalysing the conversion of zymosterol to fecosterol, and the thioredoxin peroxidase, Tsa1p (Fig. 5; arrow 3) were more abundant in Δ*ysl2* vacuoles. It is not clear why Erg6p appears as a double spot, since according to the predictions (SGD) it is supposed to have a single isoelectric point.
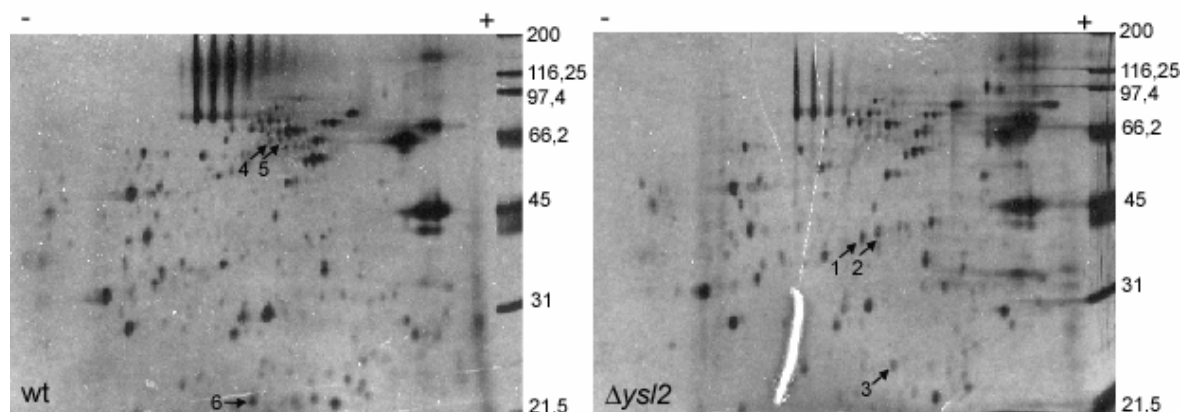

Fig. 5: Protein composition of isolated vacuoles from wild type and Δ*ysl2* cells resolved by two-dimensional gel electrophoresis. Vacuoles from wt (RH1201) and Δ*ysl2* cells (BS747) were isolated by centrifugation in a Ficoll gradient as described in 2.2.3.9. Aliquots of approximately 50 µg (for qualitative analysis) or 125 µg (for mass spectroscopic analysis) of purified vacuoles were trichloroacetic acid-precipitated and subjected to two dimensional gel electrophoresis as described in 2.2.3.3 (first dimension with 7 cm IEF stripes pH 3-10, second by 12% SDS-PAGE) and finally stained according to the silver stain (for qualitative analysis) or colloidal Coomassie procedure (for mass spectroscopic analysis). The arrows indicate the isolated proteins sent for mass spectrometry: 1) + 2) Erg6p; 3) Tsa1p; 4) Ssb1p; 5) Ssb2p; 6) Fba1p.

The total vacuolar levels of the identified proteins were analysed by immunoblotting to validate the results obtained by mass spectroscopy. The immunoblot analysis of vacuoles isolated from wild type and Δ*ysl2* strains, containing Erg6p C-terminally tagged with GFP, demonstrated increased Erg6p levels in vacuoles of Δ*ysl2* cells, while in wild type vacuoles no Erg6p-GFP could be detected (Fig. 6). Thus, the results of the mass spectroscopic analysis could be verified for Erg6p. In contrast to that, the analysis of the vacuolar levels of Fba1p and Tsa1p did not confirm changes indicated by results from mass spectroscopy. While the total cellular levels of both proteins were not altered, the amounts of Fba1p were rather equal than decreased in vacuoles of Δ*ysl2* cells compared to the wild type, and the amounts of Tsa1p were rather decreased than increased. The proteins Ssb1p and Ssb2p were not further analysed, because changes in the expression levels of these chaperons are probably secondary effects of the *YSL2* deletion. Thus, out of all proteins identified by the mass spectroscopic analysis, only the increase of Erg6p levels on the Δ*ysl2* vacuoles could be confirmed by the

analysis of the vacuolar levels by one-dimensional SDS-PAGE and immunoblotting. For that reason even the identification of Erg6p has to be handled with caution. Anyhow, the Erg6p double spot was the most prominent difference between the protein pattern of Δ*ysl2* and wild type vacuoles separated by two-dimensional gel electrophoresis. Thus, even if variations during the preparation of vacuoles have caused isolation of false proteins, Erg6p still emerged in every experiment as the most obvious candidate. The missorting of Erg6p to the vacuole may have caused changes in ergosterol levels in the cell, since Erg6p regulates one of the final steps of the ergosterol synthesis (Parks *et al*., 1995). This may have multiple cellular effects such as inhibition of vacuole fusion and alterations in lipid rafts (Kato and Wickner, 2001; Tedrick *et al*., 2004). Thus, the phenotypes of Δ*ysl2* cells could partially be caused by the missorting of Erg6p.

Additionally, the effect of the *YSL2* deletion on the cellular and vacuolar levels was analysed for several proteins, which are known to be transported through TGN/endosomes. The cytosolic marker protein phosphoglycerokinase (PGK) did not show any changes in cellular or vacuolar levels upon *YSL2* deletion (Fig. 6) and served therefore as a control. Early pulse chase experiments proposed a role for Ysl2p in processing and sorting of vacuolar enzymes carboxypeptidase Y (CPY) and alkaline phosphatase (ALP) (Singer-Krüger and Ferro-Novick, 1997; Bonangelino *et al*., 2002). The accumulation of precursor forms of CPY in total cell lysates of Δ*ysl2* cells (Fig. 6), observed in the present study, is in agreement with the previous results. On the other hand, Δ*ysl2* cells seem to accumulate an additional ALP form which is smaller than in the wild type cells. It remains to be shown if this form is the soluble, luminal form of ALP while the higher mass band represents the mature, membrane bound form (Stepp *et al*., 1997) or if the smaller size protein is a degradation product of ALP. Interestingly, the vacuolar level is significantly reduced in the case of ALP but not for CPY in Δ*ysl2* cells compared to wild type (Fig. 6). Furthermore, the levels of Kex2p, a serin protease which cycles between the TGN and early endosomes, were found to be reduced in total cell lysates upon deletion of *YSL2* (Fig. 6). Since Kex2p is not transported to the vacuole, its quantities in vacuolar fractions were not determined. Anyhow, a cycloheximide chase did not demonstrate any differences in the degradation kinetics for HA-Kex2p (data not shown).

	lysates		vacuoles	
	wt	Δ*ysl2*	wt	Δ*ysl2*
Erg6p-GFP				
Tsa1p-GFP				
Fba1p				
PGK				
CPY				
ALP				
HA-Kex2p				
actin				
V-ATPase 60 kDa				
69 kDa				
100 kDa				
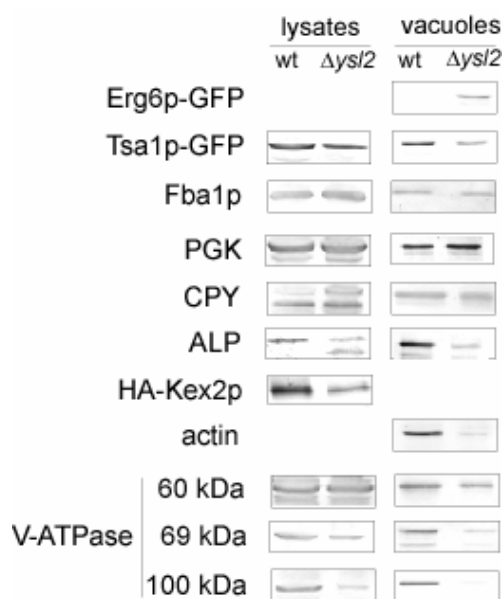
Fig. 6. Effect of the *YSL2* deletion on the on the cellular and vacuolar levels of various proteins involved in vesicular transport and vacuolar function. Same amounts of total cell lysates and isolated vacuoles (5 µg) of wt (RH1201, YML165, YML173) and Δ*ysl2* (BS747, YML164, YML172) cells were analysed by SDS-PAGE and immunoblotting using appropriate antibodies according to 2.1.4.1. For Kex2p detection BS188 and BS695 were transformed with the pHAKex2 plasmid and detected with the mouse anti-HA antibody.

The visualisation of the actin cytoskeleton in previous studies did not provide uniform results considering the effect of the *YSL2* deletion. Whereas Bonangelino *et al*. (2002) observed no changes in actin distribution in Δ*ysl2* cells compared to wild type, Singer-Krüger and Ferro-Novick (1997) reported that cortical actin patches were more randomly distributed over the periphery of both mother and daughter cell during all stages of the cell cycle. In the present study the levels of peripherally associated actin on isolated vacuoles of Δ*ysl2* cells (Fig. 6A) seemed to be reduced. It is conceivable that the changes in the distribution of cortical actin patches (Singer-Krüger and Ferro-Novick, 1997) and the changes in the levels of peripherally associated actin on isolated vacuoles of Δ*ysl2* cells could have the same origin. Possible origin could consist in alterations of the ergosterol cellular levels, since Tedrick *et al*. (2004) provided links between ergosterol, the cytoskeleton and membrane fusion.

Finally, the loss of *YSL2* may have an influence on the distribution of the V-ATPase, a proton pump responsible for the acidification of endosomes and the vacuole (see section 1.1.2.3), since the amounts of the 69 and 100 kDa subunits (subunits of the V_1 and V_0 sectors, respectively) were found to be reduced in vacuoles (Fig. 6). Moreover, the 100 kDa subunit appeared to be less abundant at the cellular level (Fig. 6). Anyhow, although the 60 kDa and 69 kDa subunits are both part of the V_1 complex, inexplicably only the level of the 69 kDa

subunit is reduced in Δ*ysl2* vacuoles. Since it has been demonstrated, that the assembly of the V_0 and V_1 subunit is performed on the early endosomes (Sipos *et al*., 2004) by the RAVE complex, and since Ysl1p, a subunit of the RAVE complex, and Ysl2p show the same synthetic lethality with Δ*ypt51*, a subcellular fractionation was performed to analyse if the explanation for reduced vacuolar levels of V-ATPase subunits could be that Ysl2p plays a role in the endosomal sorting of the V-ATPase (see section 3.2). Anyhow, the reduction of vacuolar levels does not seem to be caused by accumulation of the V-ATPase in endosomal compartments, since subcellular fractionation experiments could not demonstrate differences in the subcellular distribution of the 100 kDa V-ATPase subunit between wild type and Δ*ysl2* cells (Fig. 7). Recently, the V-ATPase was identified as the major component of lipid rafts (Yoshinaka *et al*., 2004). Thus, the reduced vacuolar levels of the V-ATPase could rather be caused by the changes in ergosterol distribution and possible loss of rafts. Anyhow, the analysis of the vacuole levels should be repeated for all examined proteins since the present analysis were performed from single vacuole isolation experiments respectively and need therefore independent repetitions for their significance.

Summarized, although Ysl2p does seem to be important for the transport of several proteins e.g. Kex2p or ALP, this may not be its only role. The potential role of Ysl2p in the localisation of Erg6p remains to be determined.

3.2 Deletion of YSL2 has no effect on the localization of a subset of TGN/endosomal marker proteins

Mutants *ysl1-1* and *ysl2-1* were identified in a synthetic lethality screen using Δ*ypt51* mutant cells (Singer-Krüger and Ferro-Novick, 1997). A recent study demonstrated that Ysl1p (also named Soi3p or Rav1p, see section 1.1.3) resides on early endosomes (Sipos *et al*., 2004) and is as a part of the RAVE complex responsible for the assembly of the V-ATPase (Seol *et al.*, 2001). Ysl2p also seems to localise to early endosomes (Jochum *et al*., 2002; see section 1.2.1) and results from present work indicate its importance for the stability of the V-ATPase subunits (see section 3.1; Fig. 6). Since Ysl1p and Ysl2p probably localise both on early endosomes and show the same genetic interaction with Δ*ypt51*, the two proteins could play a role in related pathways. Thus, it is possible that the Ysl2p importance for the stability of the V-ATPase subunits is connected to Ysl1p, e.g. Ysl2p could retrieve Ysl1p from vacuolar degradation by mediating its early endosomal localisation. To approach that question, the effect of the deletion of *YSL2* on the distribution of Ysl1p, the V-ATPase and

other endosomal and TGN marker proteins was examined by cell fractionation of early endosomes and TGN/late endosomes based on their physio-chemical characteristics (Sipos *et al.*, 2004).

In experiments performed by Sipos *et al.* (2004) Ysl1p/Soi3p was found in high-density gradient fractions distinct from that of the PVC SNARE Pep12p and the bulk of the TGN-marker protein Kex2p, although each of these proteins was present in small amounts in the dense fractions containing Ysl1p-HA. The high density of Ysl1p membranes was suggestive of early endocytic membranes, because studies of α-factor internalization demonstrated a higher density for early versus late endocytic carriers (Singer-Krüger *et al.*, 1993). Additionally, Ysl1p cofractionated with the dense fraction of Chs3p (Sipos *et al.*, 2004), which is thought to reside on early endosomal membranes (Valdivia *et al.*, 2002). Thus, Ysl1p was also postulated to reside on early endosomal membranes. If the deletion of *YSL2* has an effect on the localisation of Ysl1p or V-ATPase, it should be possible to observe changes in the subcellular fractionation pattern of these proteins when Δ*ysl2* and wild type cells are compared. Additionally, the subcellular localisation of Ysl2p has not been clearly proven yet. While data from the B. Singer-Krüger group provide indices for an early endosomal localisation (Jochum *et al.*, 2002), the subcellular fractionation experiments from Efe *et al.* (2005) propose a TGN localisation. Thus, it was conceivable to use the subcellular fractionation in the present work to approach this question.

Spheroblasted wild type or Δ*ysl2* cells were homogenised and separated by differential sucrose centrifugation. After fractionation by sequential centrifugation at 15,000 x g and 100,000 x g the enriched high-speed pellet was resuspended and loaded on the top of a sucrose gradient (29–60 %) and centrifuged at 100,000 x g for 18 hours (see section 2.2.3.9). The collected fractions were separated by SDS-PAGE and analysed by immunoblotting.

The distribution of the analysed proteins was in agreement with experiments performed by Sipos *et al.* (2004), since Ysl1p was found in distinct fractions from the TGN/late endosome markers Kex2p and Pep12p (Fig. 7). While Ysl1p and the 100 kDa subunit of the V-ATPase were found mainly in high density fractions (Fig. 7, Fr. 8-12; 36-48% of sucrose), suggested to contain early endocytic membranes, TGN/LE marker proteins Tlg2p, Vps10p, Pep12p, and Kex2p localised mainly in low density fractions (Fig. 7, Fr. 3-8; 29-36% of sucrose).
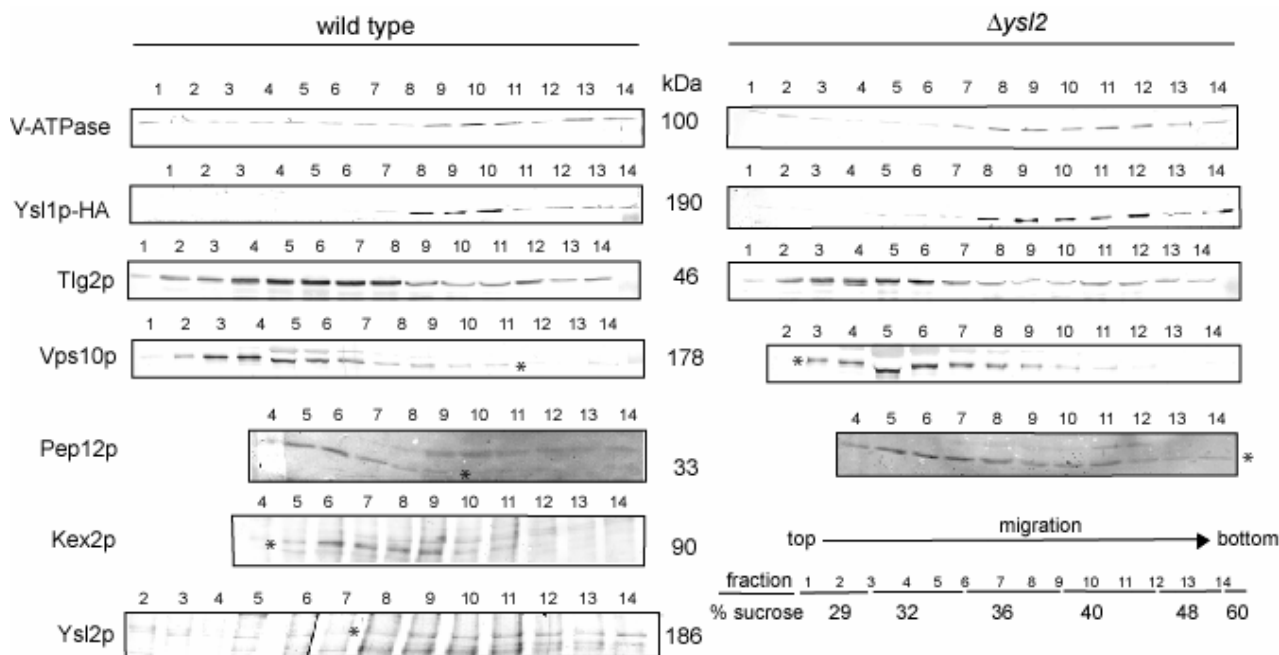
Fig. 7: Subcellular fractionation of TGN/endosomal proteins in wild type and Δ*ysl2* cells. Lysates of wild type (YML231) and Δ*ysl2* (YML233) cells were prepared by homogenisation of spheroblasts as described in 2.2.3.8. After fractionation by sequential centrifugation at 15,000 x g and 100,000 x g, the high-speed pellet was loaded on the top of a sucrose gradient (29 – 60 %) and centrifuged for 18 h at 100,000 x g. The gradient was collected in 14 fractions (fraction 1 is on the top, fraction 14 on the bottom of the gradient), after precipitation 10% of each fraction was analysed by SDS-PAGE and immunoblotting using appropriate antibodies according to 2.1.4.1. Asteriks indicate the size of the desired protein.

Anyhow, the deletion of *YSL2* did not seem to influence the localisation of Ysl1p or V-ATPase or any other analysed protein, since their sedimentation profiles revealed no differences between wild type and Δ*ysl2* cells (Fig. 7). These findings suggest that either Ysl2p may not be implicated in the sorting of e.g. V-ATPase, or that this pump is able to use alternative routes to reach its final destination. The analysis of Kex2p subcellular fractionation pattern in Δ*ysl2* cells (data not shown) provided no clear result, probably due to the reduction of its total cellular level upon deletion of *YSL2* as observed in present work (see section 3.1; Fig. 6).

The distribution of Ysl2p in this study (Fig. 7) was not in accordance with recently published subcellular fractionation experiments of Efe *et al*. (2005) since in their experiments Ysl2p was detected in fractions containing Kex2p and Pep12p, whereas in the present study Pep12p and Kex2p were found in lower density fractions (Fig. 7, fraction 6-9) then Ysl2p (Fig. 7, fraction 8-12). The high density fractions, which contain Ysl2p, contain also Ysl1p-HA and V-ATPase (Fig. 7). According to Sipos *et al*. (2004) these high density fractions correspond to the early endosomes. Thus, Ysl2p does seem to localise primarily on early

endosomes. The additional pool of Ysl2p in low density fractions (Fig. 7, fraction 2-6) allows the possibility that Ysl2p localises additionally on TGN, as indicated by former studies (Efe *et al.*, 2005; Gillingham *et al.*, 2006). It remains dubious why Efe *et al.* (2005) did not observe any difference between the fractionation of Ysl2p on the one side and Pep12p and Kex2p on the other side, although they have used an analogous fractionation experiment. Nevertheless, the result of the present subcellular fractionation supports the previous observations from the B. Singer-Krüger group (Jochum *et al.* 2002), which postulate an endosomal localisation for Ysl2p.

3.3 Search for novel Ysl2 interaction partners

3.3.1 The two hybrid screen offers several putative interaction partners of Ysl2p

A two-hybrid screen is usually the fastest and easiest method for the initial analysis of protein-protein interaction networks, especially if it is performed by a robot. For that reason it was the method of choice in the search for novel Ysl2p interaction partners. All genes from *S. cerevisiae* are available as a collection of prey plasmids for a two hybrid screen (group of Dr. P. Uetz). For the two hybrid screen, the gene of interest has to be inserted in a bait-plasmid, so that it can be analysed in combination with the prey collection in a search for novel interaction partners. Since Ysl2p is a large protein of 186 kDa (Fig. 8A), there is a high risk of misfolding or mislocalisation upon expression. Thus, the screen was performed not only with the entire *YSL2* gene, but also with different subdomains of Ysl2p (see section 2.2.2; Ysl2N-term (amino acids 1-505), Ysl2C-term (amino acids 505-1071), Ysl2PILT (amino acids 662-1077), Ysl2MKLF (amino acids 529-723), Ysl2EPLL (amino acids 1100-1636) and Ysl2PELD (amino acids 1417-1636); Fig. 8A). The constructs were analysed for cellular expression levels by immunodetection of the included HA-epitope. Some bait constructs tend to show a high self-activation, i.e. cells transformed with these bait plasmids have high expression rates of the reporter genes *lacZ* and *HIS3* even in the absence of any prey construct. For that reason all Ysl2-constructs were additionally analysed by the ß-galactosidase assay after co-transformation with the empty prey-plasmid (data not shown). Cells showed a very high ß-galactosidase expression only after transformation with the pAS1-Ysl2EPLL plasmid (data not shown); therefore it was not used in the screen. pAS1-Ysl2PILT is a moderate self-activator, i.e. the ß-galactose assay showed a modest reaction in cells which

were co-transformed with the pAS1-Ysl2PILT and an empty pACTII plasmid. Cells transformed with the pAS1-Ysl2PILT plasmid showed two different growth phenotypes. Analysis of the Ysl2PILT expression levels in the two types of colonies demonstrated that the cells with high expression levels of Ysl2PILT gave rise to small colonies, indicating that the recombinant protein may be toxic to the cell. In agreement, all putative interaction partners of Ysl2PILT showed a much stronger interaction when small colonies were specifically chosen for the analysis.

The screen was performed by the group of Dr. Peter Uetz (Karlsruhe) and several possible Ysl2p interaction partners were obtained. All putative interaction partners (Fig. 8B) were retested in the Y190 strain. The cells were tested for growth on 3-amino-1,2,4-triazole (3-AT) and for ß-galactosidase activity (Fig. 8C). For the ß-galactosidase test with Ysl2-PILT as bait, the transformed cells were preincubated for two days on SD$_{-Leu-Trp-His}$ plates containing 25 mM 3-AT prior to the ß-galactosidase assay to minimize the reaction caused by the self-activator activity of Ysl2PILT. The intensities of the ß-galactosidase reaction of strains expressing Ysl2PILT with respective partners varied during experimental repetitions, possibly due to different expression levels of Ysl2PILT. As a negative control, all positive prey plasmids were tested for interaction with pAS1-Sjl2p to exclude the possibility of high self-activator activity (data not shown).

Surprisingly, only the interactions obtained for Ysl2PILT as bait could be reproduced upon retesting of the isolated plasmids in the strain Y190 (Fig. 8C), none of the other putative interaction partners of Ysl2 subdomains showed a positive reaction upon retesting (Fig. 8C). Nevertheless, some prey proteins were found in more than one screen, e.g. Izh4p, membrane protein involved in zinc metabolism with a possible role in sterol metabolism (Lyons *et al*., 2004), was found in screen with Ysl2PELD and also with Ysl2C-term. The identified prey partners of Ysl2PILT were the gene product of YMR279C, a protein of unknown function, Ent4p, an uncharacterised protein with an N-terminal epsin-like domain and Bud27p, an URI-type prefoldin (Tronnersjö *et al*., 2007) (Fig. 8C). Mrs6p, a Rab escort protein (Benito-Moreno *et al*., 1994), showed also a significant interaction with Ysl2PILT (Fig. 8C), but at the same it was identified in 14 screens (according to P. Uetz), what indicated strong unspecific binding to other proteins. For that reason it was not considered in further studies. The interaction with Atr1p was not reproducible through the repetitions although it was identified in the screen as an interaction partner of Ysl2PILT and Ysl2N-term. Anyhow, since the interaction between Ysl2N-term and Atr1p was also not reproducible (Fig. 8C), it was not further considered in the studies.

It was of interest to verify the putative interaction partners with alternative biochemical assays. Ent4p is a close homologue of Ent3p and Ent5p, which are both already known to participate in endosomal transport processes (Eugster *et al.*, 2004; Costaguta *et al.*, 2006; Copic *et al.*, 2007). For that reason Ent4p was an interesting putative Ysl2p binding partner and thus was analysed *in vitro* and *in vivo* for interaction with Ysl2p. GST-pull down experiments were performed to test the interaction between Ent4p-HA and different GST-constructs containing subdomains of Ysl2p. A GST-fusion of Gga2p was included in the experiment, since Gga2p is already known to interact with Ent3p and Ent5p (Costaguta *et al.*, 2006). Furthermore, it is a possible effector of Ysl2p and Arl1p (see section 3.5). Glutathione S-transferase (GST) fusions containing amino acids 1-326 of Gga2p (GST-Gga2$_{1-326}$) or amino acids 1-505 (Ysl2N-term), 662-1077 (Ysl2PILT) or 1100-1636 (Ysl2EPLL) of Ysl2p were expressed in *E. coli* and purified by glutathione-Sepharose affinity purification (see section 2.2.3.5). A GST-Ypt7p fusion was provided by Dr. Birgit Singer-Krüger as a negative control. GST-fusions were immobilized on glutathione-Sepharose beads and incubated with a yeast cell lysate containing Ent4p-HA (see section 2.2.3.6). No binding of Ent4p-HA to GST-Ypt7p and negligible binding to GST-EPLL could be observed (Fig. 8D), whereas Ent4p-HA revealed a weak binding to GST-Ysl2PILT, GST-Ysl2N-term and GST-Gga2$_{1-326}$. Although Ent4p was detected as an Ysl2PILT binding partner in the two hybrid screen (Fig. 8C) and the two hybrid screen with Ysl2Nterm did not reveal Ent4p as a potential interaction partner, in the GST-pull down analysis the strongest binding of Ent4p-HA was detected with GST-Ysl2N-term (Fig. 8D). This could be because the GST-Ysl2PILT fusion protein was isolated in a very low yield or because GST-Ysl2N-term has a higher level of unspecific binding.
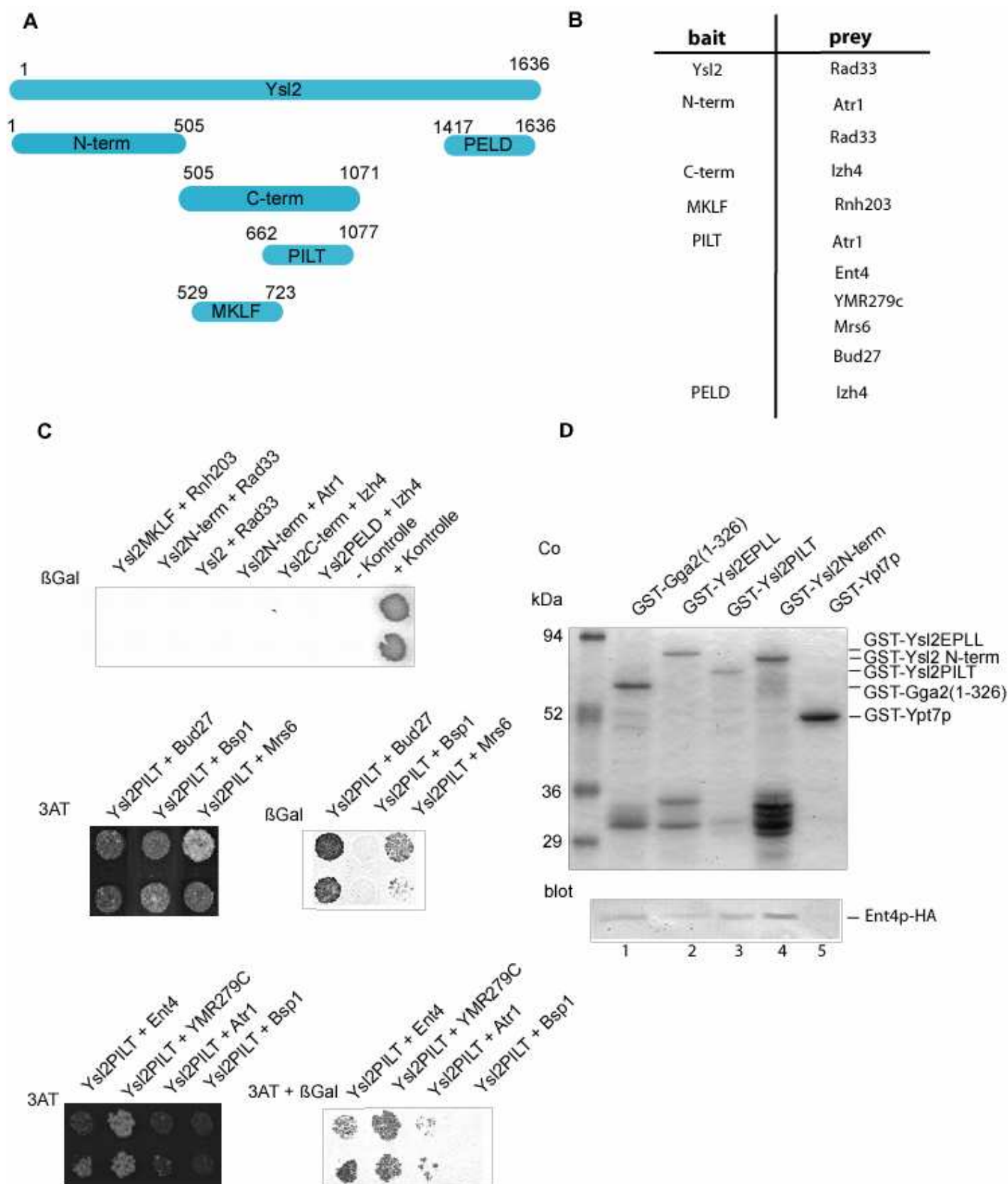
**Fig. 8: The PILT domain of Ysl2p interacts with several proteins in the two-hybrid system**. (A) Scheme of different subdomains of Ysl2p, which were used to generate the pAS1- and pGEX-constructs, in approximate relation to the full length protein. The numbers indicate the beginning and ending amino acids of the subdomains. (B) List of all putative interaction partners from the two hybrid screen performed in the P. Uetz

group. (C) Yeast strain Y190 was co-transformed with combinations of pAS1-Ysl2Nterm, pAS1-Ysl2MKLF, pAS1-Ysl2Cterm, pAS1-Ysl2PELD, pGBD-C2-Ysl2 or pAS1-Ysl2PILT as bait plasmids and pOAD-Rnh203, pOAD-Rad33, pOAD-Atr1, pOAD-Izh4, pOAD-Bud27, pOAD-YMR279C, pOAD-Mrs6, pACTII-Bsp1 or pACTII-Ent4 as prey plasmids. Strains BS714 (Y190 transformed with pAS1-YPT51 and clone #14) and BS934 (Y190 transformed with pAS1-Sjl2-588 and pYPR171-C1#9) served as a negative and positive control, respectively. Transformants were streaked out on SD$_{-Leu-Trp-His}$ plates either with or without 25 mM 3-amino-1,2,4-triazole (3-AT) and analysed for ß-galactosidase activity or growth on 3-AT, respectively, as described in Materials and Methods (see section 2.2.2). (D) Ent4p binds *in vitro* to several Ysl2p-subdomains and the VHS-GAT domain of Gga2p. 80 µg of GST-Ypt7p, GST-Ysl2N-term, GST-Ysl2PILT, GST-Ysl2EPLL and GST-Gga2$_{1-326}$ were immobilised onto glutathione-Sepharose beads and incubated with a yeast cell lysate containing Ent4p-HA (YML221). After extensive washing, bound proteins were eluted and separated by SDS-PAGE. Recombinant proteins were stained with Coomassie brilliant blue (Co), Ent4p-HA was detected by immunoblotting.

Nevertheless, the *in vitro* binding of Ent4p-HA to GST-fusion constructs of Ysl2p and Gga2p provides a further hint for the Ent4-Ysl2 interaction although the co-immunoprecipitation experiments performed to verify *in vivo* the interaction between Ysl2p-TAP and Ent4p-HA were negative (data not shown). For that reason, further studies are required to determine whether Ent4p and Ysl2p are true binding partners.

Additionally, Bud27p and Ymr279c were detected as positive interaction partners of Ysl2PILT in the two hybrid analysis (Fig. 8B, C). YMR279c was identified as a heat-induced gene in a high-throughput screen (Sakaki *et al*., 2003) whose gene product is predicted to have a molecular weight of 60 kDa and 13 transmembrane domains (SGD). It was not possible to express C-terminally HA-epitope tagged Ymr279c, although the epitope sequence was properly inserted, as verified by PCR. Possibly, the epitope tag may generate a non-functional protein that is degraded. Therefore, the interaction between Ysl2p and Ymr279c could not be further analysed. Co-immunoprecipitation experiments performed with Ysl2p-TAP and Bud27p-HA, another putative Ysl2p interaction partner, were negative (data not shown). Since Bud27p is involved in distinct cellular process, e.g. transcription, sumoylation and DNA repair (Tronnersjö *et al*., 2007), it is improbable that it is a real interaction partner of Ysl2p *in vivo*.

Summarized, out of all analysed proteins Ent4p remains the most probable interaction partner of Ysl2p *in vivo*, since the two hybrid interaction was reproducible and also supported by the result from the GST-pull down. Further experiments remain necessary for the verification of the Ent4-Ysl2 interaction.

3.3.2 Ysl2-TAP large scale purification did not provide novel interaction partners

A large scale purification of Ysl2p-TAP was applied as an alternative approach to identify further Ysl2p interaction partners by co-immunoprecipitation. The TAP-epitope consists of the IgG-binding units of protein A from *Staphylococcus aureus* (ProtA) and the <u>C</u>almodulin <u>B</u>inding <u>P</u>eptide (CBP), fused in tandem and separated by a TEV protease cleavage site allowing for <u>T</u>andem <u>A</u>ffinity <u>P</u>urification (TAP) (Rigaut *et al.*, 1999). Ysl2p and putative binding proteins were isolated from a yeast strain expressing Ysl2p with a C-terminal TAP epitope (BS986). Sjl2p-TAP (BS906) was used as a negative control.

Growth of the yeast cells and the purification of the TAP-fusion proteins were performed as described in Wicky *et al.* (2004), the duration of the incubation with the IgG Sepharose (2 h) and the amounts of Sepharose (15 µl IgG Sepharose / 1 g cells (wet weight)) were optimized according to the Ysl2p yield. Cells were grown at 30°C either in 2 l flask culture or in 20 l fermentation culture, harvested, and stored as cell drops at -80°C. Upon gentle lysis by grinding under liquid nitrogen (Kellogg and Moazed, 2002; section 2.2.3.8), Ysl2p-TAP and possible interacting proteins were isolated from the total cellular extracts in presence of 0.2% NP-40 by affinity purification via IgG-sepharose and released from the matrix by cleavage with the site specific TEV-protease. After elution proteins were either subjected to TCA precipitation and separation by SDS-PAGE or further purified by the calmodulin binding domain. Whereas after the TEV cleavage numerous matching co-isolated proteins could be observed in the Ysl2p- and Sjl2p-eluates (Fig. 9A; lane 1 and 2), the second purification step of rebinding to the calmodulin-Sepharose strongly reduced unspecific protein binding (Fig. 9A; lane 3 and 4). Ysl2p could be enriched with a high purity (Fig. 9A; lane 3). Unfortunately, under the conditions published by Rigaut *et al.* (1999) no prominent copurifying proteins were detected (Fig. 9A), independently of the increase of cell amounts or duration of the silver staining (Fig. 9B).

In an analogous large-scale purification of Ysl2p tagged with two copies of the IgG-binding Z domain of protein A Gillingham *et al.* (2006) have identified Dop1p as an interaction partner of Ysl2p. Moreover, Dop1p was found to co-purify equimolar to Ysl2p, indicating that the two proteins stably interact and coexist in a complex. Co-immunoprecipitation experiments (Efe *et al.*, 2005) and immunofluorescence analysis (Gillingham *et al.*, 2006) supported this finding (see section 1.2.1). This result is in the contrast to the findings of the present study, in which no band could be specifically co-isolated.

Fig. 9: Comparison of Ysl2p purification after TEV cleavage and elution from calmodulin beads. (A) Immunoprecipitations were performed with lysates of cells (wet weight ~3 g) expressing TAP-tagged Ysl2p (BS986) or Sjl2p (BS906). Eluates were analysed after the TEV cleavage (lane 1 and 2) or elution from calmodulin beads (lane 3 and 4). 15% of the eluates were separated by SDS-PAGE and stained with silver (3-5 min). (B) Immunoprecipitations were performed with lysates of cells (wet weight ~ 18 g) expressing TAP-tagged Ysl2p or Sjl2p. Eluates were analysed after the elution from calmodulin beads (lane 1-3 represent eluates 1-3) 50% of the eluates were separated by SDS-PAGE and silver stained for a much longer period (15 min) than in (A). (C) Estimation of the isolated Ysl2p quantities in different experiments by comparison with different quantities of a BSA standard. Co-immunoprecipitations were performed with lysates of cells expressing TAP-tagged Ysl2p. Eluates were analysed after the TEV cleavage (lane 1) or after elution from calmodulin beads. The eluates from calmodulin beads were compared for cultures grown in 2 l flask culture (lane 2) and in 20 l fermentation culture (lane 3). The proteins were separated by SDS-PAGE and analysed with the silver staining procedure.

An estimation of the isolated Ysl2p quantities was done by comparison of the intensity of the Ysl2p band with different quantities (1-100 ng) of the BSA standard after SDS-PAGE and silver staining (Fig. 9C). Estimation was performed for eluates after the TEV cleavage (Fig. 9C, lane 1) and for the 2 l flask culture (Fig. 9C, lane 2) and the 20 l fermentation culture (Fig. 9C, lane 3) after binding to the calmodulin-Sepharose beads. Whereas after TEV cleavage ~170 ng of Ysl2p could be isolated per 1 g cells (wet weight), the additional binding to calmodulin Sepharose-beads reduced the amounts of isolated Ysl2p to 20 ng/ 1 g cells for 2 l flask culture or even to less than 10 ng in the case of 20 l fermentation culture (Fig. 9C). Therefore, the increase in protein purity by the second purification step is coupled to an 8-28 fold reduction of isolated protein amounts.

3.4 Further analysis of Ysl2p

3.4.1 Importance of the C-terminal 100 amino acids of Ysl2p

Since it was known that the deletion of *YSL2* causes a strong growth defect as well as a delay in the endocytosis and biosynthetic delivery to the vacuole (Jochum *et al*., 2002), it was interesting to analyse which domains of the wild type protein are important for its function. To approach this question, a deletion series of Ysl2p was created, in which the C-terminal 100, 200, 300, 400, 500, 750, or 900 amino acids were exchanged by insertion of the TAP-epitope (see section 3.3.2) by homologous recombination in a diplod strain (BS811) with subsequent sporulation and dissection of tetrads. The strain BS811 was deficient in one copy of *NEO1* (see section 2.1.1). After homologous recombination it was sporulated either upon transformation with a plasmid encoding HA-NEO1 to generate haploid Δ*neo1* strains

expressing plasmid-derived HA-Neo1p for co-immunoprecipitations with Ysl2Δxp-TAP and HA-Neo1p (see section 3.4.2, selection on SD$_{-leu}$ plates) or without transformation to generate haploid strains expressing wild-type Neo1p for growth tests at 30°C and 37°C (selection on YPD plates). Surprisingly, the deletion of the last C-terminal 100 amino acids caused a strong growth defect at 30°C and abolished growth at 37°C (Fig. 10A), both phenotypes known from Δ*ysl2* cells (Jochum *et al*., 2002). All other deletions had the same effect (Fig. 10A). The Ysl2Δ400p-TAP construct and some of Ysl2Δ100p-TAP clones (deletion of 100 amino acids did not produce consistent phenotypes) caused even a stronger growth phenotype than Δ*ysl2*, indicating that the expression of these modified proteins may inhibit the processes in which Ysl2p commonly participates. The immunoblot analysis of protein levels demonstrated that expression levels of the Ysl2ΔXp-TAP (X=100, 200, 300, 400, 500, 750, or 900 amino acids) mutants were only partially reduced when compared to Ysl2p-TAP (Fig. 10B). In other experiments the levels of Ysl2p-TAP and Ysl2Δ100p-TAP seemed even comparable (Fig. 10C, anti-Ysl2 blot). Consequently, it is not the degradation of Ysl2ΔXp-TAP molecules that induces the Δ*ysl2*-like phenotype.

A possible explanation for the severe growth phenotype upon the deletion of C-terminal 100 amino acids could be that the C-terminus is crucial for the localisation of Ysl2p. To approach that question the localisation of full length Ysl2p and Ysl2Δ100p were compared by indirect immunofluorescence. These localisation studies could not be performed with strains expressing Ysl2p-TAP, since the TAP-tag is not suitable for detection via indirect immunofluorescence. Unfortunately, the attempt to add an alternative epitope to Ysl2ΔXp demonstrated that the addition of a C-terminal triple HA-epitope to the Ysl2Δ100p construct induced high instability of the protein. The total protein amounts in all lysates were comparable, since the cellular levels of the control protein CPY were similar (Fig. 10C, anti-CPY blots). The cellular levels of Ysl2Δ100p-HA were much lower than of Ysl2p-HA after comparison of lysates upon immunoblotting with the anti-HA antibody (Fig. 10C, anti-HA blot). Surprisingly, the difference between the expression levels seems to be induced by the addition of the HA-tag since the expression levels of Ysl2p-TAP and Ysl2Δ100p-TAP were more similar (Fig. 10C, anti-Ysl2 blot). The additional phenotypes of strains expressing Ysl2Δ100p-HA observed by indirect immunofluorescence, e.g. fragmented vacuoles, clumping of cells and reduced adhesion to polylysine, are all known as phenotypes of Δ*ysl2* cells. An explanation for these phenotypes could be either the importance of the C-terminus for Ysl2p function or the reduction of Ysl2Δ100p-HA cellular levels. Since the expression of Ysl2Δ100p-TAP has the same effect on the cell growth, although cellular levels of

Ysl2Δ100p-TAP are not reduced (Fig. 10C, anti-Ysl2 blot), it seems that the relevance of the C-terminus for the Ysl2p function and not its cellular level is the explanation for the severe phenotype.
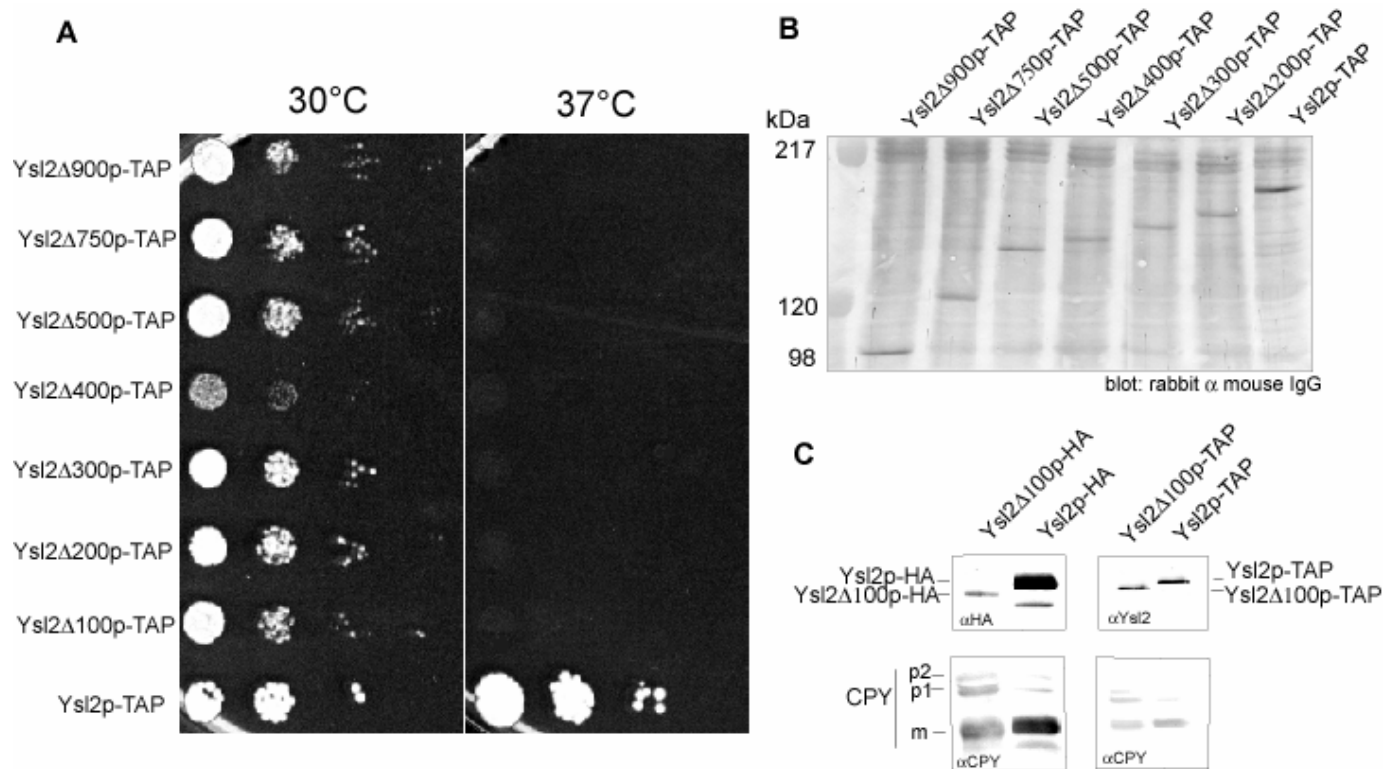

Fig. 10: The C-terminal 100 amino acids of Ysl2p are extraordinary important for its function. (A) Dilution series of strains with sequential deletions of Ysl2p: Ysl2p-TAP (BS986), Ysl2Δ100p-TAP (YML138), Ysl2Δ200p-TAP (YML101), Ysl2Δ300p-TAP (YML103), Ysl2Δ400p-TAP (YML97), Ysl2Δ500p-TAP (YML107), Ysl2Δ750p-TAP (YML110), and Ysl2Δ900p-TAP (YML113) were incubated at 30°C and 37°C. (B) Lysates of YML113 (Ysl2Δ900p-TAP), YML109 (Ysl2Δ750p-TAP), YML107 (Ysl2Δ500p-TAP), YML121 (Ysl2Δ400p-TAP), YML103 (Ysl2Δ300p-TAP), YML102 (Ysl2Δ200p-TAP), and BS986 (Ysl2p-TAP) were prepared with glass beads, same amounts were separated by SDS-PAGE. (C) Lysates of YML440 (Ysl2Δ100p-HA), BS1121 (Ysl2p-HA), YML138 (Ysl2Δ100p-TAP) and BS986 (Ysl2p-TAP) were prepared with glass beads, same amounts were separated by SDS-PAGE and analysed by immunoblotting.

Although the indirect immunofluorescence demonstrated the loss of punctuate staining for Ysl2Δ100p-HA (YML440) when compared to the Ysl2p-HA (BS1121) localisation (data not shown), it was unclear if it occurred due to incapability of membrane localisation of Ysl2Δ100p-HA or due to its reduced levels as demonstrated by the immunoblot analysis (Fig. 10C). A possible solution could be the addition of another epitope (e.g. 13xMyc, GFP), which may stabilise the Ysl2Δ100p construct similar to the TAP-epitope and which possibly would allow its detection by indirect immunofluorescence. Anyhow, localisation studies performed by Efe *et al*. (2005) indicated that the A and B domains (representing the N-terminus) of

Ysl2p are sufficient for membrane binding, while Ysl2(d-F)p-GFP did not appear to associate with membranes. Thus, the relevance of the C-terminus for the Ysl2p function does not seem to be related to its membrane association, but rather to its role in protein-protein interactions (see section 3.4.2).

3.4.2 Dimerisation of Ysl2p and the role of the C-terminal 100 amino acids

In earlier sucrose gradient experiments from the lab of B. Singer-Krüger, Ysl2p was found in fractions with marker proteins of higher molecular mass than the mass of the monomeric protein of 187 kDa. To analyse if Ysl2p is capable of self-interaction, in the present study a diploid strain was constructed harbouring both an Ysl2p-TAP and Ysl2p-HA chimera. Detergent-solubilized whole cell native extracts from a diploid Ysl2p-HA/Ysl2p control strain and the double tagged diploid Ysl2p-HA/Ysl2-TAP were then subjected to centrifugation at 13,000 x g and Ysl2p-TAP assemblies were isolated by affinity purification via IgG-Sepharose and released from the matrix by the site specific TEV protease (Rigaut *et al*., 1999). Eluates were analysed by immunoblotting using rabbit anti-mouse IgG and anti-HA antibodies (see section 2.1.4.1). Ysl2p-HA was found in immunoprecipitates from Ysl2p-TAP expressing cells (Fig. 11A; IP lane 2), but not in the control sample (Fig. 11A; IP lane 3), suggesting that Ysl2p-HA interacted specifically with Ysl2p-TAP *in vivo*. The interaction was not influenced by variations of the detergent concentration (data not shown). Interestingly, the loss of the C-terminal 100 amino acids, that have been shown to cause severe defects similar to the deletion of *YSL2* (see section 3.4.1), abolished the Ysl2p-Ysl2p interaction as well (Fig. 11A; IP lane 1), although Ysl2Δ100p-TAP was clearly expressed (Fig. 11A; input lane 1).

To exclude the possibility that the deletion of the C-terminal 100 amino acids caused the misfolding of the protein, the established co-immunoprecipitation of Neo1p-HA with Ysl2p-TAP (Wicky *et al*., 2004) was repeated with cell extracts of strains expressing Ysl2Δ500p-TAP and HA-Neo1p. Ysl2p-TAP or Ysl2Δ500p-TAP assemblies were isolated from total cellular extracts by affinity purification via IgG Sepharose and released from the matrix by the site specific TEV protease as described above. Immunoprecipitates were analysed by immunoblotting using rabbit anti-mouse IgG and anti-HA antibodies (see section 2.1.4.1). The analysis demonstrated that despite of the loss of C-terminal 500 amino acids of Ysl2p the Ysl2-Neo1 interaction is preserved, since HA-Neo1p could be co-isolated with

Ysl2Δ500p-TAP (Fig. 11B, lane 1). Consequently, the loss of the Ysl2p-Ysl2p interaction upon deletion of the C-terminal 100 amino acids does indicate that this region of Ysl2p is particularly important for the Ysl2p-Ysl2p interaction.
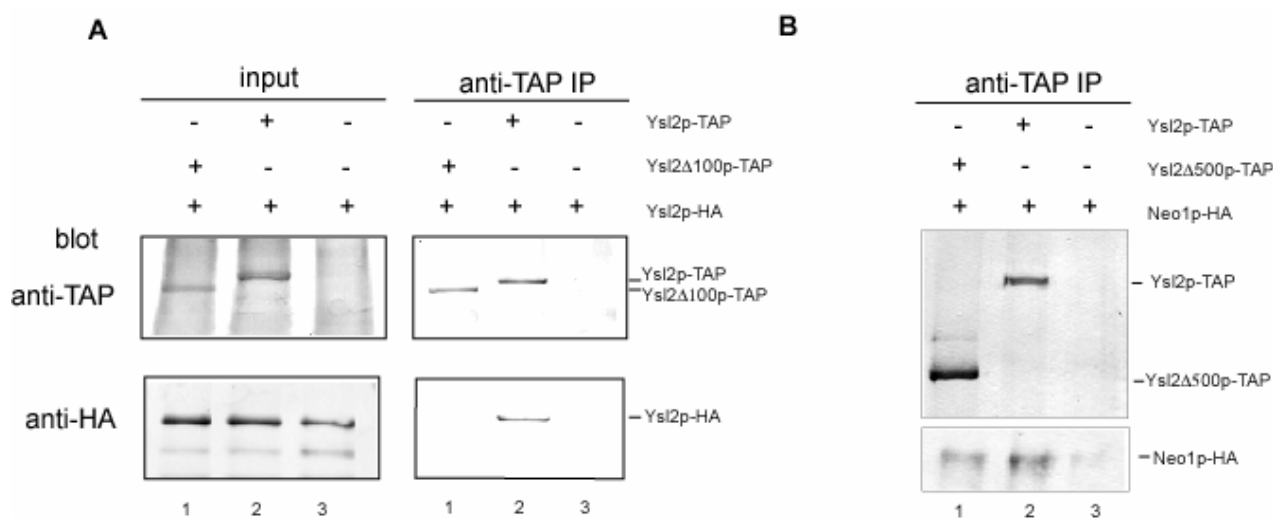

Fig. 11: Ysl2p needs the C-terminal 100 amino acids to interact with itself. (A) The deletion of the C-terminal 100 amino acids does abolish the Ysl2p-Ysl2p interaction. Detergent solubilized (0.8% NP-40) native lysates from cells (50 OD$_{600}$ units) expressing Ysl2p-HA/Ysl2p-TAP (YML174), Ysl2p-HA/Ysl2Δ100p-TAP (YML271) or only Ysl2p-HA (BS727) were cleared at 15,000 x g and subjected to immunoprecipitation using IgG Sepharose. After binding the proteins were eluted by boiling at 95°C for 5 min. 25% (for anti-TAP detection) or 12.5% (for anti-HA) of the total sample were separated by SDS-PAGE and detected by immunoblotting with rabbit anti-mouse IgG or anti-HA antibody. (lane 1 - YML271; lane 2 - YML174; lane 3 – BS727) (B) The deletion of C-terminal 500 amino acids does not abolish the Ysl2p-Neo1p interaction. Co-immunoprecipitations were performed with lysates of cells expressing Neo1p-HA/Ysl2p-TAP (BS912), Neo1p-HA/Ysl2Δ500p-TAP (YML35) or Neo1p-HA (BS862) in the presence of 0.01% (w/v) NP-40 until the TEV cleavage. 50% (for Ysl2p detection) or 12.5% (for Neo1p) of the total sample were separated by SDS-PAGE and probed with anti-Ysl2p and anti-HA antibodies, respectively, as described in section 2.1.4. (lane 1 - YML35; lane 2 - BS912; lane 3 - BS862)

To verify the Ysl2p-Ysl2p interaction with an *in vitro* assay a GST-pull down was performed with GST-fusions of different subdomains of Ysl2p: GST-Ysl2N-term (encoding amino acids 1-505), GST-Ysl2C-term (encoding amino acids 505-1071) and GST-Ysl2EPLL (encoding amino acids 1100-1636) (see section 2.2.1). A GST-Ypt7p fusion was provided by Dr. Birgit Singer-Krüger as a negative control. After expression and purification in *E. coli*, the GST-fusions were immobilized on glutathione-Sepharose beads and incubated with a yeast cell lysate containing Ysl2p-HA. Surprisingly, Ysl2p-HA did not specifically bind to any of the GST-fusions (data not shown). Alternatively, purified GST-fusions of Ysl2p (GST-

Ysl2N-term (encoding amino acids 1-505), GST-Ysl2PELD (encoding amino acids 1417-1636) and GST-Ysl2EPLL (encoding amino acids 1100-1636)) were added to the detergent-solubilized (0.8 % NP-40) yeast extract during the isolation of Ysl2p-TAP by affinity purification via IgG Sepharose, but no specific co-purification of any of the GST-fusions was detectable (data not shown). As a further approach, purified GST-Ysl2EPLL (encoding amino acids 1100-1636) was rebound to the GST-Sepharose and incubated with His-Ysl2EPLL (encoding amino acids 1100-1636) or Ysl2N-term (encoding amino acids 1-505; after expression as GST-Ysl2Secfull and subsequent thrombin cleavage). No differences could be observed for either His-Ysl2EPLL or Ysl2N-term between the binding to GST-Ypt7 and GST-Ysl2EPLL (data not shown). Thus, none of the *in vitro* methods could demonstrate the Ysl2-Ysl2 interaction.

It is surprising that although co-immunoprecipitation experiments clearly demonstrated an interaction of Ysl2p with itself, in was not possible to demonstrate this interaction by any of the *in vitro* approaches. For all *in vitro* analysis, recombinant proteins from *E. coli* were used (GST- and HIS-fusion proteins). It is possible that a modification of the C-terminus (like phosphorylation or ubiquitination) are crucial for the interactions, since these modifications are present only after expression in *S. cerevisiae*. Alternatively, the full length of Ysl2p or an additional linking protein (e.g. Dop1p) is necessary for the Ysl2-Ysl2 interaction.

3.5 The Neo1/Ysl2/Arl1 network is implicated in the recruitment of adaptor proteins to TGN/endosomal membranes

3.5.1 Deletion of *GGA2* suppresses the temperature-sensitive *neo1-69* mutant

Earlier studies from the Dr. Birgit Singer-Krüger group provided evidence for a genetic interaction between *ARL1* and *NEO1* showing that the *ARL1* deletion suppresses the temperature-sensitivity of *neo1-69* cells (Wicky *et al*. 2004, see section 1.2.3.1). Electron microscopy of the *neo1-69* mutant cells has shown an accumulation of aberrantly shaped, flattened membrane elongations, that are probably endosome-derived (Wicky *et al.* 2004). A possible explanation for the growth defect of these cells is a detrimental interaction of Neo1-69p with Arl1p and interacting partners that are functionally connected. Such assemblies may impair the process of membrane trafficking within the TGN/endosomes (for example by accumulating at endosomal membrane protrusions), thereby causing the growth inhibition in

the *neo1-69* mutant at nonpermissive temperatures. Deletion of specific components of the Neo1p-dependent machinery, like demonstrated for Arl1p (Wicky *et al*., 2004), would then prevent the accumulation of further downstream effectors and restore the growth in the *neo1-69* mutant.

To date the biochemical interaction between Ysl2p and Arl1p has been demonstrated *in vitro* (Jochum *et al*., 2002), but it is still unclear which cellular processes are regulated by their common effort. Arl1p was proposed to be implicated in tethering processes due to its role as a recruiting factor for golgins (Panic *et al*., 2003a; Setty *et al*., 2003). Anyhow, this could not explain a subset of shared effectors with Arf1p (Van Valkenburgh *et al*., 2001) or its role in the distribution of the analysed adaptors AP-1 and COP-I (Lu *et al*., 2001). Arl1p interacts together with Ysl2p and the aminophospholipid (APL)-translocase Neo1p similar to the network of the small GTPase Arf1p, Arf GEF Gea2p, and APL-translocase Drs2p, which are known to participate in vesicle budding on the TGN (Chantalat *et al*., 2004). Thus, it is possible that Arl1p participates not only in recruitment of Golgins but also in vesicle budding processes, like other Arf GTPases. If so, it should be possible to demonstrate a dependence of specific coat adaptors (see section 1.1.2.1) on Arl1p. The idea was to determine if a deletion of putative Arl1p effectors can also suppress the growth defect of *neo1-69* cells like demonstrated for the deletion of *ARL1*. Since the intention was to analyse a possible implication of Arl1p in coat assembly during vesicle formation, analysed effectors were primarily coat adaptors known to play a role in the TGN/endosome trafficking and to be recruited to membranes by Arf GTPases. If some of these adaptors do depend on Neo1p and Arl1p and for that do accumulate in the *neo1-69* mutant, their deletion could have an effect on the growth of *neo1-69* cells. Therefore, the major adaptors known to participate in TGN/endosomal transport were individually deleted in the *neo1-69* strain: the genes *GGA1* and *GGA2* (Costaguta *et al*., 2001), *APL2* (subunit of AP-1 adaptor complex; Stepp *et al*., 1995) and *APL6* (subunit of AP-3 adaptor complex; Stepp *et al*., 1997). The growth of the cells was compared at 25°C and 37 °C (Fig. 12A).

While at 25°C all mutants grew similarly and no genetic interaction was observable between the *neo1-69* mutation and any of the deletions, at 37°C the deletions of the adaptors had different effect on the growth of cells. The best suppression of the *neo1-69* growth defect at 37°C was achieved by the deletion of *GGA2* (Fig.12A), the suppression was comparable to the one caused by deletion of *ARL1*, the growth was wild-type like. Deletions of all other adaptors suppressed the *neo1-69* growth defect to a lesser extend. The suppression of *neo1-69* by deletion of *APL2* was clearly less pronounced than by deletion of *GGA2*, similar slight

rescue was achieved by deletion of *APL6* and deletion of *GGA1* has shown no effect (Fig.12A).

Additionally to the adaptors, several GTPases, which participate in TGN/endosomal transport processes, were included in the analysis to determine if the suppression of *neo1-69* growth defect is restricted to the loss of *ARL1* and its effectors. In the first place the deletion of *ARF1* was analysed and showed minor suppression (Fig. 12B), comparable to *Δapl2* (Fig. 12A). Deletion of *ARL3,* which is already known to be closely connected to *ARL1* (Panic *et al*., 2003, Setty *et al*., 2003), suppressed with same intensity as *Δarl1* (Fig. 12B). Deletion of Rab GTPases *YPT51* and *YPT7*, both essential for trafficking within the endomembrane system (Singer-Krüger *et al*., 1990; Wichmann *et al*., 1992), did not have any effect on the growth defect of *neo1-69* cells, indicating that the suppressor capability may be restricted to Arf GTPases (Fig. 12B).
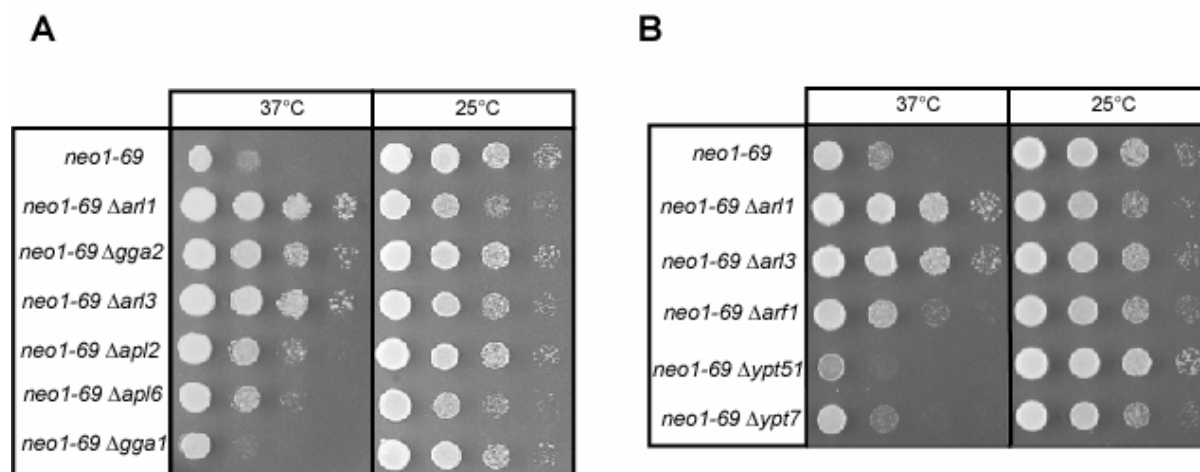
Fig. 12: The *neo1-69* mutation shows genetic interactions with adaptors and Arf GTPases. (A) Genetic interactions between the *neo1-69* mutation and deletion mutants of endosomal adaptors. Dilution series of *ARL1 neo1-69* (BS917), *Δarl1 neo1-69* (BS1323), *Δgga2 neo1-69* (YML281)*, Δarl3 neo1-69* (YML341), *Δapl2 neo1-69* (YML296)*, Δapl6 neo1-69* (YML278) *and Δgga1 neo1-69* (YML290) cells after growth at 37°C and 25°C. (B) Genetic interactions between the *neo1-69* mutation and deletions mutants of endosomal small GTPases. Dilution series of *ARL1 neo1-69* (BS917), *Δarl1 neo1-69* (BS1323), *Δarl3 neo1-69* (YML341), *Δarf1 neo1-69* (YML413), *Δypt51 neo1-69* (YML371) and *Δypt7 neo1-69* (YML376) cells after growth at 37°C and 25°C.

Since *GGA2* was the only adaptor whose deletion showed a suppression of the *neo1-69* growth phenotype comparable to *ARL1*, the implication of Gga2p in the Ysl2-Arl1p-Neo1p was further analysed.

3.5.2 Influence of the Neo1-69p mutant protein on the Gga2p localisation

The growth defect of the *neo1-69* mutant is possibly caused by accumulation of the budding machinery components on endosomes. In agreement with that theory, Arl1p and Ysl2p, both known to interact with Neo1p, are detectable in those aberrant membrane protrusions (Wicky *et al.*, 2004). Since *GGA2* shows a similar genetic interaction with *neo1-69* mutant like *ARL1* (see section 3.5.1), it was logical to analyse the subcellular distribution of Gga2p in the *neo1-69* cells. The distribution of Gga2p was analysed by indirect immunofluorescence of cells expressing Gga2p C-terminally tagged with a triple HA-epitope. In former studies Gga2p-HA has been shown to localise in wild-type cells at several discrete punctuate structures, likely representing the TGN and endosomes (Hirst *et al.*, 2001; Boman *et al.*, 2002). In the present study, the staining pattern was similar, mainly cytosolic with several punctuate structures (Fig. 13A). The pattern of Gga2p localisation was affected by the *neo1-69* mutation already at permissive temperature. While in a large fraction of cells the uniformly observed punctuate pattern of Gga2p-HA was replaced by a diffuse background-like staining, indicating a reduction in the total levels of Gga2p, in the remaining cells the Gga2p-HA positive structures were more prominent and appeared brighter and larger than in
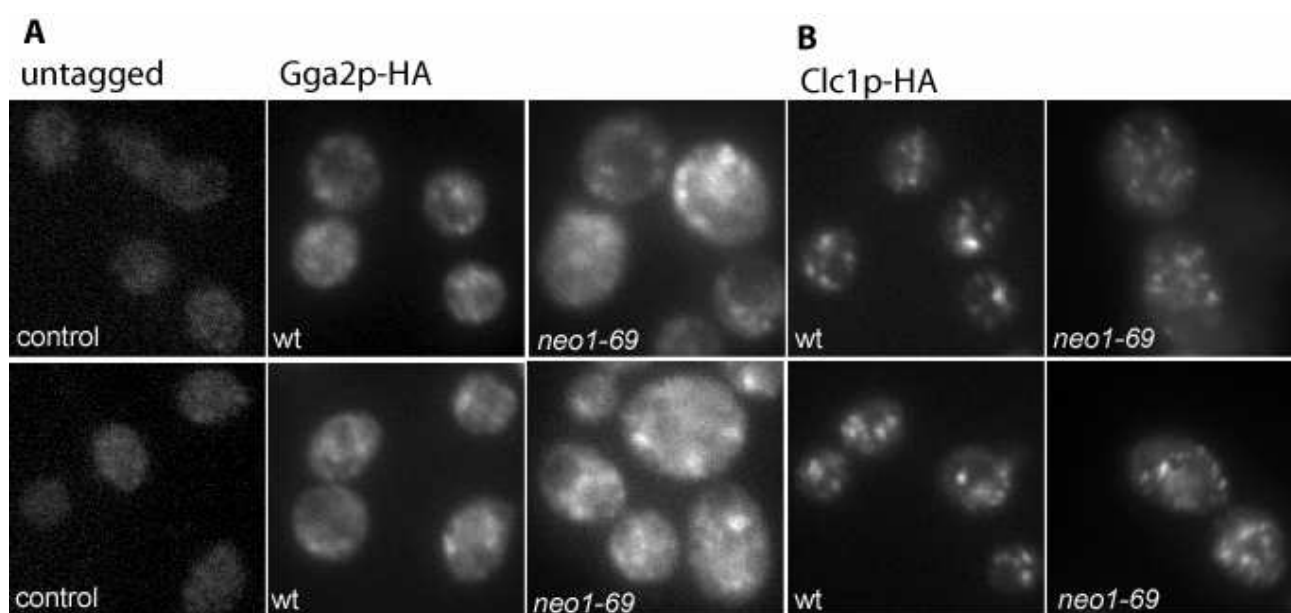
Fig. 13: Neo1-69p affects the subcellular distribution of Gga2p-HA. (A) Wild-type cells lacking the HA-epitope (BS64) (control), wild-type (wt) cells expressing Gga2p-HA (YML303), and *neo1-69* cells expressing Gga2p-HA (YML307) were grown at 25°C, fixed, and stained by indirect immunofluorescence with a monoclonal mouse anti-HA antibody as described in the Materials and Methods. (B) Indirect immunofluorescence was performed with wild type (BS1519) and *neo1-69* (BS1557) cells each expressing HA-Clc1p as described in the legend of Fig. 13A.

wild type cells (Fig. 13A). The quantification of this effect revealed that 19 % of the *neo1-69* cells (n = 241) exhibited the prominent punctuate pattern, similar to results obtained for Arl1p (25%) and Ysl2p (19%) (Wicky *et al.*, 2004). These results indicate that the examined protein Gga2p tends to accumulate in the *neo1-69* structures (brighter staining in some cells) comparable to the distribution of Ysl2p and Arl1p (Wicky *et al.*, 2004).

The staining of Clc1p, N-terminally tagged with a triple HA-epitope to preserve functionality (Böttcher *et al.*, 2006), was also analysed. No differences of the HA-Clc1p localisation in the *neo1-69* mutant could be observed compared to wild type (Fig. 13B). This observation is not unexpected, since clathrin participates in numerous processes within the cell and only a subset of clathrin molecules is possibly influenced by the *neo1-69* mutation. Thus, it remains to be proven, if a subset of clathrin molecules accumulates on abberant strunctures of the *neo1-69* mutant cells.

3.5.3 The localisation of Gga2p to endosomal structures is dependent on Arl1p

Until now the localisation of adaptor proteins was always closely related to Arf-GTPases, namely to Arf1p (Dell'Angelica *et al.*, 2000; Seaman *et al.*, 1996; Ooi *et al.*, 1998). Since the deletion of *GGA2* suppresses the *neo1-69* growth defect comparable to the deletion of *ARL1* (section 3.5.1, Wicky *et al.*, 2004), the next logical step was to analyse the possible dependence of the Gga2p localisation on the presence of Arl1p. Thus, Δ*arl1* cells expressing Gga2p-HA were stained by indirect immunofluorescence.

When compared to wild type, Δ*arl1* cells exhibited a more homogenous cytoplasmic staining pattern of Gga2p-HA. The punctuate structures were less obvious than in the wild type cells (Fig. 14). To demonstrate more clearly the possible decrease in punctuate staining between wild-type and Δ*arl1* cells, use was made of one class E *vps* mutant, *vps27*, in which abnormal, more expanded endosomal structures (class E compartment) accumulate in proximity to the vacuole (Piper *et al.*, 1995). Previously it was demonstrated that proteins such as Neo1p or Ysl2p collapse in the *vps27* cells (Wicky *et al.*, 2004; Jochum *et al.*, 2002), to form one or few large structures. Indirect immunofluorescence studies performed here confirmed the clump formation for the adaptor Gga2p already published in other recent studies (Hirst *et al.*, 2001; Boman *et al.*, 2002; Fig. 14). The deletion of *ARL1* in the *vps27* mutant resulted again in a diffuse cytoplasmic localisation of Gga2p-HA and no association

with the abnormal, expanded endosomal structures seen in *vps27 ARL1* cells (Fig. 14). Thus, Arl1p is responsible for the recruitment of Gga2p to TGN/endosomal structures.
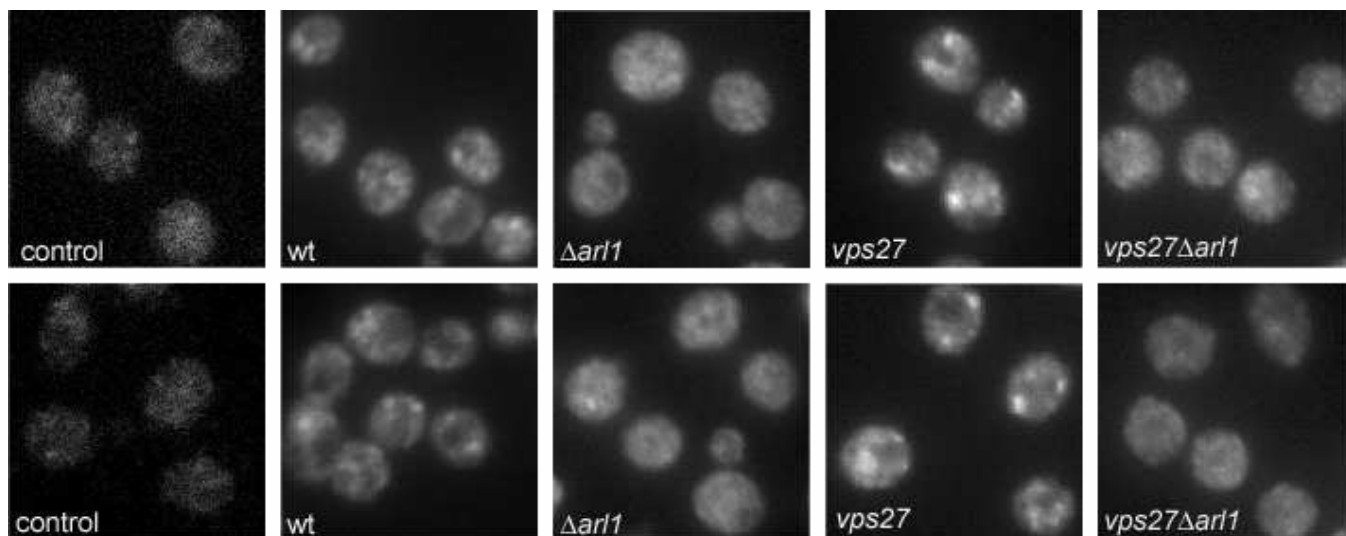

Fig. 14: Localisation of Gga2p-HA is affected by the loss of Arl1p. Indirect immunofluorescence was performed with untagged cells (BS64) (control), wild type (YML303), Δ*arl1* (YML360), *vps27* (YML333) and *vps27 Δarl1* (YML397) cells expressing Gga2p-HA as described in the legend to Fig. 13A.

From previous studies Gga2p was known to be recruited to membranes by Arf1p (Dell'Angelica *et al*., 2000). Thus, it was interesting to analyse the effect of the *ARF1* deletion on the Gga2p localisation in the *vps27* mutant. In accordance with expectations, the deletion of *ARF1* caused the same loss of punctuate staining in the *vps27* mutant as observed for the *vps27Δarl1* mutant (data not shown). Thus, the subset of Gga2p that collapses in the *vps27* mutant is dependent on both, Arl1p and Arf1p. If these two small GTPases recruit Gga2p to TGN/endosomal structures by collaboration or by independent pathways remains to be shown.

3.5.4 Deletion of *YSL2* severely perturbs the localisation of Gga2p

Since the *neo1-69* mutation has the same effect on the Ysl2p and Gga2p localisation (Wicky *et al*., 2004; section 3.5.2), it seems that both proteins are probably localized in the aberrant membrane protrusions caused by the *neo1-69* mutation. Further, in the present study Arl1p has been demonstrated to be responsible for the recruitment of Gga2p to endosomal membranes (section 3.5.3). Since Ysl2p interacts directly with Arl1p and has been proposed to be a GEF for this small GTPase (Jochum *et al*., 2002, see section 1.2.2), it was interesting to show whether Ysl2p may also be involved in this recruitment of Gga2p. Therefore, the

influence of the *YSL2* deletion on the localisation of Gga2p-HA was analysed by indirect immunofluorescence.

Remarkably, comparison of the staining pattern of Gga2p C-terminally tagged with a triple HA-epitope in wild type and Δ*ysl2* cells revealed that the deletion of *YSL2* caused a general loss of the punctuate Gga2p-HA staining (Fig. 15A). While in the wild type cells Gga2p-HA distributes between cytosol and distinct punctuate structures, the punctuate localisation of Gga2p is lost in Δ*ysl2* cells (Fig. 15A). Thus, Ysl2p has a function in the membrane association of this adaptor protein. To exclude the possibility that loss of *YSL2* results in a general mislocalization for all proteins which reside on TGN/endosomal structures, the staining pattern of Tlg1p-Myc, a SNARE protein that resides within the same compartment as Gga2p, Ysl2p, and Neo1p (Jahn and Scheller, 2006; Wicky *et al.*, 2004; see section 1.1.2.3) was also determined. However, in Δ*ysl2* cells the staining pattern of Tlg1p-Myc was similar to wild type cells (Fig. 15B), indicating that the loss of *YSL2* does not have pleiotropic effects on endosome biogenesis and membrane trafficking.

Earlier studies from the group of Dr. Birgit Singer-Kruger have demonstrated that overexpression of *ARL1* can suppress multiple defects of Δ*ysl2* cells including its impaired growth at 37°C, the defect in endocytosis and in vacuole biogenesis (Jochum *et al.*, 2002). Thus, it was consistent to analyse whether *ARL1* overexpression also restores the staining pattern of Gga2p in the Δ*ysl2* mutant cells. Therefore, Δ*ysl2* cells were transformed with 2 µm plasmids encoding *ARL1* or *ARF1*, respectively, and the staining pattern of Gga2p-HA was analysed (Fig. 15A). Consistent with previous results, *ARL1* overexpression was able to restore the Gga2p localisation to punctuate structures. In contrast, Δ*ysl2* cells overexpressing *ARF1* still exhibited the greatly diminished Gga2p-HA staining. Moreover, overexpression of *ARF1* further impaired the growth of Δ*ysl2*, while *ARL1* overexpression suppressed it (data not shown; Jochum *et al.*, 2002). Thus,Ysl2p may have a role in the localisation of Gga2p, likely mediated by Arl1p.
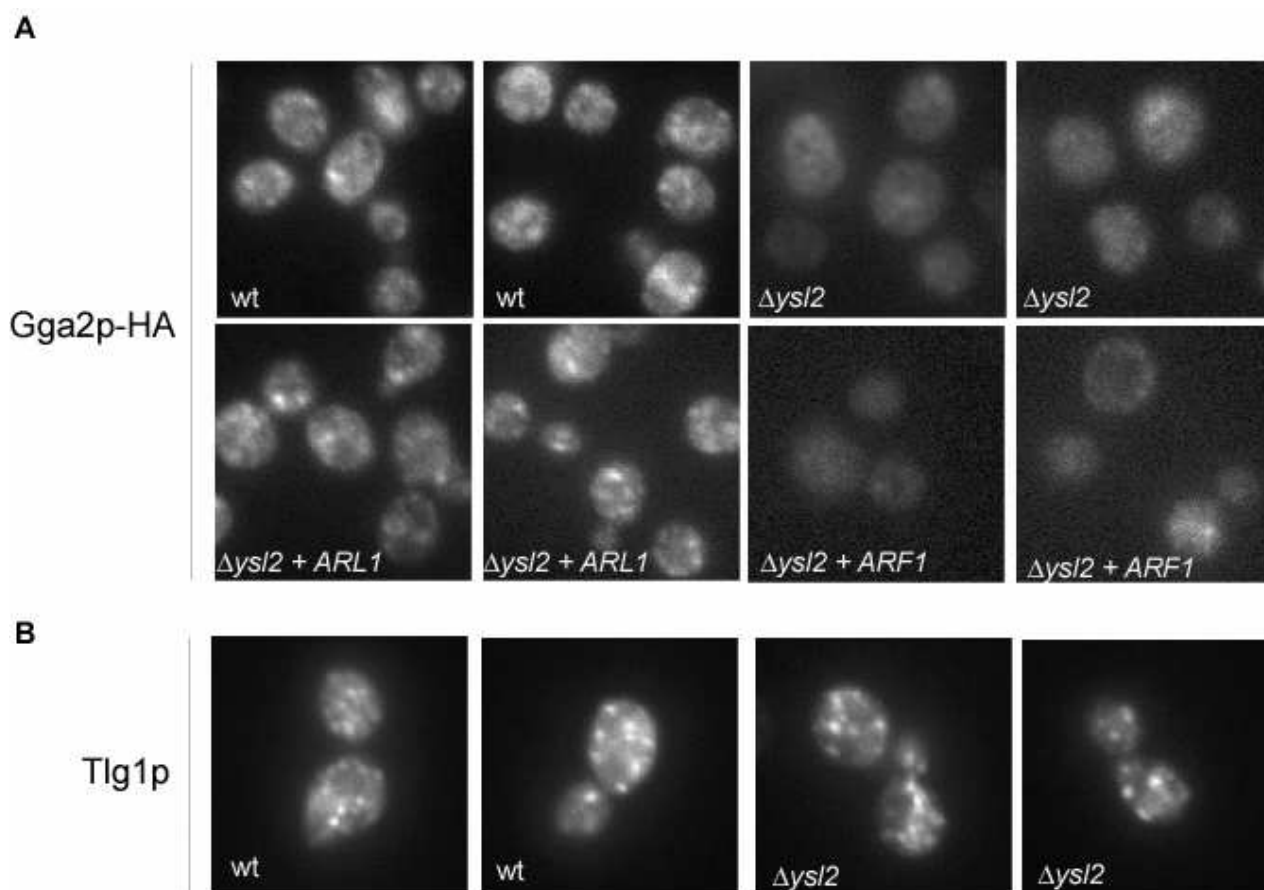
Fig. 15: Loss of Ysl2p severely affects the subcellular distribution of Gga2p-HA. (A) Indirect immunofluorescence was performed with wild type (YML303) and Δ*ysl2* (YML363) cells expressing Gga2p-HA as well as with Δ*ysl2* cells (YML363) transformed with either 2µm-based *ARL1 or 2 µ*m- based *ARF1* as described in the legend to Fig. 13A. (B) Wild-type (BS64) and Δ*ysl2* cells (BS695), each transformed with pmycTLG1 were grown in SD$_{-ura}$ medium at 25°C, fixed, and stained by indirect immunofluorescence with a rabbit anti-c-Myc antibody as described in Materials and Methods, section 2.1.4.3.

The localisation studies performed for Gga2p in Δ*arl1* and Δ*ysl2* cells have indicated a loss of punctuate structures in both deletion strains. Anyhow, the deletion of *YSL2* seems to result in a stronger loss of punctuate staining (Fig. 15), than the deletion of *ARL1* (Fig. 14). Subcellular fractionation was the method of choice to respond if the total cellular levels or/and the distribution between membranes and the cytosol is changed for Gga2p upon deletion of *ARL1* or *YSL2*. Analysis of the cell lysates of wild type, Δ*ysl2* and Δ*arl1* cells has demonstrated that the deletion of *YSL2* or *ARL1* had no effect on the total cellular levels of Gga2p-HA (Fig. 16A). For the fractionation the precleared lysate of wild type, Δ*ysl2* and Δ*arl1* cells was subjected to ultracentrifugation. The protein concentrations in the respective supernatant and pellet fractions were determined by the Microassay Bradford procedure (Bradford, 1976). Several quantities (µg) of the supernatant and pellet fractions of the

respective strain were loaded on the same SDS-gel. After immunoblotting, the intensity of the Gga2p bands derived from the pellet fractions was compared to that derived from the supernatant fractions (Fig. 16B). The amounts of pellet and supernatant fractions showing the same intensity of the Gga2p band for a given strain were determined. These values were divided by the total protein amounts of the pellet and supernatant fractions, respectively. The two ratios were then expressed using a common denominator, allowing the determination of the percentage of total Gga2p present in each fraction (see section 2.2.3.2). The Gga2p levels did not differ considerably in wild-type and the $\Delta ysl2$ mutant, approximately ~3/4 of the Gga2p-HA was found soluble and only ¼ bound to membranes (Fig. 16B).

Further, the pellet or supernatant fractions of wild type, $\Delta arl1$ and $\Delta ysl2$ cells were loaded on the same gel, respectively (Fig. 16C). Surprisingly, the quantities of Gga2p in the respective supernatant and pellet fractions were very similar. Only a slight accumulation of the higher mass band could be observed in the $\Delta ysl2$ muntant (Fig. 16C, marked with *), which could represent a covalently modified form of Gga2p (e.g. phosphorylation or ubiquitination). Previous studies by Hirst *et al.* (2001) demonstrated that the stability of membrane association upon freezing/thawing or lysis by homogenisation is much lower for GGAs than for AP-1. They used this experiment to explain why they cannot verify observed interactions of GGA proteins with biochemical methods. Therefore, the results of the subcellular fractionation performed in the present study may not reflect the real *in vivo* situation but rather artefacts of the experimental procedure.
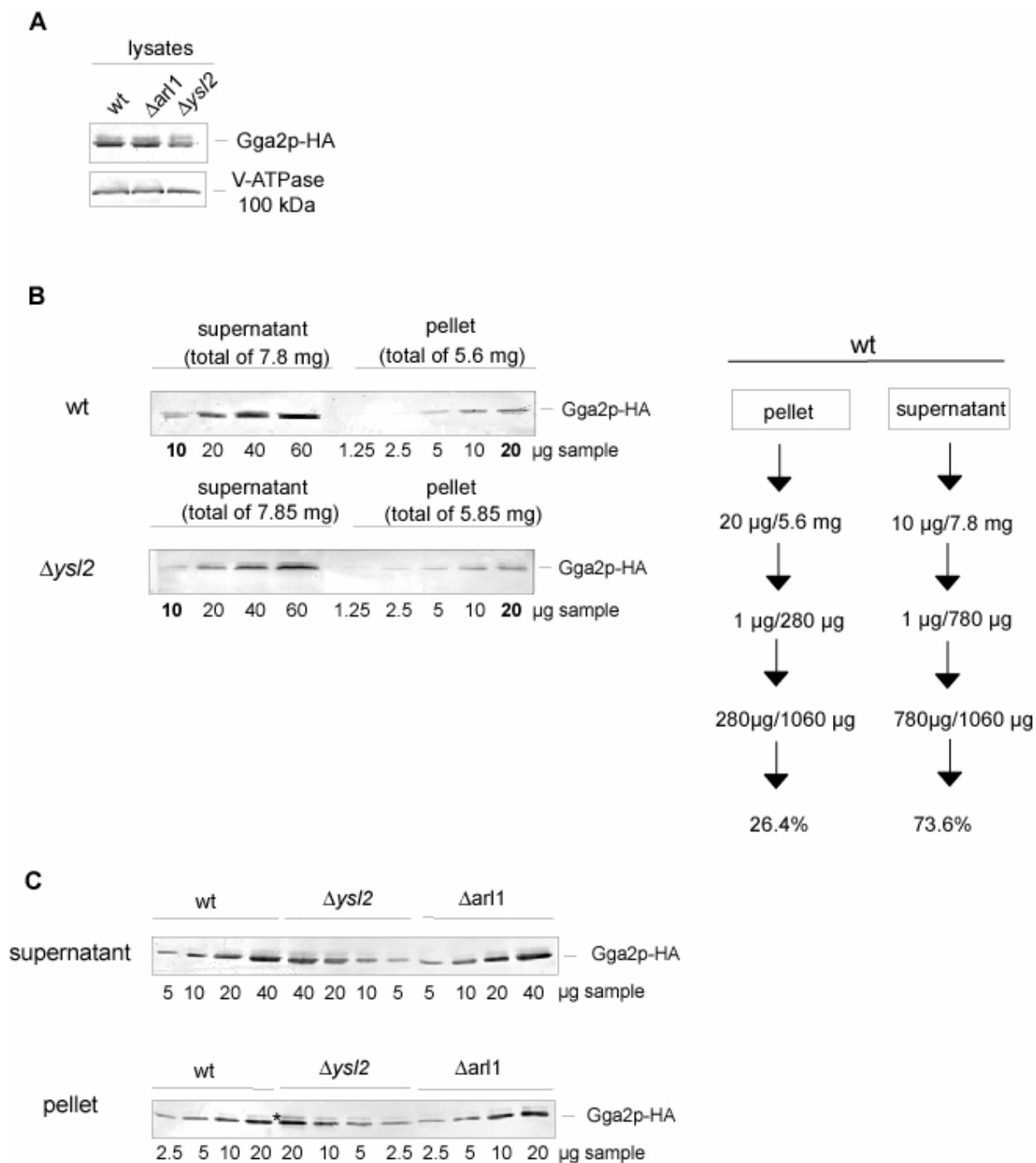
Fig. 16: Deletion of *YSL2* or *ARL1* does not perturb the subcellular distribution of Gga2p-HA according to the subcellular fractionation. (A) Lysates of Δ*ysl2* (YML363), Δ*arl1* (YML360) and wild type cells (YML303) were prepared with glass beads, same amounts were separated by SDS-PAGE. Gga2p-HA was detected by immunoblotting with monoclonal mouse anti-HA antibody. (B) Comparison of the Gga2p-HA quantities in pellet and supernatant fractions for Δ*ysl2* (YML363) and wild type cells (YML303). After a 100,000 x g centrifugation of a solubilised and precleared total cell lysate, several quantities of the supernatant and pellet fractions were analysed by SDS-PAGE. Gga2p-HA was detected by immunoblotting with the mouse anti-HA antibody. Determination of the percentage of membrane associated Gga2p was performed by loading several amounts (µg) of the pellet and supernatant fractions of either the wild type or Δ*ysl2* strain on a SDS-

polyacrylamid gel. After immunoblotting, the intensity of the Gga2p bands derived from the pellet fractions was compared to that derived from the supernatant fractions. Numbers in bold indicate the amounts in the pellet and supernatant, which are estimated to show an equivalent signal for Gga2p-HA. The calculation of the distribution (in percentage) of Gga2p-HA between the supernatant and pellet is shown for wild type cells as an example. The amounts of pellet and supernatant fractions showing the same intensity of the Gga2p band for a given strain were determined. These values were divided by the total protein amounts of the pellet and supernatant fractions, respectively. The two ratios were expressed using a common denominator, allowing the determination of the percentage of total Gga2p present in each fraction. (C) The pellet and supernatant fractions of Δarl1 (YML360), Δysl2 (YML363) and wild type cells (YML303) were compared considering the Gga2p-HA distribution. Cellfractionation was performed as in (B), several quantities of either the pellet or the supernatant fractions of all strains were loaded on the same SDS-gel. An enriched band in pellet fraction of the Δysl2 strain is indicated by an asterix (*).

3.5.5 *GGA1* and *GGA2* genetically interact with *ARL1*

Since several lines of evidence indicate a recruitment of Gga2p by Arl1p (see section 3.5.1 and 3.5.3), it was interesting to analyse the possible genetic interaction between *ARL1* and the *GGA* proteins.

Single deletions of *ARL1*, *GGA1* and *GGA2* are all known to have subtle or no growth defects and moderate deficiencies in membrane traffic (Lee *et al.*, 1997; Lu *et al.*, 2001; Dell'Angelica *et al.*, 2000; Hirst *et al.*, 2000; Zhdankina *et al.*, 2001). In the present study, the growth of the single Δgga1, Δgga2, and Δarl1 mutants, all possible double mutants and the triple Δgga1Δgga2Δarl1 mutant was compared at 25°C and 37°C (Fig. 17). At both temperatures all single and double mutants grew comparable to wild type, only for the *Δarl1Δgga2* a slight growth defect could be observed. The additional deletion of *GGA1* further impaired the growth. The defect could be observed at 25°C, but was clearly pronounced at 37°C. The result indicates that Arl1p and the GGA proteins regulate an important transport route in the TGN/endosomal system by a common effort.
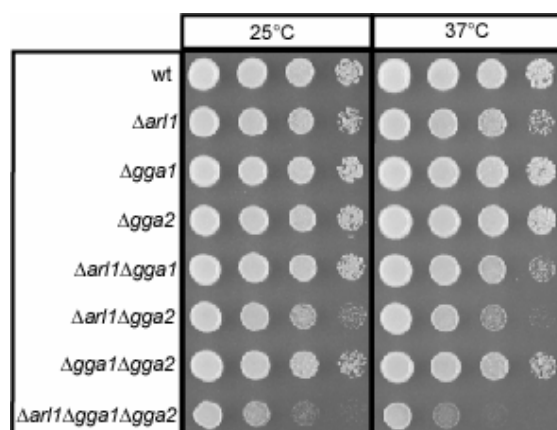
**Fig. 17: Δarl1Δgga2Δgga1 cells show strongly impaired growth.** Dilution series of wild type (BS64), Δarl1 (BS1105), Δgga2 (YML269), Δgga1 (YML268), Δgga2Δarl1 (YML318), Δgga1Δarl1 (YML355), Δgga1Δgga2 (CB255) and Δarl1Δgga2Δgga1 (YML460) cells were grown at 25° and 37°C.

3.5.6 Arl1p and Ysl2p interact physically with Gga2p

The immunofluorescence and genetic data (section 3.5.1-3.5.5) are highly indicative of a close connection between Gga2p and the Ysl2p-Arl1p-Neo1p network. Thus, it was of interest to analyse if the Gga2p localisation is mediated by direct interaction with these proteins. The interaction between Arl1p and Gga2p was of major interest, since the GGA proteins were to date regarded to be recruited to membranes in an Arf-dependent manner, but solely by the action of Arf1p (Zhdankina *et al.*, 2001). In former binding assays GGA subdomains were expressed as GST-fusions in *E. coli*, Arf1p was used either from bovine brain cytosol or was recombinantly expressed. GST-fusions were prebound to the glutathione-Sepharose and subsequently incubated with the Arf1p-containing sample in presence or absence of GTPγS (Boman *et al.*, 2000; Dell'Angelica *et al.*, 2000). Since GGAs are Arf1p effectors, the GTPase could be isolated only with constructs containing the GAT domain in a GTP dependent manner.

In the present work Gga2p was expressed as a GST-fusion that contains amino acids 1-326 of Gga2p including the VHS (Vps27, HRS, and STAM) domain that recognizes acidic-cluster-dileucine signals present in the cytosolic tails of cargo (Puertollano *et al.*, 2001a; Zhu *et al.*, 2001) and the GAT (GGA and TOM) domain that interacts with the GTP-bound form of ADP-ribosylation factors (Arfs) (Boman *et al.*, 2000; Dell'Angelica *et al.*, 2000; Puertollano *et al.*, 2001b). GST-Gga2$_{1-326}$ is similar to a construct of the homologous Gga1p previously used to demonstrate the interaction of Gga1p with Arf1p (Zhdankina *et al.*, 2001). The purified GST-fusions of Gga2p and the control proteins were rebound to the glutathion-Sepharose and incubated with a yeast cell lysate containing chromosomally HA-epitope tagged proteins. GST-pull down with Arl1p was of major interest, but Ysl2p and Neo1p were also analysed as well as several other proteins (Ysl1p, Vps13p and Sjl2p) as negative controls.

To analyse the physical interaction between Arl1p and Gga2p, GST-Gga2$_{1-326}$ was immobilized on glutathione-Sepharose beads and incubated with a yeast cell lysate containing Arl1p-HA (Fig. 18A). Purified GST and a GST-Ypt7p fusion were provided by Dr. Birgit Singer-Krüger as negative controls. GST-Ysl2N-term was previously demonstrated to interact with *in vitro* translated Arl1p (Jochum *et al.*, 2002) and was therefore included as a positive control. Although the intensity of the Arl1p-HA interaction with GST-Gga2$_{1-326}$ (Fig. 18A; lane 3) is weaker than with GST-Ysl2N-term (~50%) (Fig. 18A; lane 4), it is clearly distinguishable from the negative controls (Fig. 18A; lane 1 and 2) which show no binding of Arl1p-HA. Thus, Arl1p can bind to Gga2p *in vitro*.

Since Ysl2p was shown to be important for the Gga2p localisation (see section 3.5.4), it was further analysed if this dependence is caused by a direct interaction of the two proteins. Like for the GST-pull down with Arl1p-HA, GST-Gga2$_{1-326}$ was immobilized on glutathione-Sepharose beads and incubated with a yeast cell lysate containing Ysl2p-HA (Fig. 18A). Purified GST and a GST-Ypt7p fusion were provided Dr. Birgit Singer-Krüger as negative controls. Specific binding of Ysl2p-HA to GST-Gga2$_{1-326}$ (Fig. 18B; lane 3) but no binding to the control recombinant proteins GST and GST-Ypt7 (Fig. 18B; lane 1 and 2) could be detected. Thus, Ysl2p can bind to Gga2p *in vitro*. Since the membrane recruitment of adaptor proteins is thought to be mediated mainly by Arf-GTPases, the GST-Gga2$_{1-326}$ pull down with Ysl2p-HA was repeated with a Δ*arl1* lysate. The immunoblot analysis showed only a moderate reduction of isolated Arl1p-HA compared to the pull down in the wild type strain (Fig. 18C; lane 3 and 6), indicating that the interaction between Ysl2p and Gga2p is independent of Arl1p. In the reverse GST pull down experiment, different regions of Ysl2p were expressed as GST fusions and incubated with yeast lysate containing Gga2p-HA, but unfortunately, no interaction could be observed between the two proteins (data not shown). This may indicate that either the complete length or additional modifications of Ysl2p are necessary to mediate the interaction. Anyhow, it is also possible that the GST-Gga2$_{1-326}$ construct binds unspecifically to proteins so that the interactions demonstrated here are not representative.

Thus, to analyse the specificity of the GST-Gga2$_{1-326}$ interactions with Ysl2p-HA and Arl1p-HA other proteins known to participate in cellular transport processes were also included in the analysis (Fig.18D). Neo1p was analysed, since it is closely linked to Ysl2p and Arl1p (Wicky *et al.*, 2004) and has in this study been demonstrated to be important for the membrane recruitment of Gga2p (see section 3.5.1-3.5.2). Ysl1p localises to early endosomes (Sipos *et al.*, 2004), but does not seem to function in dependence on Ysl2p (see section 3.2), Vps13p is known to regulate the cycling of Kex2p on the TGN (Brickner and Fuller, 1997) and Sjl2p is known to regulate early endocytic processes (Böttcher *et al.*, 2006). Thus, all three proteins were included in the analysis as controls to exclude the possibility that proteins which participate in vesicular transport are generally enriched upon incubation on Sepharose beads with GST-Gga2$_{1-326}$. GST-Ypt7p and GST-Gga2$_{1-326}$ were immobilized on glutathione-Sepharose beads and incubated with a yeast cell lysate containing HA-Neo1p, Ysl1p-HA, Vps13p-HA or Sjl2p-HA. 0.8% NP-40 were used for the solubilisation of the proteins except in the case of HA-Neo1p, where 0.01% are known to preserve the interaction with Ysl2p (Wicky *et al.*, 2004).
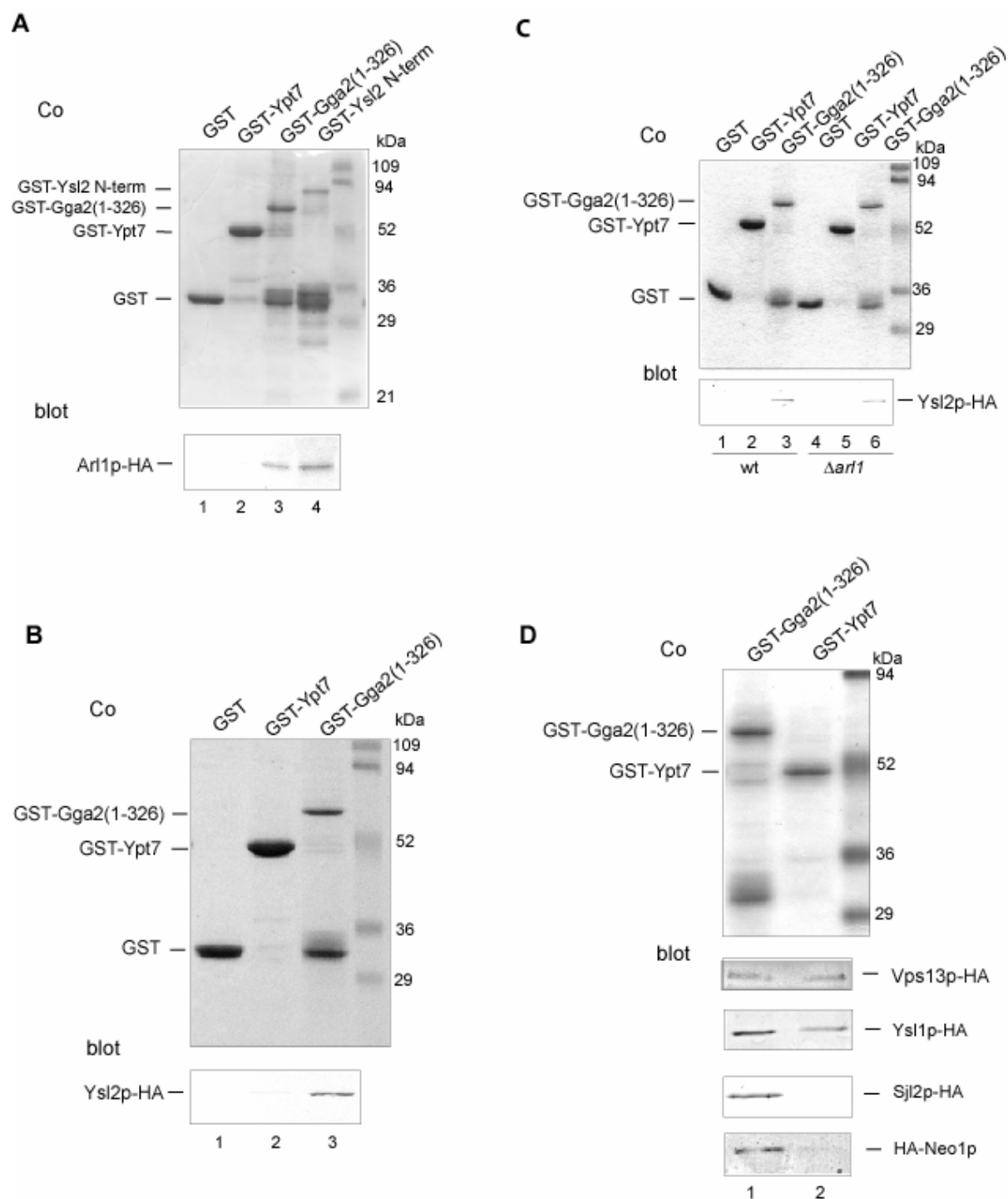
Fig. 18: Gga2p interacts *in vitro* with the Ysl2p/Arl1p/Neo1p network. (A) Arl1p-HA binds *in vitro* to Gga2p via a region containing the VHS-GAT domains of Gga2p. 80 µg of GST, GST-Ypt7, GST-Ysl2N-term and GST- Gga2$_{1-326}$ were immobilised onto glutathione-Sepharose beads and incubated with a detergent-solubilized (0.6 % Triton X-100) yeast cell lysate containing Arl1p-HA (YML346). After extensive washing, bound proteins were eluted and separated by SDS-PAGE. Recombinant proteins were stained with Coomassie brilliant blue (Co), Arl1p-HA was detected by immunoblotting using a monoclonal mouse anti-HA antibody. (B) Ysl2p-HA binds *in vitro* to Gga2p via the VHS-GAT domain of Gga2p. 80 µg of GST, GST-Ypt7 and GST- Gga2$_{1-326}$ were immobilised onto glutathione-Sepharose beads and incubated with a detergent-solubilized (0.6 % Triton X-100) yeast cell lysate containing Ysl2p-HA (BS1121). After extensive washing, bound proteins were eluted and separated by SDS-PAGE. Recombinant proteins were stained with Coomassie brilliant blue (Co), Ysl2p-HA was

detected by immunoblotting using a monoclonal mouse anti-HA antibody. (C) Ysl2p-HA binds *in vitro* to Gga2p via the VHS-GAT domain of Gga2p independently of Arl1p. 80 µg of GST, GST-Ypt7 and GST- Gga2$_{1-326}$ were immobilised onto glutathione-Sepharose beads and incubated with a wild type (BS1121) or *Δarl1* (YML424) detergent-solubilized (0.6 % Triton X-100) yeast cell lysate containing Ysl2p-HA. After extensive washing, bound proteins were eluted and separated by SDS-PAGE. Recombinant proteins were stained with Coomassie brilliant blue (Co), Ysl2p-HA was detected by immunoblotting using a monoclonal mouse anti-HA antibody. (D) Possible specificity of 80 µg of GST-Ypt7 and GST-Gga2$_{1-326}$ were immobilised onto glutathione-Sepharose beads and incubated with a yeast cell lysate containing Vps13p-HA (CB8), Ysl1p-HA (YML231), HA-Neo1p (BS1488) or Sjl2p-HA (BS1127). For the solubilisation of the yeast proteins 0.6% Triton X-100 was used, except for HA-Neo1p 0.01% NP-40. After extensive washing, bound proteins were eluted and separated by SDS-PAGE. Recombinant proteins were stained with Coomassie brilliant blue (Co), HA-tagged proteins were detected by immunoblotting using a monoclonal mouse anti-HA antibody.

HA-Neo1p was isolated by GST-Gga2$_{1-326}$ and not by GST-Ypt7 (Fig. 18D). Thus, like Ysl2p and Arl1p also Neo1p seemed to interact with Gga2p. Unfortunately, also Sjl2p-HA, which has a role in distinct early endocytic processes, was isolated specifically by GST-Gga2$_{1-326}$ and not by GST-Ypt7. Ysl1p-HA showed only a slight increase after isolation with GST-Gga2$_{1-326}$ compared to GST-Ypt7p. The GST-pull down with Vps13p-HA suggested that the GST-Gga2$_{1-326}$ construct did not enrich every protein similarly, since there is no difference between the weak interactions in the negative control (Fig.18D; lane 2) and GST-Gga2$_{1-326}$ (Fig.18D; lane 1). Anyhow, the specific interaction with Sjl2p and also the increase in the amount of isolated Ysl1p suggest that the GST-Gga2$_{1-326}$ construct interacts *in vitro* with many proteins which *in vivo* do not interact with Gga2p. Thus, the positive interactions with Ysl2p, Arl1p and Neo1p have also to be regarded with caution and to be confirmed by additional methods.

To confirm the interaction of Gga2p with Ysl2p and Arl1p co-immunoprecipitation experiments were performed in strains expressing Gga2p-HA/Ysl2p-Myc, Gga2p-Myc/Ysl2p-HA or Gga2p-Myc/Arl1p-HA by isolation of Gga2p via the respective antibody and immunoblot analysis of the coisolated proteins. Anyhow, no or only minor enrichment of Ysl2p or Arl1p could be observed when compared to strains with untagged Gga2p (data not shown). Remarkably, the analysis of the interaction of Gga2p with Ysl2p and Arl1p reminds of experiments considering the Ent4p-Ysl2p interaction (see section 3.3.1). In both cases the interaction could be shown by GST-pull down experiments but not by co-imunoprecipitations. For mammalian GGA proteins it has been shown that cycles of phosphorylation/ dephosphorylation regulate their binding to cargo proteins *in vivo* although *in vitro* the VHS domain of the GGAs could clearly bind to the respective cargo protein (Doray *et al*., 2002a).

Similar, cycles of phosphorylation could also regulate the interaction of Gga2p with Ysl2p or Arl1p. Mutations in the respective phosphorylation site in the hinge segment of Gga2p could help to analyse if the interactions to Ysl2p or Arl1p depend on this modification. Further, the dependence of the Gga2p-Arl1p interaction on the nucleotide state of Arl1p has not been analysed yet. If Gga2p is an effector of Arl1p, their interaction should be stabilized by the addition of nonhydrolysable GTP-analogue GTPγS to the co-immunoprecipitation experiment.

The controls in the GST-pull down (Fig. 18D) have demonstrated that GST-Gga2$_{1\text{-}326}$ seems to have a high rate of false positives partners in the GST-pull down assay. Thus, it is still possible that the Gga2p *in vivo* does not directly interact with Ysl2p or Arl1p. Anyhow, the genetic (section 3.5.1. and 3.5.5.) and microscopy data (section 3.5.3. and 3.5.4) have clearly demonstrated that Gga2p participates in common pathways with Arl1p and Ysl2p and that the localisation of Gga2p depends on the presence of Ysl2p and Arl1p. Additionally, the positive result from the GST-pull down assays with Ysl2p and Arl1p indicate that the dependence in Gga2p localisation is mediated by a direct interaction of Gga2p with Ysl2p and Arl1p. If the interaction is direct or mediated by e.g. Arf1p remains to be analysed by alternative biochemical assays.

3.6 Further studies considering physical interactions of the novel protein Tvp38p with Ysl2p

3.6.1 *In vitro* binding experiments verify the two hybrid interaction between Tvp38p and the N-terminus of Ysl2p

A two hybrid screen was recently performed in the group of Dr. Birgit Singer-Krüger with the Sec7 domain of Ysl2p (amino acids 211 to 514). The region has a remote homology to Sec7 family members and in known to be responsible for the Ysl2p-Arl1p interaction (Jochum *et al.*, 2002). Among the interacting partners a novel protein named Tvp38p was identified. The name originates from an experiment in which Tvp38p (Tlg2 compartment vesicle protein) was discovered in Tlg2-containing membrane fraction by proteomic analysis of immunoisolated Golgi subcompartments of *S. cerevisiae* (Inadome *et al.*, 2005). In agreement, indirect immunofluorescence studies performed in the group of Dr. Singer-Krüger demonstrated a TGN/early endosomal localisation for Tvp38p (A. Ziegler, Diplomarbeit). Its conserved sequence is found in higher eukaryotes, but these homologues have not been

characterized yet. Tvp38p is nonessential and the processing of CPY and ALP occurred in Δ*tvp38* cells as in the wild type (Inadome *et al*., 2005). Interestingly, pulse chase experiments performed in the group of B. Singer-Krüger showed that Vps10p seems to be more stabile in Δ*tvp38* cells than in wild type (A. Ziegler, Diplomarbeit). There is a genetic interaction between Tvp38p and Ypt51p, but Tvp38p does not seem to participate in the endocytic processes since LY and Ste2p transport are not perturbed.
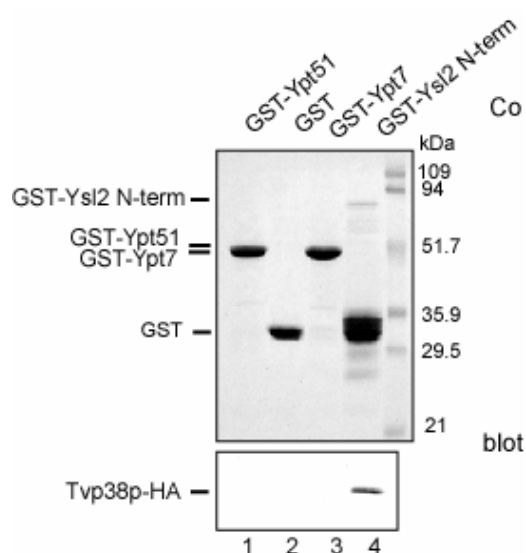
Fig. 19: Tvp38p interacts *in vitro* with the N-terminus of Ysl2p. GST and GST fusions were immobilized onto glutathione-Sepharose beads and incubated with a detergent-solubilized (0.6 % Triton x-100) yeast cell lysate containing HA-epitope tagged Tvp38p. After extensive washing, bound proteins were eluted and separated by SDS-PAGE. Recombinant proteins were stained with Coomassie Brilliant Blue (Co), Tvp38p-HA was detected by immunoblotting.

Co-immunoprecipitation experiments performed with Ysl2p-TAP and Tvp38p-HA in the group of Dr. Singer-Krüger confirmed the result of the two hybrid analysis. In the present work it was analysed if the result from the two hybrid and co-immunoprecipitation experiments can be verified with an *in vitro* GST-pull down experiment. For that purpose, the N-terminal region of Ysl2p (amino acids 2-514), containing the Sec7 domain used in the initial two-hybrid screen, was expressed in *E. coli* as a GST-fusion and purified by glutathione-Sepharose affinity purification. Purified GST, GST-Ypt7 and GST-Ypt51 were provided by the Dr. Birgit Singer-Krüger as negative controls. GST and GST-fusions were immobilized on glutathione-Sepharose beads and incubated with a detergent-solubilized yeast cell lysate containing triple HA-epitope tagged Tvp38p. The immunoblot analysis of the eluates revealed that Tvp38p-HA bound specifically to GST-Ysl2N-term (Fig. 19; lane 4) and

not to the control recombinant proteins (Fig. 19; lane 1-3). Thus, co-immunoprecipitation analysis could be verified, Tvp38p-HA can bind Ysl2p *in vitro*.

3.6.2 Tvp38p interacts with Sys1p *in vivo*

Recent large scale analysis of protein-protein interactions in *S. cerevisiae* using a split-ubiquitin technique, specifically applied for putative integral membrane proteins, identified Sys1p as a possible interaction partner of Tvp38p (Miller *et al*., 2005). Sys1p is an integral membrane protein that localizes to the TGN (Setty *et al*., 2004; Behnia *et al*., 2004). It has recently been demonstrated that Sys1p is the sole membrane receptor for the acetylated Arl3p, while Arl3p in turn is necessary for the Arl1p membrane binding (Setty *et al*., 2003; Setty *et al*., 2004; Behnia *et al*., 2004; Panic *et al*., 2003a; see section 1.2.2). Since Ysl2p has yet not been proven to be the GEF for Arl1p although their common role has been demonstrated (Jochum *et al*., 2002, Wicky *et al*., 2004; section 3.5), it would be highly interesting to prove if Tvp38p is a common interacting partner for Sys1p and Ysl2p. By that, an additional hint for a role of Ysl2p in the Sys1p/Arl3p/Arl1p network would be provided.

The putative *in vivo* interaction between Tvp38p and Sys1p was analysed in the present work by co-immunoprecipitation experiments. The co-immunoprecipitations were carried out using extracts of cells expressing either both Tvp38p-HA and Sys1p-Myc, or Tvp38p-HA alone (control strain). A strain expressing Sys1p C-terminally tagged with a Myc epitope was provided by the group of Dr. Birgit Singer-Krüger. After the lysis proteins were solubilized from the total cellular lysates by different concentrations of the detergent (0.01-1.25% NP-40). This titration of the detergent was applied, since for Neo1p, which is also an integral membrane protein, it has already been demonstrated that the increase of the detergent concentration abolishes the co-immunoprecipitation with Ysl2p (Wicky *et al*., 2004). Sys1p-Myc assemblies were isolated from the precleared lysate by affinity purification with an anti-Myc antibody coupled to protein A-Sepharose and released from the matrix by boiling in SDS-PAGE sample buffer. Immunoprecipitates were then analysed by immunoblotting using anti-HA and anti-Myc antibodies (see section 2.1.4.1). Sys1-Myc was solubilised in similar quantities at all detergent concentrations (Fig. 20A, anti-Myc blot). However, Tvp38p was found in immunoprecipitates from Sys1p-Myc expressing cells and not in the negative control, but as already shown for Neo1-Ysl2 interaction (Wicky *et al*., 2004), only in the presence of 0.01% NP-40 (Fig. 20A, anti-HA blot). The increase of the detergent concentration led to the complete loss of the interaction between Sys1p and Tvp38p.
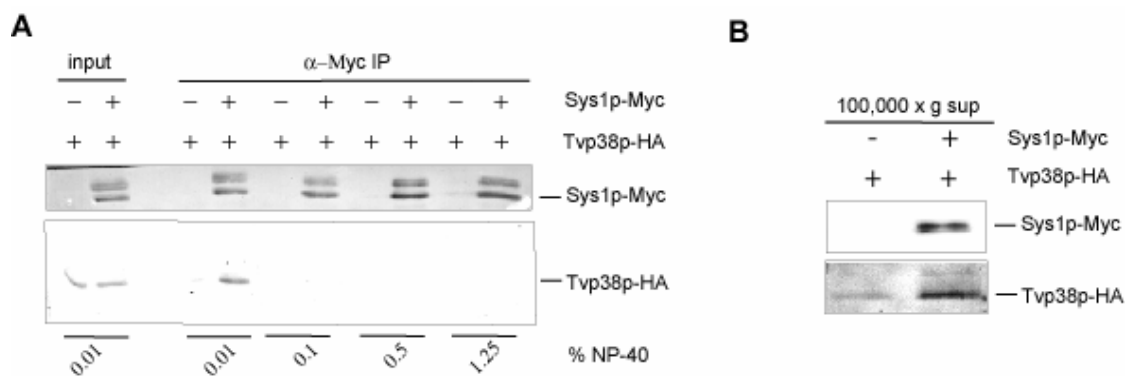
Fig. 20: Tvp38p associates with the integral membrane protein Sys1p. (A) Detergent (0.01% - 1.25% NP-40) solubilized lysates from cells (50 OD_{600} units) expressing Sys1p-Myc/Tvp38p-HA (CB223) or only Tvp38p-HA (BS1299) were cleared at 15,000 x g and subjected to immunoprecipitation using anti-Myc antibody and protein A-Sepharose. Isolated proteins (33.3 % of the total precipitates) were separated by SDS-PAGE and detected by immunoblotting using mouse monoclonal anti-Myc and anti-HA antibodies. (B) Detergent (0.01 % NP-40) solubilized lysates from cells (150 OD_{600} units) expressing Sys1p-Myc/Tvp38p-HA (CB223) or only Tvp38p-HA (BS1299) were cleared at 15,000 x g and subsequently at 100,000 x g. The supernatant was subjected to immunoprecipitation using an anti-Myc antibody and protein A-Sepharose. After binding, the proteins were eluted by heating in SDS-PAGE buffer with 8M urea at 50°C for 10 min. 33,3 % (for anti-HA detection) or 16,6 % (for anti-Myc) of the total precipitate were separated by SDS-PAGE and detected by immunoblotting with anti –Myc or anti-HA antibody as described in section 2.1.4.1.

To exclude the possibility that the Sys1p-Tvp38p interaction is mediated by membranes which include both proteins, Sys1p-Myc assemblies were isolated from precleared cell lysates, solubilised with 0.01% NP-40 and subsequently centrifuged for 1h at 100,000 x g to pellet unsolubilized material. The solubilized Tvp38p-HA still co-purified specifically with Sys1p-Myc (Fig. 20B, anti-HA blot). These data indicate that the *in vivo* interaction of Sys1p and Tvp38p is most likely mediated by the solubilised proteins and not by membranes.

4 Discussion

4.1 Loss of YSL2 perturbs the sorting of several components of the vacuolar fusion machinery

In the present work the compositions of Δ*ysl2* and wild type vacuoles were compared using two-dimensional electrophoresis and mass spectroscopy to identify proteins which are either strongly enriched or reduced in the vacuoles of the Δ*ysl2* mutant. By identification of these proteins the role of Ysl2p in transport processes could possibly be further specified.

The most prominent alteration upon *YSL2* deletion is the increase of vacuolar levels for Erg6p. In wild type cells Erg6p localises mainly in lipid droplets and the ER (Müllner *et al*., 2004; see section 1.1.4). There, on the contact zone between ER and lipid particles, Erg6p regulates one of the final maturation steps of the ergosterol synthesis, the C-24 methylation of zymosterol (Zinser *et al*., 1993; Parks *et al*., 1995). Interestingly, recent study has demonstrated that the lipid particles directly contact with early endosomes through the action of Rab GTPases (Liu *et al*., 2007), probably to transport lipids between these compartments. Erg6p could possibly be missorted in Δ*ysl2* cells during such contact from the lipid particle to endosomes and finally to the vacuole. That could explain its accumulation in the vacuoles of Δ*ysl2* cells, which was observed in the present study. If this mislocalisation causes changes in ergosterol levels remains to be determined.

Secondly, reduced actin levels could be observed on vacuoles of Δ*ysl2* cells. In wild type cells actin associates with vacuoles and its dynamic disassembly and reassembly has been implicated in several membrane fusion systems (Stamnes *et al.*, 2002; Eitzen*,* 2003). Recent reports have defined a role for lipids in the regulation of actin cytoskeleton remodelling in conjunction with vesicular trafficking (Friant *et al.,* 2001; Anes *et al.,* 2003). Further, Tedrick *et al*. (2004) provide links between ergosterol, the cytoskeleton and membrane fusion. They demonstrated that both growth defects and vacuole fragmentation caused by defects in the actin-remodelling machinery can be suppressed by the vacuolar sterol enrichment and greatly enhanced vacuole membrane fusion of *ERG6* upregulated cells. Thus, some perturbations in ergosterol synthesis could have conditioned reduced actin levels on Δ*ysl2* vacuoles. On the other hand, there are also several lines of evidence for a connection of Ysl2p with the actin network. Efe *et al*. (2005) observed a polarized accumulation of the N-terminal Ysl2p fragments in nascent buds (neck and cortical anchor) and a colocalization with cytoskeletal elements. Further, Singer-Krüger and Ferro-Novick (1997) reported that in *ysl2-1*

cells cortical actin patches were more randomly distributed over the periphery of both mother and daughter cell during all stages of the cell cycle. Thus, changes in the Ysl2p function could have a ubiquitous influence on the actin distribution.

Thirdly, the reduced vacuolar levels of some V-ATPase subunits could as well be observed in Δ*ysl2* cells. The V-ATPase was identified as an important component of lipid rafts (Yoshinaka *et al*., 2004) and Vma1p, a V-ATPase subunit, interacts also with Vrp1p, a part of the actin remodelling machinery (Gavin *et al*., 2002). Since additionally the V_0 complex is known to participate in the formation of the vacuole fusion channel (Peters *et al*., 2001; Bayer *et al*., 2003), the V-ATPase seems to be together with actin a component of the vacuole fusion machinery. Possible changes in ergosterol biosynthesis may cause defects in the assembly of the vacuole fusion machinery. If missorting of Erg6p to the vacuole causes alterations in ergosterol levels remains to be determined.

Mass spectroscopic analysis from the present work proposes a reduction of the aldolase level on the vacuole upon *YSL2* deletion. Former studies have already proposed a close connection between the aldolase and V-ATPase (Lu *et al*, 2001; Lu *et al*., 2004, see section 1.1.3). Thus, the reduction of the Fba1p levels on the vacuole could be caused by the reduction of the V-ATPase levels as observed in present study. In spite of that it remains astonishing that in the present study the mass spectroscopic result could not be confirmed by immunoblot analysis using a Fba1p-specific antibody. In the immunoblot analysis the Fba1p level was altered neither in the vacuole nor in the total cellular lysates.

The delay in the maturation of Ape1p, which is transported to the vacuole via the Cvt (cytoplasm to vacuole transport) pathway, is described for Δ*ysl2* cells by Efe *et al.* (2005, see also section 1.2.1). The Cvt vesicles fuse with the vacuolar membrane using the common vacuole fusion machinery. Further, as shown in present work probably one or more parts of this fusion machinery is missorted or its levels are reduced in the Δ*ysl2* cells. Thus, the problem in the Cvt pathway of Δ*ysl2* cells could have the same origin as the vacuole fragmentation and by that be a secondary effect of the *YSL2* deletion and not an evidence for a direct role of *YSL2* in the cytoplasm to vacuole transport, as proposed by Efe *et al*. (2005).

It would be interesting to compare the lipid composition of Δ*ysl2* and wild type cells to see if the *YSL2* deletion causes changes in ergosterol levels. The analysis of the vacuolar levels of other components of the vacuole fusion machinery could possibly show whether they are missorted as well. Cells with reduced ergosterol levels are more resistant to nystatin (Tedrick *et al*., 2004), thus it would be interesting to compare the growth of wild type and Δ*ysl2* cells after addition of this drug.

4.2 Ysl2p is possibly involved in the sorting of Kex2p

Since on the one hand the vacuole levels of the V-ATPase are reduced in Δ*ysl2* cells (see section 3.1) and on the other hand Ysl1p, a protein involved in the assembly of the V-ATPase is resident on early endosomes like Ysl2p (Sipos *et al*., 2004), it was conceivable that the Ysl2p role in the V-ATPase sorting is interceded by Ysl1p. For that reason, subcellular fractionation studies were conducted to analyse the effect of the *YSL2* deletion on the distribution of Ysl1p and the V-ATPase. The protocol used for the subcellular fractionation enables a separation of the early endosome on the one side from TGN and late endosome on the other side according to their physio-chemical characteristics (Sipos *et al*., 2004). The organelle fractionation was successful, since Ysl1p, known as an early endosomal marker, was found in distinct fractions than Kex2p or Pep12p, which are used as TGN and late endosome marker, respectively. Neither the localisation of Ysl1p, the V-ATPase 100 kDa subunit nor of any of the other TGN/endosome markers was affected by the deletion of *YSL2*. Thus, the subcellular fractionation experiment indicated that Ysl2p does not seem to be crucial for the sorting of Ysl1p or the V-ATPase proteins. Recently, Efe *et al*. (2005) analysed the distribution of Snc1p, Tlg2p and Chs3p, all known to be transported between TGN and endosomes, but have not observed any changes in Δ*ysl2* cells compared to wild type. Only at 37°C, where Δ*ysl2* cells display a severe growth defect, Efe *et al*. (2005) observed different internal distributions of Snc1p and Tlg2p, indicating a general membrane trafficking defect. Additionally, a slight missorting of p2CPY to the extracellular space observed in Δ*ysl2* cells (Jochum *et al*., 2002) could also be caused by a general trafficking defect. Thus, these minor changes in the distribution of analysed proteins (Jochum *et al*., 2002; Efe *et al*., 2005), support the result of the present fractionation experiment indicating that Ysl2p is not directly involved in the sorting of Ysl1p, V-ATPase, Pep12p, Tlg2p or Vps10p.

Interestingly, in the present study a 50% reduction of Kex2p cellular level in Δ*ysl2* cells could be observed. Therefore, it is possible that Ysl2p participates in the sorting of Kex2p. Similar reduction of the Kex2p cellular level could be observed in the Δ*gga1*Δ*gga2* strain (Mullins and Bonifacino, 2001). Further, *GGA* deficient cells show like *YSL2* deficient cells a delay in alpha factor maturation and in contrast to the reduced Kex2p levels, the Vps10p sorting is not perturbed (Hirst *et al*., 2000). This result is highly interesting with the view on the results from the present study, which have demonstrated a dependency of Gga2p on the Ysl2p network (see section 4.5). It would be interesting to analyse the putative common role of Ysl2p and Gga2p in the sorting of Kex2p between endosomes and TGN with alternative methods, e.g. pulse chase experiments.

Former fluorescence analysis of the Ysl2p localisation indicated both endosomal and TGN localisation for Ysl2p (Jochum *et al.*, 2002; Efe *et al.*, 2005, Gillingham *et al.*, 2006). The subcellular distribution of Ysl2p performed in this work demonstrates a major pool of Ysl2p in the same fractions as the early endosomal marker Ysl1p. Thus, the results from the present work support former results (Jochum *et al.*, 2002), which propose a primarily endosomal localisation for Ysl2p. Furthermore, the subcellular fractionation experiments from the present work specify the Ysl2p localisation as early endosomal.

4.3 Novel interaction partners of Ysl2

4.3.1 Ent4p is a putative interaction partner of Ysl2p

Two novel phosphoinositide-binding proteins, Ent3p and Ent5p, were identified in a two-hybrid screen for accessory proteins that interact with AP-1 and the GGAs in yeast (Duncan *et al.*, 2003). Capability of clathrin and cargo binding identified them as monomeric adaptors for sorting vesicles between the TGN and endosomes (Legendre-Guillemin *et al.*, 2004; Duncan *et al.*, 2003; Mills *et al.*, 2003; Chidambaram *et al.*, 2004; Hirst *et al.*, 2004) and also in the sorting of proteins into multivesicular bodies (Duncan *et al.*, 2003; Eugster *et al.*, 2004; Copic *et al.*, 2007). The interactions of Ent-proteins with AP-1 and GGAs were confirmed by biochemical methods. Remarkably, the proteins show different affinities for AP-1 and GGAs. Ent3p acts primarily with GGA proteins, whereas Ent5p acts with both AP-1 and GGA proteins but is more critical for AP-1-mediated transport (Costaguta *et al.*, 2006). Together, AP-1, Ent3p, Ent5p, and the GGAs cooperate in different ways to sort proteins between the TGN and the endosomes.

In the present work, a homologue of Ent3p and Ent5p, the uncharacterized protein Ent4p was identified as a novel putative interaction partner of Ysl2p in a two hybrid screen. Among all the identified clones it is the most interesting one, since Δ*ent4* is synthetic lethal with *ric1* and *ypt6* (Tong *et al.*, 2004) similar to the components of the Ysl2p-Arl1p-Neo1p network. Even more important was the identified cooperation between Ent proteins and Gga2p (Costaguta *et al.*, 2006), the novel interaction partner of Ysl2p and Arl1p (see section 3.5 and 4.5). To analyse if the two hybrid interaction between the PILT domain of Ysl2p (amino acids 662-1077) and Ent4p could be confirmed with alternative biochemical methods, a GST-pull down was performed, where only a weak interaction of Ent4p with the PILT subdomain of Ysl2p could be observed. The low specificity of the interaction could be caused by low amounts of the GST-Ysl2PILT fusion, since the quantities of purified GST-Ysl2PILT

were much lower than of GST-Ysl2N-term or GST-Ysl2EPLL. It is possible, that this subdomain of Ysl2p is only partially functional upon expression in *E. coli*, and therefore the comparably week interaction with Ent4p not representative. The N-terminus of Ysl2p interacted as well with Ent4p in the GST-pull down assay, despite of the negative two hybrid test with Ysl2N-term and Ent4p. It is possible that the interaction with Ent4p is mediated by the 3-dimensional structure of Ysl2p or that the N-terminus of Ysl2p has a higher level of unspecific binding. Unfortunately, the interaction between Ysl2p and Ent4p could not be verified *in vivo* although the procedure was performed similarly to the co-immunoprecipitation method used to demonstrate the interaction between Ent3p and Gga2p (Duncan *et al*., 2003).

Additionally to the interaction with Ysl2p, the GST-pull down experiment performed in present work demonstrated the interaction between Ent4p and Gga2p. This interaction would support further the analogy of Ent4p role to the adaptors Ent3p and Ent5p since these proteins were already shown to interact with GGAs. Nevertheless, it should be mentioned that for Ent3p and Ent5p the interaction was shown with the γ–ear domain of Gga2p and not with the VHS-GAT domain as found for Ent4p. Thus, it is possible that the co-purification of Ent4p-HA is indirect or caused by strong unspecific binding of the GST-Gga2p$_{(1-326)}$ construct. Experiments which demonstrate *in vivo* an interaction between Ent4p and Ysl2p or Gga2p would support the importance of the Ysl2p-Arl1p-Neo1p network for the Gga2p localisation (see section 3.5).

Another putative Ysl2p interaction partner identified by the two hybrid screen is Bud27p. However, a recent study has identified this URI-type (for Unconventional prefoldin RPB5 Interactor) prefoldin as a part of a larger complex involved in transcription, sumoylation and DNA repair (Tronnersjö *et al*., 2007). The same study has identified 16 putative interaction partners of Bud27p using a two hybrid approach. This high amount of two hybrid interaction partners could indicate a high rate of unspecific interactions for Bud27p in two hybrid screens. Due to this unspecific binding and the involvement of Bud27p in distinct cellular process it seems unlikely that Bud27p interacts *in vivo* with Ysl2p.

4.3.2 Possible explanations for lack of success in large scale purification of Ysl2p-TAP

Identification of interaction partners is one of the most successful methods to improve the understanding of the role for a given protein. Since the two hybrid screen did not reveal

novel interaction partners except Ent4p (see section 4.3.1), a large scale co-immunoprecipitation approach using Ysl2p-TAP was applied to search for proteins that physically interact with Ysl2p. However, the SDS-PAGE analysis of the Ysl2p isolate could not reveal any specific band purified only in the presence of Ysl2p and not with the negative control. Even the upscaling of the isolation did not allow the identification of Ysl2p-copurifying proteins. Astonishingly, Gillingham *et al*. (2006) were recently successful with a similar approach in their search for novel binding partners of Ysl2p. They inserted two copies of the IgG-binding Z domain of protein A at the C terminus of the *YSL2* gene in a strain that lacks the four major vacuolar proteases. Upon Coomassie staining of the immunoprecipitates, a prominent doublet could be observed. The bands were identified by mass spectroscopy as the Ysl2-ZZ fusion protein and Dop1p. The converse experiment confirmed this result (Gillingham *et al*., 2006) as well as the co-immunoprecipitation experiments by Efe *et al*. (2005), in which Ysl2p-GFP could be co-purified with Dop1p-HA.

There are several explanations for the loss of the Ysl2-Dop1 interaction during the purification procedure applied in the present work. The most prominent differences between the experimental conditions applied in the present work and the procedure used by Gillingham *et al*. are the choice of the epitope-tag and the strain background on the one side and the lysis method on the other side. Gillingham *et al*. have used a strain deficient in four major vacuolar proteases to increase the half-life of proteins in general. However, even in the presence of proteases the Ysl2-Dop1 interaction could be detected by Efe *et al*. (2005). Still, Efe *et al*. analysed their samples solely by immunoblotting and not by silver staining, thus it is unclear if the co-immunoprecipitation of Dop1p and Ysl2p is stochiometrical. An alternative explanation for the failure to detect the Ysl2p/Dop1p interaction in this work could be that upon TEV cleavage Ysl2p (186 kDa) tagged with the remaining calmodulin binding protein (CBP; 4kDa) was undistinguishable from Dop1p (194 kDa) due to similar sizes. Finally, the lysis method used in the present work could have been inappropriate for the identification of Ysl2p interaction partners. It consisted of grinding cells under liquid nitrogen, a method developed by Kellogg and Moazeed (2002) to preserve existing protein-protein interactions. Gillingham *et al*. (2006) used homogenisation of spheroblasted cells as the method of choice, which could probably be gentler than the grinding performed in this work and therefore may be more suitable for identification of interaction partners.

An interesting observation from the present work was that the growth of in the 20 l fermentation culture reduces the amounts of isolated Ysl2p per gram cells compared to the growth in the 2 l flask culture. This could be explained by the high density of the cell culture

at the harvest. While in the 2 l flask culture cells were harvested at ~ 1 OD_{600}/ml, in the continuous 20 l fermentation culture the pH and O_2 saturation of the culture were adjusted, so that cells were grown until 25 OD_{600} per ml cells. The high density may have caused changes in the Ysl2p expression but further analysis should be performed to confirm this observation, e.g. Ysl2p amounts should be compared at different densities for the 2 l and 20 l culture, respectively.

4.4 The C-terminus of Ysl2p is crucial for the interaction of the protein with itself

Since Ysl2p is a very large protein of 186 kDa, it was interesting to address which domains of the protein are important for function. Therefore, a deletion series was constructed in the present work, by which up to 900 C-terminal amino acids of Ysl2p were deleted in approximately 100 amino acid steps and exchanged by the TAP-epitope. Subsequently, the effect on the cell growth was analysed for the respective *YSL2*-deletions.

Remarkably, the last 100 amino acids of Ysl2p seem to have a crucial role for the protein function since their loss causes a similar growth defect as the deletion of the complete *YSL2* gene. This result is in agreement with studies from Efe *et al*. (2005), in which the deletion of only the F domain of Ysl2p (corresponds to the C-terminus) led to reduced restoration of cell growth when expressed from a 2 μ plasmid in a Δ*ysl2* strain. Analogous tests with chlorpromazine (CPZ), a cationic amphipathic molecule that changes the lateral organisation of cellular membranes (Jutila *et al*., 2001) and interacts with negatively charged lipids (Chen *et al*., 2003), show that only the constructs which contain the F-domain can suppress the CPZ sensitivity of the Δ*ysl2* cells (Efe *et al*., 2005). Thus, the C-terminal part of *YSL2* seams to be crucial for its function. Interestingly, this role seems to be independent of Arl1p, since the N-terminal region of Ysl2p is sufficient for the interaction between Ysl2p and Arl1p (Jochum *et al*., 2002). The putative role as an Arl1p GEF would in that case be only one of the functions of the Ysl2p protein. It is yet possible and remains to be shown, if the dimerisation of Ysl2p, which could here be specified for the C-terminus, is necessary for the interaction with Arl1p. The idea of Ysl2p having additionally to the putative GEF function also other roles in the cell is also supported by differences in deletion phenotypes: while Δ*arl1* cells show only slight growth and sorting defects (Lu *et al*., 2001; Jochum *et al*., 2002), the loss of *YSL2* severely inhibits the cell growth (Jochum *et al*., 2002). In this context

it remains puzzling, how the overexpression of *ARL1* suppresses all defects caused by the *YSL2* deletion analysed to date (Jochum *et al.*, 2002).

Unfortunately, no localisation studies could be performed with the mutant expressing Ysl2Δ100p-HA due to the high instability of the shortened version of Ysl2p. This would have helped to determine whether the crucial role of Ysl2p is connected to its membrane association and/or to its dimerisation. However, recently Efe *et al.* (2005) have demonstrated by fluorescence microscopy that while the construct encoding domains A and B of Ysl2p (N-terminus) is localised to punctuate structures, a construct encoding the C-terminal half of the protein is entirely cytosolic. Thus, the membrane association seems to primarily be mediated by the N-terminus (Efe *et al.*, 2005). On the other hand, the co-immunoprecipitation of Ysl2p-HA with Ysl2p-TAP performed in the present work and elsewhere (Efe *et al.*, 2005) was abolished by the C-terminal deletion of only 100 of the ~1600 amino acids as could be shown in the present study. Since the co-immunoprecipitation of Neo1p by Ysl2p is preserved even upon deletion of 500 amino acids, the C-terminal deletions do not seem to cause a protein misfolding but rather to disturb directly the dimerisation of Ysl2p. Thus, Ysl2p seems to dimerise via its C-terminal domain. Since the loss of the dimerisation is coupled to the severe growth defect, it seems probable that this dimerisation is crucial for the function of the entire protein, e.g. the putative role of Ysl2p as a scaffolding protein (Gillingham *et al.*, see section 1.2.1). Nevertheless, it is still unclear how the dimerisation is accomplished. In *vitro* analysis could not demonstrate an interaction between the C-terminus and any other part of the Ysl2p protein (see section 3.4.2). It is possible that a C-terminal modification (phosphorylation, ubiquitination) is necessary for the interaction or, alternatively, that the Ysl2-Ysl2 binding is not direct but mediated by a further component e.g. Dop1p. That could explain the inconsistence between the *in vivo* and *in vitro* analysis.

4.5 Gga2 is recruited to TGN/endosomal membranes by the Ysl2-Arl1-Neo1 network

The Neo1p-Arl1p-Ysl2p network is similar to the complex composed of the APL translocase Drs2p, Arf1p and the Sec7 family Arf GEF Gea2p, demonstrated to regulate vesicle formation on the TGN (Chantalat *et al.*, 2004). Due to that similarity, a role in vesicle budding is highly indicative for the Neo1p-Arl1p-Ysl2p network. However, since a family of Arl1 effectors, the GRIP domain proteins, function as vesicle tethers that promote vesicle targeting by mediating long-range contacts between opposing membranes (Whyte and Munro,

2002; Barr and Short, 2003; Graham, 2004), Arl1p was as well proposed to play a role in recruitment of vesicle tethers to membranes (Graham, 2004, Burd *et al.*, 2004; Munro, 2005). Nevertheless, earlier studies in mammalian cells suggested common effectors for Arf1p and Arl1p, e.g. Arfaptin1 and MKLP1 (Van Valkenburgh *et al.*, 2001). Further, the importance of Arl1p for the association of the adaptors COPI and AP-1 with the Golgi apparatus could be demonstrated (Lu *et al.*, 2001). These results were difficult to integrate in a proposed role of Arl1p, being solely a regulator of tethering. Thus, it was highly interesting to analyse whether the role of Arl1p upon membrane recruitment comprises as well the initiation of the vesicle formation.

In the present work the first evidence for the role of the Neo1p-Arl1p-Ysl2p network in the budding of vesicles was obtained by identifying additional suppressors of the *neo1-69* mutant. The *neo1-69* mutant accumulates aberrant membrane protrusions (Wicky *et al.*, 2004). Arl1p and Ysl2p possibly aggregate in such protrusions and the deletion of *ARL1* suppresses the *neo1-69* growth defect (Wicky *et al.*, 2004). To explain this suppression a model was proposed, in which the accumulation of Arl1p and its effectors may be responsible for the *neo1-69* growth defect so that the removal of Arl1p and associated proteins could restore the growth of the *neo1-69* mutant (Wicky *et al.*, 2004).

The identification of other *neo1-69* suppressors described here supports the role of Arl1p and its accessory proteins in the vesicle budding: while deletion of Ypt GTPases, which mainly regulate the tethering of vesicles, had no effect on the growth of the *neo1-69* mutant, the deletion of Arf GTPases caused suppression of the *neo1-69* growth defect to different extend. Arl3p is known to recruit Arl1p to membranes (Setty *et al.*, 2003; .Panic *et al.*, 2003, see section 1.2.2). Thus, the finding that the *ARL3* deletion suppresses the *neo1-69* growth defect similar to the deletion of *ARL1* is in agreement with the present model. It is interesting that the deletion of *ARF1* partially suppresses the *neo1-69* defect. This could be explained by the involvement of Arf1p in proximate reactions.

Suppressions obtained by deletion of adaptor proteins in the *neo1-69* mutant support the role of Arl1p in vesicle formation, but also further underline the specificity of this approach. Although all tested adaptors are principally known to be recruited to membranes by Arf1p (Stamnes and Rothman, 1993; Ooi *et al.*, 1998; Zhdankina *et al.*, 2001), their deletion had different effects on the growth of the *neo1-69* mutant; while the deletion of *GGA2* caused wild-type like growth, the deletion of other adaptors showed only a partial (AP-1, AP-3) or no suppression (*GGA1*). According to the model, the deletion of an Arl1-effector should cause suppression of the *neo1-69* growth defect with the similar strength like the loss of *ARL1* itself.

If Gga2p would be primarily recruited by Arf1p, loss of Arf1p should rescue similarly or better than loss of Arl1p. However, this was not the case. Therefore, it seems more likely that Gga2p is recruited by Arl1p/Arl3p. On the other hand, AP-1 and AP-3 are probably recruited by Arf1p to structures in proximity to Neo1p, since they suppress the *neo1-69* mutant in a similar range. Deletion of *GGA1* has no effect on the growth of the *neo1-69* mutant. A reason could be that Gga2p is much more abundant in the cell than Gga1p (Costaguta *et al.*, 2001). Thus, the *neo1-69* supression experiment does not provide any clear evidence concerning the Gga1-Arl1 interdependency, Gga1p could be an Arl1p effector as well.

The relationship between GGAs and AP-1 has up to date not been fully understood. Several biochemical studies have proven a close connection or even direct interaction (Costaguta *et al.*, 2001; Doray *et al.*, 2002a; Bai *et al.*, 2004). In contrast, results from genetic studies in yeast and mammalian cells are consistent with GGA and AP-1 function in distinct pathways (Black and Pelham, 2000; Meyer *et al.*, 2000; Puertollano *et al.*, 2001b, Ha *et al.*, 2003). In the present work, the partial suppression of the *neo1-69*-associated growth defect by deletion of *ARF1* and *APL2* indicates a close spatial connection between Arl1p and Arf1p and associated proteins.

The immunofluorescence results are in agreement with the model, in which the Ysl2-Neo1-Arl1p network recruits Gga2p to membranes and indicate a role for each of the three components for the localisation of Gga2p. Firstly, Gga2p accumulates in the aberrant membrane protrusions of the *neo1-69* mutant like earlier observed for Ysl2p and Arl1p (Wicky *et al.*, 2004). Secondly, localisation of Gga2p in the Δ*ysl2* and Δ*arl1* strains supported the independent role of both proteins in the recruitment of Gga2p. While the deletion of *YSL2* has a severe effect on the distribution of Gga2p, the deletion of *ARL1* had a less pronounced effect on the Gga2p localisation. The Gga2-Ysl2 interaction seems to be independent of Arl1p, since the interaction between GST-Gga2$_{(1-326)}$ and Ysl2p-HA could be partially reproduced in the absence of Arl1p. This would be consistent with the suggestion that the interaction between Gga proteins and Arf1p is not sufficient for the GGA recruitment (Boman *et al.*, 2002). Additionally to Arf GTPases other factors are thought to ensure the specific localization of adaptors (Bonifacino, 2004; Hirst *et al.*, 2001). Possibly, an additional interaction with Ysl2p stabilizes the Gga2p recruitment by Arl1p. On the other hand, it is remarkable that the *ARL1* overexpression suppresses all defects caused by the *YSL2* deletion tested so far, including the growth defect, vacuole fragmentation (Jochum *et al.*, 2002) and as shown in present work the severe mislocalisation of Gga2p. The specific suppression of the Gga2p mislocalisation in *Δysl2* cells by the overexpression of *ARL1* and not of *ARF1*

underlines also that the effect of Ysl2p on the Gga2p localisation is primarily linked to Arl1p and not Arf1p.

It remains unclear, if Gga2p is recruited to membranes by Arf1p and Arl1p independently of each other or by a common effort of the two GTPases. Lu *et al*. (2001) have proposed a shared role for the two GTPases in mammals, since dominantly active hARL1 also increases the Golgi localisation of hARF1. For yeast, it appears that the first interpretation is better applicable, since the search for suppressors of the *neo1-69* mutant from present work suggests a closer proximity between Arl1p and Gga2p than with Arf1p. Further biochemical experiments are necessary to demonstrate the nucleotide dependence of the Gga2p-Arl1p interaction, i.e. in the case that Gga2p is an Arl1p effector, an addition of GTPγS should increase the affinity of Gga2p for Arl1p. Interestingly, the GRIP-domain protein p56 has been identified in mammals as an accessory protein of GGAs and AP-1 (Lui *et al*., 2003; Bonifacino, 2004). Since GRIP domain proteins are identified as specific effectors of Arl1p (Panic *et al*., 2003a; Setty *et al*., 2003; Lu *et al*., 2003), this could be a further link for an implication of Arl1p in recruitment of coat adaptors. It would be interesting to analyse if there is a functional link between the yeast GRIP-domain protein Imh1p and GGAs.

The synthetic sickness of the triple Δ*arl1*Δ*gga2*Δ*gga1* mutant can be explained by a role for Arl1p and GGAs in both parallel and common pathways. Anyhow, since both Arl1p and Gga2p show a similar genetic interaction with the *neo1-69* mutant and interact in a biochemical assay and since the localisation of Gga2p depends on the presence of Arl1p, it seems probable that the GGA proteins and Arl1p play a role in a common pathway.

It is still unclear which transport pathway is regulated concertedly by Gga2p and the Ysl2-Arl1-Neo1 network. GGAs may be implicated in the anterograde and retrograde transport between the TGN and endosomes as well as in the selection of cargo during the MVB formation (Black and Pelham, 2000; Puertollano and Bonifacino, 2004; Scott *et al*., 2004; see section 1.1.2). On the other hand, the Ysl2-Arl1-Neo1 network has been suggested to regulate endocytosis, vacuolar protein sorting and vacuole biogenesis (Jochum *et al*., 2002; see section 1.2). Thus, Gga2p and the Ysl2-Arl1-Neo1-network could possibly play together a role in the maturation of early endosomes. This hypothesis is supported by the synthetic lethality of *ysl2-1* and Δ*ypt51*, a Rab GTPase known to regulate the early to late endosome transport (Singer-Krüger and Ferro-Novick, 1997). Further, the loss of the Gga2p-HA association with the *vps* E compartment of the Δ*arl1vps27* mutant, as observed in the present work, indicates that a fraction of Gga2p, which is dependent on Arl1p has an endosomal localisation. This endosomal localisation would as well be applicable to a role of Gga2p and

the Ysl2p-Arl1p-Neo1p network in retrograde transport from early endosome to TGN. This would be in agreement with the findings in mammalian cells which demonstrate that the depletion of hArl1 by RNA interference causes an early endosomal accumulation of proteins which normaly cycle between the TGN and endosomes, such as TGN46 (Lu and Hong, 2003; Yoshino et al., 2003). These experiments indicate a regulatory role for Arl1p in retrograde transport from endosomes to the TGN. On the other hand, similar CPY and Kex2p missorting exhibited by the Δysl2 and Δgga1Δgga2 mutants together with an additional TGN localisation of Arl1p and Ysl2p (Efe et al., 2005; Gillingham et al., 2006) could point to a related role for Gga2p and the Ysl2p-Arl1p-Neo1p network in the sorting from the TGN.

Although it is concievable that Gga2p and the Ysl2-Arl1-Neo1 network regulate multiple pathways, probably only a specific pathway is regulated by their combination. Thus, additional experiments e.g. the analysis of cargo sorting will be necessary to identify the common pathway for these proteins.

4.6 Tvp38p could unify the Ysl2-Arl1-Neo1 with the Sys1-Arl3-Arl1 network

A two hybrid screen performed previously in the group of B. Singer-Krüger with Ysl2N-term as bait identified Tvp38p as a possible interaction partner of Ysl2p. Subsequent co-immunoprecipitation studies using Ysl2p-TAP and Tvp38p-HA confirmed this interaction. The GST-pull down experiment performed in the present work provided additional support for these results. Further, the GST-pull down has demonstrated that the N-terminus of Ysl2p is sufficient for this interaction. Thus, Tvp38p seems to represent a Ysl2p-binding protein.

Interestingly, a large scale split ubiquitin screen developed to discover interactions between transmembrane proteins, identified Sys1p as an interaction partner of Tvp38p (Miller et al., 2005). Sys1p has been recently identified as a factor responsible for membrane association of Arl3p, which in turn recruits Arl1p to membranes (Behnia et al., 2004; Setty et al., 2004, see section 1.2.2). The Tvp38-Sys1 interaction could be confirmed in the present work by a co-immunoprecipitation approach. The solubilisation conditions (0.01% NP-40) identified to detect the Ysl2p-Neo1p interaction allowed to unravel the Tvp38-Ysl2 interaction and thus may be necessary to somehow preserve the conformation and/or lipid environment of the transmembrane proteins Neo1p and Tvp38p.

The finding that the integral membrane protein Tvp38p interacts with both Sys1p and Ysl2p allows postulating a model which combines the Sys1-Arl3-Arl1 network with the Ysl2-

Arl1-Neo1 network and confirms the close links between Ysl2p and Arl1p. Depletion of Arl3p causes a loss of the TGN localisation for Arl1p and its effector Imh1p (Behnia *et al*., 2004; Setty *et al*., 2003; Panic *et al*., 2003). Burd *et al*. (2004) proposed that Arl3p and Arl1p are activated sequentially and that the GEF for Arl1p might be an effector of Arl3p. It is possible that Ysl2p is this missing link that connects Arl3p and Arl1p to form an Arf GTPase cascade. Whether this is a correct idea remains to be shown by analysing the connection between Ysl2p and Arl3p.

Interestingly, the same large-scale split-ubiquitin screen also identified Gcs1p as an interaction partner of Tvp38p (Miller *et al*., 2005). Recently, Gcs1p was shown to be a GAP not only for Arf1p but also for Arl1p (Liu *et al*., 2005). Verification of the Gcs1-Tvp38 interaction by further biochemical studies would support a possible role of Tvp38p in the Arl1-network. The precise role of Tvp38p in this network still remains to be uncovered.

4.7. Future projects

Results from the present work revealed an importance of Ysl2p for the localisation of Erg6p. In the absence of Ysl2p, Erg6p mislocalises to the vacuole and its total cellular levels are reduced. To substantiate these results, it would be necessary to determine whether the mislocalisation of Erg6p can be demonstrated by an alternative method, e.g. subcellular fractionation. Moreover, it would be interesting to analyse whether this mislocalisation causes reduced cellular ergosterol levels. If this is the case, one could analyse wheter supplementation with ergosterol rescues the Δ*ysl2*-associated defects.

In the present work, Ent4p was identified in a two hybrid screen as a putative interaction partner of Ysl2p. This interaction was supported by a GST-pull down assay. Further binding studies, e.g. a reverse GST-pull down assay with recombinant Ent4p and yeast extract expressing Ysl2p-HA, would support this interaction. Furthermore, immunofluorescence studies with Ent4p in a Δ*ysl2* strain could help to analyse the dependence of the Ent4p localisation on the presence of Ysl2p. A possible genetic interaction of the Δe*nt4* deletion with the *neo1-69* or Δ*ysl2* mutations could be of interest as well. The interaction between Ent4p and Gga2p could also be verified with alternative methods, e.g. by analysing if the localisation of Ent4p depends on the presence of Gga2p like in the case of its homologues Ent3p and Ent5p (Duncan *et al*., 2003; Costaguta *et al*., 2006).

The positive Ysl2-Ysl2 co-immunoprecipitation and the relevance of the C-terminal 100 amino acids for this interaction is a further result of the present work. It remains to be

analysed whether the interaction is fulfilled by the C-terminus itself or if only a C-terminal modification (e.g. phosphorylation, ubiquitination) is needed for the dimerisation.

Finally, the role of the Ysl2-Arl1-Neo1 network for the localisation of Gga2p could be further analysed, e.g. the dependence of the Arl1-Gga2 interaction on GTP still remains to be shown. Further, the pathway, which is regulated commonly by the Ysl2-Arl1-Neo1 network and Gga2p, could be specified by e.g. analysis of the sorting for specific markers like Kex2p. Additionally, it would be interesting whether Arl1p also regulates the recruitment of other adaptors like AP-1 or Gga1p and whether this regulation is direct or mediated through Arf1p. Finally, it would be interesting, whether in the mammalian system hARL1 fulfils an analogous role by the analysis of the dependence of the hGGA3 (human homologue of Gga2p) localisation on the presence of hARL1 and hMON2.

5 Literature

Almers, W. (2001) Fusion needs more than SNAREs. *Nature*, **409**, 567-568.

Anes, E., Kuhnel, M.P., Bos, E., Moniz-Pereira, J., Habermann, A. and Griffiths, G. (2003) Selected lipids activate phagosome actin assembly and maturation resulting in killing of pathogenic mycobacteria. *Nat Cell Biol*, **5**, 793-802.

Antonny, B., Beraud-Dufour, S., Chardin, P. and Chabre, M. (1997) N-terminal hydrophobic residues of the G-protein ADP-ribosylation factor-1 insert into membrane phospholipids upon GDP to GTP exchange. *Biochemistry*, **36**, 4675-4684.

Araki, S., Kikuchi, A., Hata, Y., Isomura, M. and Takai, Y. (1990) Regulation of reversible binding of smg p25A, a ras p21-like GTP-binding protein, to synaptic plasma membranes and vesicles by its specific regulatory protein, GDP dissociation inhibitor. *J Biol Chem*, **265**, 13007-13015.

Arighi, C.N., Hartnell, L.M., Aguilar, R.C., Haft, C.R. and Bonifacino, J.S. (2004) Role of the mammalian retromer in sorting of the cation-independent mannose 6-phosphate receptor. *J Cell Biol*, **165**, 123-133.

Avaro, S., Belgareh-Touze, N., Sibella-Arguelles, C., Volland, C. and Haguenauer-Tsapis, R. (2002) Mutants defective in secretory/vacuolar pathways in the EUROFAN collection of yeast disruptants. *Yeast*, **19**, 351-371.

Babst, M., Katzmann, D.J., Snyder, W.B., Wendland, B. and Emr, S.D. (2002) Endosome-associated complex, ESCRT-II, recruits transport machinery for protein sorting at the multivesicular body. *Dev Cell*, **3**, 283-289.

Bagnat, M., Keranen, S., Shevchenko, A. and Simons, K. (2000) Lipid rafts function in biosynthetic delivery of proteins to the cell surface in yeast. *Proc Natl Acad Sci U S A*, **97**, 3254-3259.

Bai, H., Doray, B. and Kornfeld, S. (2004) GGA1 interacts with the adaptor protein AP-1 through a WNSF sequence in its hinge region. *J Biol Chem*, **279**, 17411-17417.

Balasubramanian, K. and Schroit, A.J. (2003) Aminophospholipid asymmetry: A matter of life and death. *Annu Rev Physiol*, **65**, 701-734.

Barlowe, C., Orci, L., Yeung, T., Hosobuchi, M., Hamamoto, S., Salama, N., Rexach, M.F., Ravazzola, M., Amherdt, M. and Schekman, R. (1994) COPII: a membrane coat formed by Sec proteins that drive vesicle budding from the endoplasmic reticulum. *Cell*, **77**, 895-907.

Barr, F.A. and Short, B. (2003) Golgins in the structure and dynamics of the Golgi apparatus. *Curr Opin Cell Biol*, **15**, 405-413.

Bayer, M.J., Reese, C., Buhler, S., Peters, C. and Mayer, A. (2003) Vacuole membrane fusion: V0 functions after trans-SNARE pairing and is coupled to the Ca2+-releasing channel. *J Cell Biol*, **162**, 211-222.

Becherer, K.A., Rieder, S.E., Emr, S.D. and Jones, E.W. (1996) Novel syntaxin homologue, Pep12p, required for the sorting of lumenal hydrolases to the lysosome-like vacuole in yeast. *Mol Biol Cell*, **7**, 579-594.

Bednarek, S.Y., Orci, L. and Schekman, R. (1996) Traffic COPs and the formation of vesicle coats. *Trends Cell Biol*, **6**, 468-473.

Behnia, R., Panic, B., Whyte, J.R. and Munro, S. (2004) Targeting of the Arf-like GTPase Arl3p to the Golgi requires N-terminal acetylation and the membrane protein Sys1p. *Nat Cell Biol*, **6**, 405-413.

Benito-Moreno, R.M., Miaczynska, M., Bauer, B.E., Schweyen, R.J. and Ragnini, A. (1994) Mrs6p, the yeast homologue of the mammalian choroideraemia protein: immunological evidence for its function as the Ypt1p Rab escort protein. *Curr Genet*, **27**, 23-25.

Black, M.W. and Pelham, H.R. (2000) A selective transport route from Golgi to late endosomes that requires the yeast GGA proteins. *J Cell Biol*, **151**, 587-600.

Boman, A.L., Zhang, C., Zhu, X. and Kahn, R.A. (2000) A family of ADP-ribosylation factor effectors that can alter membrane transport through the trans-Golgi. *Mol Biol Cell*, **11**, 1241-1255.

Boman, A.L., Salo, P.D., Hauglund, M.J., Strand, N.L., Rensink, S.J. and Zhdankina, O. (2002) ADP-ribosylation factor (ARF) interaction is not sufficient for yeast GGA protein function or localization. *Mol Biol Cell*, **13**, 3078-3095.

Bonangelino, C.J., Chavez, E.M. and Bonifacino, J.S. (2002) Genomic screen for vacuolar protein sorting genes in Saccharomyces cerevisiae. *Mol Biol Cell*, **13**, 2486-2501.

Bonifacino, J.S. (2004) The GGA proteins: adaptors on the move. *Nat Rev Mol Cell Biol*, **5**, 23-32.

Bonifacino, J.S. and Rojas, R. (2006) Retrograde transport from endosomes to the trans-Golgi network. *Nat Rev Mol Cell Biol*, **7**, 568-579.

Böttcher, C., Wicky, S., Schwarz, H. and Singer-Kruger, B. (2006) Sjl2p is specifically involved in early steps of endocytosis intimately linked to actin dynamics via the Ark1p/Prk1p kinases. *FEBS Lett*, **580**, 633-641.

Bradford, M.M. (1976) A rapid and sensitive method for the quantitation of microgram quantities of protein utilizing the principle of protein-dye binding. *Anal Biochem*, **72**, 248-254.

Bravo, J., Karathanassis, D., Pacold, C.M., Pacold, M.E., Ellson, C.D., Anderson, K.E., Butler, P.J., Lavenir, I., Perisic, O., Hawkins, P.T., Stephens, L. and Williams, R.L. (2001) The crystal structure of the PX domain from p40(phox) bound to phosphatidylinositol 3-phosphate. *Mol Cell*, **8**, 829-839.

Brickner, J.H. and Fuller, R.S. (1997) SOI1 encodes a novel, conserved protein that promotes TGN-endosomal cycling of Kex2p and other membrane proteins by modulating the function of two TGN localization signals. *J Cell Biol*, **139**, 23-36.

Brown, D.A. and London, E. (2000) Structure and function of sphingolipid- and cholesterol-rich membrane rafts. *J Biol Chem*, **275**, 17221-17224.

Brugger, B., Sandhoff, R., Wegehingel, S., Gorgas, K., Malsam, J., Helms, J.B., Lehmann, W.D., Nickel, W. and Wieland, F.T. (2000) Evidence for segregation of sphingomyelin and cholesterol during formation of COPI-coated vesicles. *J Cell Biol*, **151**, 507-518.

Burd, C.G., Strochlic, T.I. and Gangi Setty, S.R. (2004) Arf-like GTPases: not so Arf-like after all. *Trends Cell Biol*, **14**, 687-694.

Chantalat, S., Courbeyrette, R., Senic-Matuglia, F., Jackson, C.L., Goud, B. and Peyroche, A. (2003) A novel Golgi membrane protein is a partner of the ARF exchange factors Gea1p and Gea2p. *Mol Biol Cell*, **14**, 2357-2371.

Chantalat, S., Park, S.K., Hua, Z., Liu, K., Gobin, R., Peyroche, A., Rambourg, A., Graham, T.R. and Jackson, C.L. (2004) The Arf activator Gea2p and the P-type ATPase Drs2p interact at the Golgi in Saccharomyces cerevisiae. *J Cell Sci*, **117**, 711-722.

Chen, C.Y., Ingram, M.F., Rosal, P.H. and Graham, T.R. (1999) Role for Drs2p, a P-type ATPase and potential aminophospholipid translocase, in yeast late Golgi function. *J Cell Biol*, **147**, 1223-1236.

Chen, L. and Davis, N.G. (2000) Recycling of the yeast a-factor receptor. *J Cell Biol*, **151**, 731-738.

Chen, J.Y., Brunauer, L.S., Chu, F.C., Helsel, C.M., Gedde, M.M. and Huestis, W.H. (2003) Selective amphipathic nature of chlorpromazine binding to plasma membrane bilayers. *Biochim Biophys Acta*, **1616**, 95-105.

Chidambaram, S., Mullers, N., Wiederhold, K., Haucke, V. and von Mollard, G.F. (2004) Specific interaction between SNAREs and epsin N-terminal homology (ENTH) domains of epsin-related proteins in trans-Golgi network to endosome transport. *J Biol Chem*, **279**, 4175-4179.

Chvatchko, Y., Howald, I. and Riezman, H. (1986) Two yeast mutants defective in endocytosis are defective in pheromone response. *Cell*, **46**, 355-364.

Conibear, E. and Stevens, T.H. (1998) Multiple sorting pathways between the late Golgi and the vacuole in yeast. *Biochim Biophys Acta*, **1404**, 211-230.

Cooper, A.A. and Stevens, T.H. (1996) Vps10p cycles between the late-Golgi and prevacuolar compartments in its function as the sorting receptor for multiple yeast vacuolar hydrolases. *J Cell Biol*, **133**, 529-541.

Copic, A., Starr, T. and Schekman, R. (2007) Ent3p and Ent5p Exhibit Cargo-specific Functions in Trafficking Proteins between the Trans-Golgi Network and the Endosomes in Yeast 3. *Mol Biol Cell*. **18**, 1803-1815

Costaguta, G., Stefan, C.J., Bensen, E.S., Emr, S.D. and Payne, G.S. (2001) Yeast Gga coat proteins function with clathrin in Golgi to endosome transport. *Mol Biol Cell*, **12**, 1885-1896.

Costaguta, G., Duncan, M.C., Fernandez, G.E., Huang, G.H. and Payne, G.S. (2006) Distinct roles for TGN/endosome epsin-like adaptors Ent3p and Ent5p. *Mol Biol Cell*, **17**, 3907-3920.

Cowles, C.R., Odorizzi, G., Payne, G.S. and Emr, S.D. (1997) The AP-3 adaptor complex is essential for cargo-selective transport to the yeast vacuole. *Cell*, **91**, 109-118.

Darsow, T., Burd, C.G. and Emr, S.D. (1998) Acidic di-leucine motif essential for AP-3-dependent sorting and restriction of the functional specificity of the Vam3p vacuolar t-SNARE. *J Cell Biol*, **142**, 913-922.

Dascher, C. and Balch, W.E. (1994) Dominant inhibitory mutants of ARF1 block endoplasmic reticulum to Golgi transport and trigger disassembly of the Golgi apparatus. *J Biol Chem*, **269**, 1437-1448.

Daum, G., Lees, N.D., Bard, M. and Dickson, R. (1998) Biochemistry, cell biology and molecular biology of lipids of Saccharomyces cerevisiae. *Yeast*, **14**, 1471-1510.

Dell'Angelica, E.C., Klumperman, J., Stoorvogel, W. and Bonifacino, J.S. (1998) Association of the AP-3 adaptor complex with clathrin. *Science*, **280**, 431-434.

Dell'Angelica, E.C., Puertollano, R., Mullins, C., Aguilar, R.C., Vargas, J.D., Hartnell, L.M. and Bonifacino, J.S. (2000) GGAs: a family of ADP ribosylation factor-binding proteins related to adaptors and associated with the Golgi complex. *J Cell Biol*, **149**, 81-94.

Deloche, O., Yeung, B.G., Payne, G.S. and Schekman, R. (2001) Vps10p transport from the trans-Golgi network to the endosome is mediated by clathrin-coated vesicles. Mol Biol Cell, 12, 475-485.

Dittie, A.S., Hajibagheri, N. and Tooze, S.A. (1996) The AP-1 adaptor complex binds to immature secretory granules from PC12 cells, and is regulated by ADP-ribosylation factor. *J Cell Biol*, **132**, 523-536.

Doray, B., Ghosh, P., Griffith, J., Geuze, H.J. and Kornfeld, S. (2002a) Cooperation of GGAs and AP-1 in packaging MPRs at the trans-Golgi network. *Science*, **297**, 1700-1703.

Doray, B., Bruns, K., Ghosh, P. and Kornfeld, S. (2002b) Interaction of the cation-dependent mannose 6-phosphate receptor with GGA proteins. *J Biol Chem*, **277**, 18477-18482.

Duncan, M.C., Costaguta, G. and Payne, G.S. (2003) Yeast epsin-related proteins required for Golgi-endosome traffic define a gamma-adaptin ear-binding motif. *Nat Cell Biol*, **5**, 77-81.

Efe, J.A., Plattner, F., Hulo, N., Kressler, D., Emr, S.D. and Deloche, O. (2005) Yeast Mon2p is a highly conserved protein that functions in the cytoplasm-to-vacuole transport pathway and is required for Golgi homeostasis. *J Cell Sci*, **118**, 4751-4764.

Eitzen, G. (2003) Actin remodeling to facilitate membrane fusion. *Biochim Biophys Acta*, **1641**, 175-181.

Eugster, A., Pecheur, E.I., Michel, F., Winsor, B., Letourneur, F. and Friant, S. (2004) Ent5p is required with Ent3p and Vps27p for ubiquitin-dependent protein sorting into the multivesicular body. *Mol Biol Cell*, **15**, 3031-3041.

Fields, S. and Song, O. (1989) A novel genetic system to detect protein-protein interactions. *Nature*, **340**, 245-246.

Foote, C. and Nothwehr, S.F. (2006) The clathrin adaptor complex 1 directly binds to a sorting signal in Ste13p to reduce the rate of its trafficking to the late endosome of yeast. *J Cell Biol*, **173**, 615-626.

Forgac, M. (1999) Structure and properties of the clathrin-coated vesicle and yeast vacuolar V-ATPases. *J Bioenerg Biomembr*, **31**, 57-65.

Franzusoff, A. and Schekman, R. (1989) Functional compartments of the yeast Golgi apparatus are defined by the sec7 mutation. *Embo J*, **8**, 2695-2702.

Friant, S., Lombardi, R., Schmelzle, T., Hall, M.N. and Riezman, H. (2001) Sphingoid base signaling via Pkh kinases is required for endocytosis in yeast. *Embo J*, **20**, 6783-6792.

Futerman, A.H. and Riezman, H. (2005) The ins and outs of sphingolipid synthesis. *Trends Cell Biol*, **15**, 312-318.

Gaber, R.F., Copple, D.M., Kennedy, B.K., Vidal, M. and Bard, M. (1989) The yeast gene ERG6 is required for normal membrane function but is not essential for biosynthesis of the cell-cycle-sparking sterol. *Mol Cell Biol*, **9**, 3447-3456.

Gagescu, R., Demaurex, N., Parton, R.G., Hunziker, W., Huber, L.A. and Gruenberg, J. (2000) The recycling endosome of Madin-Darby canine kidney cells is a mildly acidic compartment rich in raft components. *Mol Biol Cell*, **11**, 2775-2791.

Gallusser, A. and Kirchhausen, T. (1993) The beta 1 and beta 2 subunits of the AP complexes are the clathrin coat assembly components. *Embo J*, **12**, 5237-5244.

Garcia-Mata, R. and Sztul, E. (2003) The membrane-tethering protein p115 interacts with GBF1, an ARF guanine-nucleotide-exchange factor. *EMBO Rep*, **4**, 320-325.

Gavin, A.C., Bosche, M., Krause, R., Grandi, P., Marzioch, M., Bauer, A., Schultz, J., Rick, J.M., Michon, A.M., Cruciat, C.M., Remor, M., Hofert, C., Schelder, M., Brajenovic, M., Ruffner, H., Merino, A., Klein, K., Hudak, M., Dickson, D., Rudi, T., Gnau, V., Bauch, A., Bastuck, S., Huhse, B., Leutwein, C., Heurtier, M.A., Copley, R.R., Edelmann, A., Querfurth, E., Rybin, V., Drewes, G., Raida, M., Bouwmeester, T., Bork, P., Seraphin, B., Kuster, B., Neubauer, G. and Superti-Furga, G. (2002) Functional organization of the yeast proteome by systematic analysis of protein complexes. *Nature*, **415**, 141-147.

Ghosh, P., Griffith, J., Geuze, H.J. and Kornfeld, S. (2003) Mammalian GGAs act together to sort mannose 6-phosphate receptors. *J Cell Biol*, **163**, 755-766.

Gillingham, A.K. and Munro, S. (2003) Long coiled-coil proteins and membrane traffic. *Biochim Biophys Acta*, **1641**, 71-85.

Gillingham, A.K., Tong, A.H., Boone, C. and Munro, S. (2004) The GTPase Arf1p and the ER to Golgi cargo receptor Erv14p cooperate to recruit the golgin Rud3p to the cis-Golgi. *J Cell Biol*, **167**, 281-292.

Gillingham, A.K., Whyte, J.R., Panic, B. and Munro, S. (2006) Mon2, a relative of large Arf exchange factors, recruits Dop1 to the Golgi apparatus. *J Biol Chem*, **281**, 2273-2280.

Gomes, E., Jakobsen, M.K., Axelsen, K.B., Geisler, M. and Palmgren, M.G. (2000) Chilling tolerance in Arabidopsis involves ALA1, a member of a new family of putative aminophospholipid translocases. *Plant Cell*, **12**, 2441-2454.

Graham, T.R., Scott, P.A. and Emr, S.D. (1993) Brefeldin A reversibly blocks early but not late protein transport steps in the yeast secretory pathway. *Embo J*, **12**, 869-877.

Graham, T.R. (2004) Membrane targeting: getting Arl to the Golgi. Curr Biol, 14, R483-485.

Grosshans, B.L., Ortiz, D. and Novick, P. (2006) Rabs and their effectors: achieving specificity in membrane traffic. *Proc Natl Acad Sci U S A*, **103**, 11821-11827.

Gruenberg, J. (2003) Lipids in endocytic membrane transport and sorting. *Curr Opin Cell Biol*, **15**, 382-388.

Gu, F., Crump, C.M. and Thomas, G. (2001) Trans-Golgi network sorting. *Cell Mol Life Sci*, **58**, 1067-1084.

Ha, S.A., Torabinejad, J., DeWald, D.B., Wenk, M.R., Lucast, L., De Camilli, P., Newitt, R.A., Aebersold, R. and Nothwehr, S.F. (2003) The synaptojanin-like protein Inp53/Sjl3 functions with clathrin in a yeast TGN-to-endosome pathway distinct from the GGA protein-dependent pathway. *Mol Biol Cell*, **14**, 1319-1333.

Haas, A. (1995) A quantitative assay to measure homotypic vacuole fusion in vitro. *Methods in Cell Science*, **17**, 283-294.

Hanahan, D. (1983) Studies on transformation of Escherichia coli with plasmids. *J Mol Biol*, **166**, 557-580.

Hao, M., Lin, S.X., Karylowski, O.J., Wustner, D., McGraw, T.E. and Maxfield, F.R. (2002) Vesicular and non-vesicular sterol transport in living cells. The endocytic recycling compartment is a major sterol storage organelle. *J Biol Chem*, *277*, 609-617.

Hechtberger, P., Zinser, E., Saf, R., Hummel, K., Paltauf, F. and Daum, G. (1994) Characterization, quantification and subcellular localization of inositol-containing sphingolipids of the yeast, Saccharomyces cerevisiae. *Eur J Biochem*, **225**, 641-649.

Heese-Peck, A., Pichler, H., Zanolari, B., Watanabe, R., Daum, G. and Riezman, H. (2002) Multiple functions of sterols in yeast endocytosis. *Mol Biol Cell*, **13**, 2664-2680.

Hirst, J., Lui, W.W., Bright, N.A., Totty, N., Seaman, M.N. and Robinson, M.S. (2000) A family of proteins with gamma-adaptin and VHS domains that facilitate trafficking between the trans-Golgi network and the vacuole/lysosome. *J Cell Biol*, **149**, 67-80.

Hirst, J., Lindsay, M.R. and Robinson, M.S. (2001) GGAs: roles of the different domains and comparison with AP-1 and clathrin. *Mol Biol Cell*, **12**, 3573-3588.

Hirst, J., Miller, S.E., Taylor, M.J., von Mollard, G.F. and Robinson, M.S. (2004) EpsinR is an adaptor for the SNARE protein Vti1b. *Mol Biol Cell*, **15**, 5593-5602.

Holthuis, J.C., Nichols, B.J. and Pelham, H.R. (1998) The syntaxin Tlg1p mediates trafficking of chitin synthase III to polarized growth sites in yeast. *Mol Biol Cell*, **9**, 3383-3397.

Hong, W. (2005) SNAREs and traffic. *Biochim Biophys Acta*, **1744**, 493-517.

Horazdovsky, B.F., Davies, B.A., Seaman, M.N., McLaughlin, S.A., Yoon, S. and Emr, S.D. (1997) A sorting nexin-1 homologue, Vps5p, forms a complex with Vps17p and is required for recycling the vacuolar protein-sorting receptor. *Mol Biol Cell*, **8**, 1529-1541.

Hornick, C.A., Hui, D.Y. and DeLamatre, J.G. (1997) A role for retrosomes in intracellular cholesterol transport from endosomes to the plasma membrane. *Am J Physiol*, **273**, C1075-1081.

Hua, Z., Fatheddin, P. and Graham, T.R. (2002) An essential subfamily of Drs2p-related P-type ATPases is required for protein trafficking between Golgi complex and endosomal/vacuolar system. *Mol Biol Cell*, **13**, 3162-3177.

Huttner, W.B. and Zimmerberg, J. (2001) Implications of lipid microdomains for membrane curvature, budding and fission. *Curr Opin Cell Biol,* **13**, 478-484

Inadome, H., Noda, Y., Adachi, H. and Yoda, K. (2005) Immunoisolaton of the yeast Golgi subcompartments and characterization of a novel membrane protein, Svp26, discovered in the Sed5-containing compartments. *Mol Cell Biol*, **25**, 7696-7710.

Ito, H., Fukuda, Y., Murata, K. and Kimura, A. (1983) Transformation of intact yeast cells treated with alkali cations. *J Bacteriol*, **153**, 163-168.

Jackson, C.L. and Casanova, J.E. (2000) Turning on ARF: the Sec7 family of guanine-nucleotide-exchange factors. *Trends Cell Biol*, **10**, 60-67.

Jackson, C.L. (2003) The Sec7 Family of Arf Guanine nucleotide Exchange Factors. ARF family GTPases by *Kluwer academic publishers*. 71-100

Jahn, R., Lang, T. and Sudhof, T.C. (2003) Membrane fusion. **Cell**, *112*, 519-533.

Jahn, R. and Scheller, R.H. (2006) SNAREs--engines for membrane fusion. *Nat Rev Mol Cell Biol*, **7**, 631-643.

Jenness, D.D. and Spatrick, P. (1986) Down regulation of the alpha-factor pheromone receptor in S. cerevisiae. *Cell*, **46**, 345-353.

Jochum, A., Jackson, D., Schwarz, H., Pipkorn, R. and Singer-Kruger, B. (2002) Yeast Ysl2p, homologous to Sec7 domain guanine nucleotide exchange factors, functions in endocytosis and maintenance of vacuole integrity and interacts with the Arf-Like small GTPase Arl1p. *Mol Cell Biol*, **22**, 4914-4928.

Jones, D.H., Bax, B., Fensome, A. and Cockcroft, S. (1999) ADP ribosylation factor 1 mutants identify a phospholipase D effector region and reveal that phospholipase D participates in lysosomal secretion but is not sufficient for recruitment of coatomer I. *Biochem J*, **341**, 185-192.

Jutila, A., Soderlund, T., Pakkanen, A.L., Huttunen, M. and Kinnunen, P.K. (2001) Comparison of the effects of clozapine, chlorpromazine, and haloperidol on membrane lateral heterogeneity. *Chem Phys Lipids*, **112**, 151-163.

Kahn, R.A. (2003) The ARF family. ARF family GTPases by *Kluwer academic publishers*, VII-XXIII.

Kaksonen, M., Toret, C.P. and Drubin, D.G. (2006) Harnessing actin dynamics for clathrin-mediated endocytosis. *Nat Rev Mol Cell Biol*, **7**, 404-414.

Kato, M. and Wickner, W. (2001) Ergosterol is required for the Sec18/ATP-dependent priming step of homotypic vacuole fusion. *Embo J*, **20**, 4035-4040.

Katzmann, D.J., Stefan, C.J., Babst, M. and Emr, S.D. (2003) Vps27 recruits ESCRT machinery to endosomes during MVB sorting. *J Cell Biol*, **162**, 413-423.

Kellogg, D.R. and Moazed, D. (2002) Protein- and immunoaffinity purification of multiprotein complexes. *Methods Enzymol*, **351**, 172-183.

Kirchhausen, T. (1999) Adaptors for clathrin-mediated traffic. *Annu Rev Cell Dev Biol*, **15**, 705-732.

Kirchhausen, T. (2000) Clathrin. *Annu Rev Biochem*, **69**, 699-727.

Kübler, E., Dohlman, H.G. and Lisanti, M.P. (1996) Identification of Triton X-100 insoluble membrane domains in the yeast Saccharomyces cerevisiae. Lipid requirements for targeting of heterotrimeric G-protein subunits. *J Biol Chem*, **271**, 32975-32980.

Lafont, F., Abrami, L. and van der Goot, F.G. (2004) Bacterial subversion of lipid rafts. *Curr Opin Microbiol*, **7**, 4-10.

Lange, Y., Swaisgood, M.H., Ramos, B.V. and Steck, T.L. (1989) Plasma membranes contain half the phospholipid and 90% of the cholesterol and sphingomyelin in cultured human fibroblasts. *J Biol Chem*, **264**, 3786-3793.

Lange, Y., Ye, J. and Steck, T.L. (1998) Circulation of cholesterol between lysosomes and the plasma membrane. *J Biol Chem*, **273**, 18915-18922.

Leammli, U.K. (1970) Cleavage of structural proteins during the assembly of the head of bacteriophage T4. *Nature*, **227**, 680-685.

Leber, R., Zinser, E., Zellnig, G., Paltauf, F. and Daum, G. (1994) Characterization of lipid particles of the yeast, Saccharomyces cerevisiae. *Yeast*, **10**, 1421-1428.

Lee, F.J., Huang, C.F., Yu, W.L., Buu, L.M., Lin, C.Y., Huang, M.C., Moss, J. and Vaughan, M. (1997) Characterization of an ADP-ribosylation factor-like 1 protein in Saccharomyces cerevisiae. *J Biol Chem*, **272**, 30998-31005.

Legendre-Guillemin, V., Wasiak, S., Hussain, N.K., Angers, A. and McPherson, P.S. (2004) ENTH/ANTH proteins and clathrin-mediated membrane budding. *J Cell Sci*, **117**, 9-18.

Lemmon, S.K. and Traub, L.M. (2000) Sorting in the endosomal system in yeast and animal cells. *Curr Opin Cell Biol*, **12**, 457-466.

Lewis, M.J., Nichols, B.J., Prescianotto-Baschong, C., Riezman, H. and Pelham, H.R. (2000) Specific retrieval of the exocytic SNARE Snc1p from early yeast endosomes. *Mol Biol Cell*, **11**, 23-38.

Li, H., Adamik, R., Pacheco-Rodriguez, G., Moss, J. and Vaughan, M. (2003) Protein kinase A-anchoring (AKAP) domains in brefeldin A-inhibited guanine nucleotide-exchange protein 2 (BIG2). *Proc Natl Acad Sci U S A*, **100**, 1627-1632.

Liu, Y.W., Huang, C.F., Huang, K.B. and Lee, F.J. (2005) Role for Gcs1p in regulation of Arl1p at trans-Golgi compartments. *Mol Biol Cell*, **16**, 4024-4033.

Liu, P., Bartz, R., Zehmer, J.K., Ying, Y.S., Zhu, M., Serrero, G. and Anderson, R.G. (2007) Rab-regulated interaction of early endosomes with lipid droplets. *Biochim Biophys Acta*, **1773**, 784-793.

Longtine, M.S., McKenzie, A., 3rd, Demarini, D.J., Shah, N.G., Wach, A., Brachat, A., Philippsen, P. and Pringle, J.R. (1998) Additional modules for versatile and economical PCR-based gene deletion and modification in Saccharomyces cerevisiae. *Yeast*, **14**, 953-961.

Longva, K.E., Blystad, F.D., Stang, E., Larsen, A.M., Johannessen, L.E. and Madshus, I.H. (2002) Ubiquitination and proteasomal activity is required for transport of the EGF receptor to inner membranes of multivesicular bodies. *J Cell Biol*, **156**, 843-854.

Lowe, S.L., Wong, S.H. and Hong, W. (1996) The mammalian ARF-like protein 1 (Arl1) is associated with the Golgi complex. *J Cell Sci*, **109** (Pt 1), 209-220.

Lu, M., Holliday, L.S., Zhang, L., Dunn, W.A., Jr. and Gluck, S.L. (2001) Interaction between aldolase and vacuolar H+-ATPase: evidence for direct coupling of glycolysis to the ATP-hydrolyzing proton pump. J Biol Chem, 276, 30407-30413.

Lu, L. and Hong, W. (2003) Interaction of Arl1-GTP with GRIP domains recruits autoantigens Golgin-97 and Golgin-245/p230 onto the Golgi. *Mol Biol Cell*, **14**, 3767-3781.

Lu, M., Sautin, Y.Y., Holliday, L.S. and Gluck, S.L. (2004) The glycolytic enzyme aldolase mediates assembly, expression, and activity of vacuolar H+-ATPase. *J Biol Chem*, **279**, 8732-8739.

Lui, W.W., Collins, B.M., Hirst, J., Motley, A., Millar, C., Schu, P., Owen, D.J. and Robinson, M.S. (2003) Binding partners for the COOH-terminal appendage domains of the GGAs and gamma-adaptin. *Mol Biol Cell*, **14**, 2385-2398.

Luzio, J.P., Mullock, B.M., Pryor, P.R., Lindsay, M.R., James, D.E. and Piper, R.C. (2001) Relationship between endosomes and lysosomes. *Biochem Soc Trans*, **29**, 476-480.

Lyons, T.J., Villa, N.Y., Regalla, L.M., Kupchak, B.R., Vagstad, A. and Eide, D.J. (2004) Metalloregulation of yeast membrane steroid receptor homologs. *Proc Natl Acad Sci U S A*, **101**, 5506-5511.

Maldonado-Baez, L. and Wendland, B. (2006) Endocytic adaptors: recruiters, coordinators and regulators. *Trends Cell Biol*, **16**, 505-513.

Mattera, R., Arighi, C.N., Lodge, R., Zerial, M. and Bonifacino, J.S. (2003) Divalent interaction of the GGAs with the Rabaptin-5-Rabex-5 complex. *Embo J*, **22**, 78-88.

Meyer, C., Zizioli, D., Lausmann, S., Eskelinen, E.L., Hamann, J., Saftig, P., von Figura, K. and Schu, P. (2000) mu1A-adaptin-deficient mice: lethality, loss of AP-1 binding and rerouting of mannose 6-phosphate receptors. *Embo J*, **19**, 2193-2203.

Miller, J.P., Lo, R.S., Ben-Hur, A., Desmarais, C., Stagljar, I., Noble, W.S. and Fields, S. (2005) Large-scale identification of yeast integral membrane protein interactions. *Proc Natl Acad Sci U S A*, **102**, 12123-12128.

Mills, I.G., Praefcke, G.J., Vallis, Y., Peter, B.J., Olesen, L.E., Gallop, J.L., Butler, P.J., Evans, P.R. and McMahon, H.T. (2003) EpsinR: an AP1/clathrin interacting protein involved in vesicle trafficking. *J Cell Biol*, **160**, 213-222.

Mouratou, B., Biou, V., Joubert, A., Cohen, J., Shields, D.J., Geldner, N., Jurgens, G., Melancon, P. and Cherfils, J. (2005) The domain architecture of large guanine nucleotide exchange factors for the small GTP-binding protein Arf. *BMC Genomics*, **6**, 20.

Mukherjee, S. and Maxfield, F.R. (2004) Membrane domains. *Annu Rev Cell Dev Biol*, **20**, 839-866.

Mulholland, J., Konopka, J., Singer-Kruger, B., Zerial, M. and Botstein, D. (1999) Visualization of receptor-mediated endocytosis in yeast. *Mol Biol Cell*, **10**, 799-817.

Mullins, C. and Bonifacino, J.S. (2001) Structural requirements for function of yeast GGAs in vacuolar protein sorting, alpha-factor maturation, and interactions with clathrin. *Mol Cell Biol*, **21**, 7981-7994.

Müllner, H., Zweytick, D., Leber, R., Turnowsky, F. and Daum, G. (2004) Targeting of proteins involved in sterol biosynthesis to lipid particles of the yeast Saccharomyces cerevisiae. *Biochim Biophys Acta*, **1663**, 9-13.

Munn, A.L., Heese-Peck, A., Stevenson, B.J., Pichler, H. and Riezman, H. (1999) Specific sterols required for the internalization step of endocytosis in yeast. *Mol Biol Cell,* **10**, 3943-3957.

Munn, A.L. (2001) Molecular requirements for the internalisation step of endocytosis: insights from yeast. *Biochim Biophys Acta*, **1535**, 236-257.

Munro, S. (2005) The Arf-like GTPase Arl1 and its role in membrane traffic. *Biochem Soc Trans*, **33**, 601-605.

Muren, E., Oyen, M., Barmark, G. and Ronne, H. (2001) Identification of yeast deletion strains that are hypersensitive to brefeldin A or monensin, two drugs that affect intracellular transport. *Yeast*, **18**, 163-172.

Natarajan, P., Wang, J., Hua, Z. and Graham, T.R. (2004) Drs2p-coupled aminophospholipid translocase activity in yeast Golgi membranes and relationship to in vivo function. *Proc Natl Acad Sci U S A*, **101**, 10614-10619.

Nelson, N. and Harvey, W.R. (1999) Vacuolar and plasma membrane proton-adenosinetriphosphatases. *Physiol Rev*, **79**, 361-385.

Nikko, E., Marini, A.M. and Andre, B. (2003) Permease recycling and ubiquitination status reveal a particular role for Bro1 in the multivesicular body pathway. *J Biol Chem*, **278**, 50732-50743.

Nothwehr, S.F., Ha, S.A. and Bruinsma, P. (2000) Sorting of yeast membrane proteins into an endosome-to-Golgi pathway involves direct interaction of their cytosolic domains with Vps35p. *J Cell Biol*, **151**, 297-310.

Odorizzi, G., Cowles, C.R. and Emr, S.D. (1998b) The AP-3 complex: a coat of many colours. *Trends Cell Biol*, **8**, 282-288.

Ooi, C.E., Dell'Angelica, E.C. and Bonifacino, J.S. (1998) ADP-Ribosylation factor 1 (ARF1) regulates recruitment of the AP-3 adaptor complex to membranes. *J Cell Biol*, **142**, 391-402.

Orci, L., Glick, B.S. and Rothman, J.E. (1986) A new type of coated vesicular carrier that appears not to contain clathrin: its possible role in protein transport within the Golgi stack. *Cell*, **46**, 171-184.

Padilla, P.I., Chang, M.J., Pacheco-Rodriguez, G., Adamik, R., Moss, J. and Vaughan, M. (2003) Interaction of FK506-binding protein 13 with brefeldin A-inhibited guanine nucleotide-exchange protein 1 (BIG1): effects of FK506. *Proc Natl Acad Sci U S A*, **100**, 2322-2327.

Panic, B., Whyte, J.R. and Munro, S. (2003a) The ARF-like GTPases Arl1p and Arl3p act in a pathway that interacts with vesicle-tethering factors at the Golgi apparatus. *Curr Biol*, **13**, 405-410.

Panic, B., Perisic, O., Veprintsev, D.B., Williams, R.L. and Munro, S. (2003b) Structural basis for Arl1-dependent targeting of homodimeric GRIP domains to the Golgi apparatus. *Mol Cell*, **12**, 863-874.

Parks, L.W., Smith, S.J. and Crowley, J.H. (1995) Biochemical and physiological effects of sterol alterations in yeast--a review. *Lipids*, 30, 227-230.

Parton, R.G. and Richards, A.A. (2003) Lipid rafts and caveolae as portals for endocytosis: new insights and common mechanisms. *Traffic*, **4**, 724-738.

Pascon, R.C. and Miller, B.L. (2000) Morphogenesis in Aspergillus nidulans requires Dopey (DopA), a member of a novel family of leucine zipper-like proteins conserved from yeast to humans. *Mol Microbiol*, **36**, 1250-1264.

Patton, J.L. and Lester, R.L. (1991) The phosphoinositol sphingolipids of Saccharomyces cerevisiae are highly localized in the plasma membrane. *J Bacteriol*, **173**, 3101-3108.

Pelham, H.R. (2002) Insights from yeast endosomes. *Curr Opin Cell Biol*, **14**, 454-462.

Peter, B.J., Kent, H.M., Mills, I.G., Vallis, Y., Butler, P.J., Evans, P.R. and McMahon, H.T. (2004) BAR domains as sensors of membrane curvature: the amphiphysin BAR structure. *Science*, **303**, 495-499.

Peters, C., Bayer, M.J., Buhler, S., Andersen, J.S., Mann, M. and Mayer, A. (2001) Trans-complex formation by proteolipid channels in the terminal phase of membrane fusion. *Nature*, **409**, 581-588.

Peyroche, A., Paris, S. and Jackson, C.L. (1996) Nucleotide exchange on ARF mediated by yeast Gea1 protein. *Nature*, **384**, 479-481.

Piper, R.C., Cooper, A.A., Yang, H. and Stevens, T.H. (1995) VPS27 controls vacuolar and endocytic traffic through a prevacuolar compartment in Saccharomyces cerevisiae. *J Cell Biol*, **131**, 603-617.

Pomorski, T., Lombardi, R., Riezman, H., Devaux, P.F., van Meer, G. and Holthuis, J.C. (2003) Drs2p-related P-type ATPases Dnf1p and Dnf2p are required for phospholipid translocation across the yeast plasma membrane and serve a role in endocytosis. *Mol Biol Cell*, **14**, 1240-1254.

Prescianotto-Baschong, C. and Riezman, H. (1998) Morphology of the yeast endocytic pathway. *Mol Biol Cell*, **9**, 173-189.

Prescianotto-Baschong, C. and Riezman, H. (2002) Ordering of compartments in the yeast endocytic pathway. *Traffic*, **3**, 37-49.

Prezant, T.R., Chaltraw, W.E., Jr. and Fischel-Ghodsian, N. (1996) Identification of an overexpressed yeast gene which prevents aminoglycoside toxicity. *Microbiology*, **142**, 3407-3414.

Puertollano, R., Randazzo, P.A., Presley, J.F., Hartnell, L.M. and Bonifacino, J.S. (2001a) The GGAs promote ARF-dependent recruitment of clathrin to the TGN. *Cell*, **105**, 93-102.

Puertollano, R., Aguilar, R.C., Gorshkova, I., Crouch, R.J. and Bonifacino, J.S. (2001b) Sorting of mannose 6-phosphate receptors mediated by the GGAs. *Science*, **292**, 1712-1716.

Puertollano, R. and Bonifacino, J.S. (2004) Interactions of GGA3 with the ubiquitin sorting machinery. *Nat Cell Biol*, **6**, 244-251.

Ramaen, O., Joubert, A., Simister, P., Belgareh-Touze, N., Olivares-Sanchez, M.C., Zeeh, J.C., Chantalat, S., Golinelli-Cohen, M.P., Jackson, C.L., Biou, V. and Cherfils, J. (2007) Interactions between Conserved Domains within Homodimers in the BIG1, BIG2, and GBF1 Arf Guanine Nucleotide Exchange Factors. *J Biol Chem*, **282**, 28834-28842.

Reggiori, F. and Pelham, H.R. (2001) Sorting of proteins into multivesicular bodies: ubiquitin-dependent and -independent targeting. *EMBO J*, **20**, 5176-5186.

Reggiori, F. and Pelham, H.R. (2002) A transmembrane ubiquitin ligase required to sort membrane proteins into multivesicular bodies. *Nat Cell Biol*, **4**, 117-123.

Reggiori, F., Wang, C.W., Stromhaug, P.E., Shintani, T. and Klionsky, D.J. (2003) Vps51 is part of the yeast Vps fifty-three tethering complex essential for retrograde traffic from the early endosome and Cvt vesicle completion. *J Biol Chem*, **278**, 5009-5020.

Ridgway, N.D. (2000) Interactions between metabolism and intracellular distribution of cholesterol and sphingomyelin. *Biochim Biophys Acta*, **1484**, 129-141.

Rigaut, G., Shevchenko, A., Rutz, B., Wilm, M., Mann, M. and Seraphin, B. (1999) A generic protein purification method for protein complex characterization and proteome exploration. *Nat Biotechnol*, **17**, 1030-1032.

Robinson, M.S. (2004) Adaptable adaptors for coated vesicles. *Trends Cell Biol*, **14**, 167-174.

Russell, M.R., Nickerson, D.P. and Odorizzi, G. (2006) Molecular mechanisms of late endosome morphology, identity and sorting. *Curr Opin Cell Biol*, **18**, 422-428.

Sakaki, K., Tashiro, K., Kuhara, S. and Mihara, K. (2003) Response of genes associated with mitochondrial function to mild heat stress in yeast Saccharomyces cerevisiae. *J Biochem (Tokyo)*, **134**, 373-384.

Sambrook, J., Fritsch, E.F. and Manniatis, T. (1989) Molecular cloning - A laboratory manual. 2. edn. *Cold Spring Harbor Laboratory Press*.

Schoer, J.K., Gallegos, A.M., McIntosh, A.L., Starodub, O., Kier, A.B., Billheimer, J.T. and Schroeder, F. (2000) Lysosomal membrane cholesterol dynamics. *Biochemistry*, **39**, 7662-7677.

Scott, P.M., Bilodeau, P.S., Zhdankina, O., Winistorfer, S.C., Hauglund, M.J., Allaman, M.M., Kearney, W.R., Robertson, A.D., Boman, A.L. and Piper, R.C. (2004) GGA proteins bind ubiquitin to facilitate sorting at the trans-Golgi network. *Nat Cell Biol*, **6**, 252-259.

Seaman, M.N., Sowerby, P.J. and Robinson, M.S. (1996) Cytosolic and membrane-associated proteins involved in the recruitment of AP-1 adaptors onto the trans-Golgi network. *J Biol Chem*, **271**, 25446-25451.

Seaman, M.N., Marcusson, E.G., Cereghino, J.L. and Emr, S.D. (1997) Endosome to Golgi retrieval of the vacuolar protein sorting receptor, Vps10p, requires the function of the VPS29, VPS30, and VPS35 gene products. *J Cell Biol*, **137**, 79-92.

Seeley, E.S., Kato, M., Margolis, N., Wickner, W. and Eitzen, G. (2002) Genomic analysis of homotypic vacuole fusion. *Mol Biol Cell*, **13**, 782-794.

Seol, J.H., Shevchenko, A. and Deshaies, R.J. (2001) Skp1 forms multiple protein complexes, including RAVE, a regulator of V-ATPase assembly. *Nat Cell Biol*, **3**, 384-391.

Serafini, T., Stenbeck, G., Brecht, A., Lottspeich, F., Orci, L., Rothman, J.E. and Wieland, F.T. (1991) A coat subunit of Golgi-derived non-clathrin-coated vesicles with homology to the clathrin-coated vesicle coat protein beta-adaptin. *Nature*, **349**, 215-220.

Setty, S.R., Shin, M.E., Yoshino, A., Marks, M.S. and Burd, C.G. (2003) Golgi recruitment of GRIP domain proteins by Arf-like GTPase 1 is regulated by Arf-like GTPase 3. *Curr Biol*, **13**, 401-404.

Setty, S.R., Strochlic, T.I., Tong, A.H., Boone, C. and Burd, C.G. (2004) Golgi targeting of ARF-like GTPase Arl3p requires its Nalpha-acetylation and the integral membrane protein Sys1p. *Nat Cell Biol*, **6**, 414-419.

Short, B., Haas, A. and Barr, F.A. (2005) Golgins and GTPases, giving identity and structure to the Golgi apparatus. *Biochim Biophys Acta*, **1744**, 383-395.

Simons, K. and Ikonen, E. (1997) Functional rafts in cell membranes. *Nature*, **387**, 569-572.

Simons, K. and Vaz, W.L. (2004) Model systems, lipid rafts, and cell membranes. *Annu Rev Biophys Biomol Struct*, **33**, 269-295.

Singer-Kruger, B. and Riezman, H. (1990) Detection of an intermediate compartment involved in transport of alpha-factor from the plasma membrane to the vacuole in yeast. *J Cell Biol*, **110**, 1911-1922.

Singer-Kruger, B., Frank, R., Crausaz, F. and Riezman, H. (1993) Partial purification and characterization of early and late endosomes from yeast. Identification of four novel proteins. *J Biol Chem*, **268**, 14376-14386.

Singer-Kruger, B., Stenmark, H., Dusterhoft, A., Philippsen, P., Yoo, J.S., Gallwitz, D. and Zerial, M. (1994) Role of three rab5-like GTPases, Ypt51p, Ypt52p, and Ypt53p, in the endocytic and vacuolar protein sorting pathways of yeast. *J Cell Biol*, **125**, 283-298.

Singer-Kruger, B. and Ferro-Novick, S. (1997) Use of a synthetic lethal screen to identify yeast mutants impaired in endocytosis, vacuolar protein sorting and the organization of the cytoskeleton. *Eur J Cell Biol*, **74**, 365-375.

Sipos, G. and Fuller, R.S. (2002) Separation of Golgi and endosomal compartments. *Methods Enzymol*, **351**, 351-365.

Sipos, G., Brickner, J.H., Brace, E.J., Chen, L., Rambourg, A., Kepes, F. and Fuller, R.S. (2004) Soi3p/Rav1p functions at the early endosome to regulate endocytic trafficking to the vacuole and localization of trans-Golgi network transmembrane proteins. *Mol Biol Cell*, **15**, 3196-3209.

Slepnev, V.I. and De Camilli, P. (2000) Accessory factors in clathrin-dependent synaptic vesicle endocytosis. *Nat Rev Neurosci*, **1**, 161-172.

Smardon, A.M., Tarsio, M. and Kane, P.M. (2002) The RAVE complex is essential for stable assembly of the yeast V-ATPase. *J Biol Chem*, **277**, 13831-13839.

Sokol, J., Blanchette-Mackie, J., Kruth, H.S., Dwyer, N.K., Amende, L.M., Butler, J.D., Robinson, E., Patel, S., Brady, R.O., Comly, M.E. and et al. (1988) Type C Niemann-Pick disease. Lysosomal accumulation and defective intracellular mobilization of low density lipoprotein cholesterol. *J Biol Chem*, **263**, 3411-3417.

Söllner, T.H. (2003) Regulated exocytosis and SNARE function (Review). *Mol Membr Biol*, **20**, 209-220.

Stamnes, M.A. and Rothman, J.E. (1993) The binding of AP-1 clathrin adaptor particles to Golgi membranes requires ADP-ribosylation factor, a small GTP-binding protein. *Cell*, **73**, 999-1005.

Stamnes, M. (2002) Regulating the actin cytoskeleton during vesicular transport. *Curr Opin Cell Biol*, **14**, 428-433.

Stepp, J.D., Pellicena-Palle, A., Hamilton, S., Kirchhausen, T. and Lemmon, S.K. (1995) A late Golgi sorting function for Saccharomyces cerevisiae Apm1p, but not for Apm2p, a second yeast clathrin AP medium chain-related protein. *Mol Biol Cell*, **6**, 41-58.

Stepp, J.D., Huang, K. and Lemmon, S.K. (1997) The yeast adaptor protein complex, AP-3, is essential for the efficient delivery of alkaline phosphatase by the alternate pathway to the vacuole. *J Cell Biol*, **139**, 1761-1774.

Stevens, T.H. and Forgac, M. (1997) Structure, function and regulation of the vacuolar (H+)-ATPase. *Annu Rev Cell Dev Biol*, **13**, 779-808.

Szymkiewicz, I., Destaing, O., Jurdic, P. and Dikic, I. (2004) SH3P2 in complex with Cbl and Src. *FEBS Lett*, **565**, 33-38.

Tamkun, J.W., Kahn, R.A., Kissinger, M., Brizuela, B.J., Rulka, C., Scott, M.P. and Kennison, J.A. (1991) The arflike gene encodes an essential GTP-binding protein in Drosophila. *Proc Natl Acad Sci U S A*, **88**, 3120-3124.

Tang, X., Halleck, M.S., Schlegel, R.A. and Williamson, P. (1996) A subfamily of P-type ATPases with aminophospholipid transporting activity. *Science*, **272**, 1495-1497.

Tedrick, K., Trischuk, T., Lehner, R. and Eitzen, G. (2004) Enhanced membrane fusion in sterol-enriched vacuoles bypasses the Vrp1p requirement. *Mol Biol Cell*, **15**, 4609-4621.

Teter, S.A. and Klionsky, D.J. (2000) Transport of proteins to the yeast vacuole: autophagy, cytoplasm-to-vacuole targeting, and role of the vacuole in degradation. *Semin Cell Dev Biol*, **11**, 173-179.

Theos, A.C., Tenza, D., Martina, J.A., Hurbain, I., Peden, A.A., Sviderskaya, E.V., Stewart, A., Robinson, M.S., Bennett, D.C., Cutler, D.F., Bonifacino, J.S., Marks, M.S. and Raposo, G. (2005) Functions of adaptor protein (AP)-3 and AP-1 in tyrosinase sorting from endosomes to melanosomes. *Mol Biol Cell*, **16**, 5356-5372.

Tong, A.H., Lesage, G., Bader, G.D., Ding, H., Xu, H., Xin, X., Young, J., Berriz, G.F., Brost, R.L., Chang, M., Chen, Y., Cheng, X., Chua, G., Friesen, H., Goldberg, D.S., Haynes, J., Humphries, C., He, G., Hussein, S., Ke, L., Krogan, N., Li, Z., Levinson, J.N., Lu, H.,

Menard, P., Munyana, C., Parsons, A.B., Ryan, O., Tonikian, R., Roberts, T., Sdicu, A.M., Shapiro, J., Sheikh, B., Suter, B., Wong, S.L., Zhang, L.V., Zhu, H., Burd, C.G., Munro, S., Sander, C., Rine, J., Greenblatt, J., Peter, M., Bretscher, A., Bell, G., Roth, F.P., Brown, G.W., Andrews, B., Bussey, H. and Boone, C. (2004) Global mapping of the yeast genetic interaction network. *Science*, **303**, 808-813.

Towbin, H., Staehelin, T. and Gordon, J. (1979) Electrophoretic transfer of proteins from polyacrylamide gels to nitrocellulose sheets: procedure and some applications. *Proc Natl Acad Sci U S A*, **76**, 4350-4354.

Tronnersjö, S., Hanefalk, C., Balciunas, D., Hu, G.Z., Nordberg, N., Muren, E. and Ronne, H. (2007) The jmjN and jmjC domains of the yeast zinc finger protein Gis1 interact with 19 proteins involved in transcription, sumoylation and DNA repair. *Mol Genet Genomics*, **277**, 57-70.

Tsukada, M., Will, E. and Gallwitz, D. (1999) Structural and functional analysis of a novel coiled-coil protein involved in Ypt6 GTPase-regulated protein transport in yeast. *Mol Biol Cell*, **10**, 63-75.

Uetz, P., Giot, L., Cagney, G., Mansfield, T.A., Judson, R.S., Knight, J.R., Lockshon, D., Narayan, V., Srinivasan, M., Pochart, P., Qureshi-Emili, A., Li, Y., Godwin, B., Conover, D., Kalbfleisch, T., Vijayadamodar, G., Yang, M., Johnston, M., Fields, S. and Rothberg, J.M. (2000) A comprehensive analysis of protein-protein interactions in Saccharomyces cerevisiae. *Nature*, **403**, 623-627.

Valdivia, R.H., Baggott, D., Chuang, J.S. and Schekman, R.W. (2002) The yeast clathrin adaptor protein complex 1 is required for the efficient retention of a subset of late Golgi membrane proteins. *Dev Cell*, **2**, 283-294.

van Meer, G. and Sprong, H. (2004) Membrane lipids and vesicular traffic. *Curr Opin Cell Biol*, **16**, 373-378.

Van Valkenburgh, H., Shern, J.F., Sharer, J.D., Zhu, X. and Kahn, R.A. (2001) ADP-ribosylation factors (ARFs) and ARF-like 1 (ARL1) have both specific and shared effectors: characterizing ARL1-binding proteins. *J Biol Chem*, **276**, 22826-22837.

Vida, T.A., Huyer, G. and Emr, S.D. (1993) Yeast vacuolar proenzymes are sorted in the late Golgi complex and transported to the vacuole via a prevacuolar endosome-like compartment. *J Cell Biol*, **121**, 1245-1256.

Vogel, J.P., Lee, J.N., Kirsch, D.R., Rose, M.D. and Sztul, E.S. (1993) Brefeldin A causes a defect in secretion in Saccharomyces cerevisiae. *J Biol Chem*, **268**, 3040-3043.

Wach, A., Brachat, A., Pohlmann, R. and Philippsen, P. (1994) New heterologous modules for classical or PCR-based gene disruptions in Saccharomyces cerevisiae. *Yeast*, **10**, 1793-1808.

Wachtler, V. and Balasubramanian, M.K. (2006) Yeast lipid rafts?--an emerging view. *Trends Cell Biol*, **16**, 1-4.

Wahle, T., Prager, K., Raffler, N., Haass, C., Famulok, M. and Walter, J. (2005) GGA proteins regulate retrograde transport of BACE1 from endosomes to the trans-Golgi network. *Mol Cell Neurosci*, **29**, 453-461.

Wasiak, S., Legendre-Guillemin, V., Puertollano, R., Blondeau, F., Girard, M., de Heuvel, E., Boismenu, D., Bell, A.W., Bonifacino, J.S. and McPherson, P.S. (2002) Enthoprotin: a

novel clathrin-associated protein identified through subcellular proteomics. *J Cell Biol*, **158**, 855-862.

Whyte, J.R. and Munro, S. (2002) Vesicle tethering complexes in membrane traffic. *J Cell Sci*, **115**, 2627-2637.

Wichmann, H., Hengst, L. and Gallwitz, D. (1992) Endocytosis in yeast: evidence for the involvement of a small GTP-binding protein (Ypt7p). *Cell*, **71**, 1131-1142.

Wicky, S., Frischmuth, S. and Singer-Kruger, B. (2003) Bsp1p/Ypr171p is an adapter that directly links some synaptojanin family members to the cortical actin cytoskeleton in yeast. *FEBS Lett*, **537**, 35-41.

Wicky, S., Schwarz, H. and Singer-Kruger, B. (2004) Molecular interactions of yeast Neo1p, an essential member of the Drs2 family of aminophospholipid translocases, and its role in membrane trafficking within the endomembrane system. *Mol Cell Biol*, **24**, 7402-7418.

Wiederkehr, A., Meier, K.D. and Riezman, H. (2001) Identification and characterization of Saccharomyces cerevisiae mutants defective in fluid-phase endocytosis. *Yeast*, **18**, 759-773.

Wu, M., Lu, L., Hong, W. and Song, H. (2004) Structural basis for recruitment of GRIP domain golgin-245 by small GTPase Arl1. Nat Struct Mol Biol, 11, 86-94.

Xu, J. and Scheres, B. (2005) Dissection of Arabidopsis ADP-RIBOSYLATION FACTOR 1 function in epidermal cell polarity. *Plant Cell*, **17**, 525-536.

Yoshinaka, K., Kumanogoh, H., Nakamura, S. and Maekawa, S. (2004) Identification of V-ATPase as a major component in the raft fraction prepared from the synaptic plasma membrane and the synaptic vesicle of rat brain. *Neurosci Lett*, **363**, 168-172.

Yoshino, A., Bieler, B.M., Harper, D.C., Cowan, D.A., Sutterwala, S., Gay, D.M., Cole, N.B., McCaffery, J.M. and Marks, M.S. (2003) A role for GRIP domain proteins and/or their ligands in structure and function of the trans Golgi network. *J Cell Sci*, **116**, 4441-4454.

Zachowski, A., Henry, J.P. and Devaux, P.F. (1989) Control of transmembrane lipid asymmetry in chromaffin granules by an ATP-dependent protein. *Nature*, **340**, 75-76.

Zhdankina, O., Strand, N.L., Redmond, J.M. and Boman, A.L. (2001) Yeast GGA proteins interact with GTP-bound Arf and facilitate transport through the Golgi. *Yeast*, **18**, 1-18.

Zhu, Y., Doray, B., Poussu, A., Lehto, V.P. and Kornfeld, S. (2001) Binding of GGA2 to the lysosomal enzyme sorting motif of the mannose 6-phosphate receptor. *Science*, **292**, 1716-1718.

Ziegler, A. (2003) Untersuchungen zur Lokalizierung und Funktion eines neuen Hefeproteins Ykr088p im Endomembransystem *Diplomarbeit* Universität Stuttgart

Ziman, M., Chuang, J.S. and Schekman, R.W. (1996) Chs1p and Chs3p, two proteins involved in chitin synthesis, populate a compartment of the Saccharomyces cerevisiae endocytic pathway. *Mol Biol Cell*, **7**, 1909-1919.

Zinser, E., Paltauf, F. and Daum, G. (1993) Sterol composition of yeast organelle membranes and subcellular distribution of enzymes involved in sterol metabolism. *J Bacteriol*, **175**, 2853-2858.

Zinser, E. and Daum, G. (1995) Isolation and biochemical characterization of organelles from the yeast, Saccharomyces cerevisiae. *Yeast*, **11**, 493-536.

Acknowledgment

Als erstes möchte ich mich bei der Betreuerin meiner Doktorarbeit bedanken, PD Dr. Birgit Singer-Krüger. Ihr Engagement und umfassende wissenschaftliche Anleitung während der letzten Jahre waren unabdingbar für den Erfolg meiner Doktorarbeit. Vielen Dank für dieses spannende Projekt und die Hilfe bei der Fertigstellung dieser Arbeit.

Als nächstes möchte ich mich bei Prof. Dr. Dieter H. Wolf für die Möglichkeit bedanken, meine Arbeit am Institut für Biochemie durchführen zu können sowie für die Bereitschaft zu meinem Prüfungskomitee zu gehören.

Especially I want to thank to my colleagues from the south lab, for all the great discussions and fun we had in all the time: Claudia Böttcher-Sehlmeyer, Sónia Barbosa, Sidonie Wicky-John, Anna-Maria Bürger, Dagmar Siele, Viola Günther, Yi Wang und Svenja Kaden. Each of you has made me a richer person in your very special way.

Bei allen DokorandInnen, DipomandInnen und MitarbeiterInnen des Instituts für Biochemie der Universität Stuttgart möchte ich mich herzlich für die gute Zusammenarbeit und das großartige Arbeitsklima bedanken. Einen hrezlichen Dank im Speziellen an Elisabeth und Dragica für die Unterstützung und gewissen Mama-Ersatz ;-).

Ich danke Herrn Klaus Bökamp für das „Auf den Weg bringen". Ohne die drei Jahre im Bio-LK bei dir würde es diese Doktorarbeit nicht geben.

I naravno, last but not least, hvala mami i tati za konstantnu podršku koja mi je pomogla da izdržim kada je bilo najteže. Svaki moj uspijeh je istovremeno i vasa zasluga. Ljubim vas.

I'll miss you all!!

Curriculum Vitae

PERSONAL DATA

Name:	Maja Lasić	Current address:	Maja Lasić
Date of birth:	19.05.1979		Hohes Feld 50
	in Mostar, Bosnia-Herzegovina		D- 33611 Bielefeld
Nationality:	bosnian/croatian		
	resident of Germany since 1993		
Marital status:	married, no children		

EDUCATION

May 2007 – Okt 2007	**Marketing Trainee** at the College of Further Education in economy (FAW Bielefeld)
Sept. 2003 – 13.03.2008	**Ph.D.** project at the Institute of biochemistry at the Technical University of Stuttgart, Germany
Sept. 1998 – May 2003	**Study of biology** at the Westfalian Wilhelms-University Munster, Germany Diploma thesis: "Protein SWAP-70: Intramolecular interactions and the GDP-exchange activity for monomeric G-proteins of the Rho-family" at the Institute of General Zoology and Genetics at the University of Muenster, Germany (Supervisor: Prof. Dr. Martin Bähler)
	mark: excellent (1,0)
	final mark: excellent (1,0)
April 1999 – Sept. 2002	**Study of chemistry** at the Westfalian Wilhelms-University Muenster
Sept. 1995 – June 1998	**A-level degree** "Abitur" at the Ratsgymnasium Bielefeld, Germany

PROFESSIONAL EXPERIENCE

Since Nov. 2007	**Account manager** in Procter&Gamble Pharmaceuticals
Sept.2003 – Aug. 2006	**PhD research** at the Institute of biochemistry of Prof. D. H. Wolf, University of Stuttgart. Topic: "The yeast endosomal-TGN-localised Ysl2p/Arl1p/Neo1p network: Studies on new interaction partners", PhD defence presumably in January 2008 (Supervisor: PD Dr. Birgit Singer-Krüger)

PUBLICATIONS

Birgit Singer-Krüger, **Maja Lasić**, Anna-Maria Bürger, Angelika Haußer, Rüdiger Pipkorn, and Yi Wang: (2008) **"Yeast and human Ysl2p/hMon2 interact with Gga adaptors and mediate their subcellular distribution"** accepted in *EMBO Journal*

Lasić, M., 2003 „Das Protein SWAP-70: Intramolekulare Interaktionen und GDP-Austauschaktivität für monomere G-Proteine der Rho-Familie" unpublished Diploma thesis, Westfälische Wilhelms-Universität (WWU) in Muenster, Germany